INDUSTRIAL CARNALLITE-WASTE FOR THERMOCHEMICAL ENERGY STORAGE APPLICATION

~~CARNALLITE-WASTE: A POTENTIAL INDUSTRIAL WASTE STUDIED FOR THERMOCHEMICAL STORAGE APPLICATION~~

V. Mamani [1], A. Gutiérrez[2], A. I. Fernández[3], S. Ushak [1]*

1 Department of Chemical Engineering and Mineral Processing and Center for Advanced Study of Lithium and Industrial Minerals (CELiMIN), Universidad de Antofagasta, Campus Coloso, Av. Universidad de Antofagasta 02800, Antofagasta, Chile

[2] German Aerospace Center – DLR e. V., Institute of Engineering Thermodynamics, Pfaffenwaldring 38, 70569 Stuttgart, Germany

[3] Department of Materials Science and Physical Chemistry, Universitat de Barcelona, Martí i Franqués 1, 08028 Barcelona, Spain

Corresponding author e-mail: svetlana.ushak@uantof.cl

Abstract

The key to successful development and implementation of thermochemical storage systems is the identification of high energy density and low-cost storage materials. In this work, an industrial waste based on a double salt hydrate, coming from non-metallic mining was studied for thermochemical storage applications. Initially, chemical characterization was performed and determined that carnallite-waste material consists of 73.54 wt% of $KCl{\cdot}MgCl_2{\cdot}6H_2O$ and impurities such as NaCl (23.04 wt%), KCl (1.76 wt%) and $CaSO_4$ (1.66 wt%). Using thermal analyses methods, the operating conditions such as temperatures and partial pressures, were optimized for seasonal thermochemical storage applications to P_{Hy} = 1.3 kPa and ϑ_{Hy} = 40 °C, and to P_{De} = 4.0 kPa and ϑ_{De} = 110 °C. Under these conditions, the reaction reversibility over 10 cycles (10 years) was significantly high, with only 8.5% decrease in chemical reversibility. Furthermore, the duration of dehydration and hydration isotherms was optimized to 15 and 360 minutes, respectively. Finally, 1.129 GJ/m^3 energy storage density was calculated after the tenth cycle of hydration/dehydration for this material. Hence 7.1 m^3 of carnallite was estimated to meet the demand of 8 GJ of energy for an average household during the six months of cold seasons. These results are comparable and competitive with an energy storage density of materials such as K_2CO_3 and $MgCl_2$, reported as promising for seasonal thermochemical storage applications. It should be noted that carnallite-waste material has no commercial value so far and its use contributes to developing sustainable low-cost thermochemical energy storage systems.

Keywords: thermochemical storage energy; potassium magnesium chloride hexahydrate ~~carnallite~~; carnallite-waste ~~low-cost~~ material; doble inorganic salt; dehydration and hydration reaction; seasonal heat storage.

1. Introduction

Population growth in the last decades has brought a great industrial activity increase, which as a consequence, has also increased greenhouse gas emissions. Thereby, nowadays one of the greatest challenges that countries face in order to maintain sustainable economic development and to reduce

dependence on conventional energy sources is to increase energy efficiency based on renewable sources and thermal energy storage (TES) systems [1,2]. The principle of TES is based on storing heat while the energy source is available, and use it later for heating/cooling applications or the generation of other types of energy e. g. electric [3]. The heat can come from different sources such as industrial waste heat, solar energy, etc. Applications vary from domestic to industrial level depending on the temperature level [4]. The heat storage mechanisms can be sensible heat storage (SHS), latent heat storage (LHS) and thermochemical storage (TCS). TCS has the highest energy storage density in terms of medium of storage (~ 0.92 – 3.56 GJ/m^3), which is from 5 to 10 times higher compared to LHS (0.15-0.37 GJ/m^3) and SHS (0.033 - 0.4 GJ/m^3), respectively [3,4]. In addition, TCS systems reviewed in [5], use thermochemical materials (TCM) that store and release heat through reversible chemical reactions with practically no heat losses over time [6]. This characteristic is especially attractive for long-term TES applications such as seasonal heat storage, using for example salt hydrates, summarized in [7]. In this case, the heat is stored and released through a reversible reaction of dehydration and hydration (See eq.1) [8]. On the one hand, during summer the system is charged by means of material dehydration, flowing hot air heated by solar collectors, at maximum temperatures of 150 °C. On the other hand, during winter the discharging process is carried out, flowing humid air (e.g. p_{H2O} ~ 1.3 kPa, ϑ_{SAT} = 10°C) through the partially hydrated or totally anhydrous powder. Lastly, this discharge process, release the stored heat through the exothermic hydration reaction [9] (Figure 1).

$$M \cdot xH_2O_{(s)} + \Delta_R H \leftrightarrow M \cdot yH_2O_{(S)} + (x-y)H_2O_{(g)} \quad \text{(eq. 1)}$$

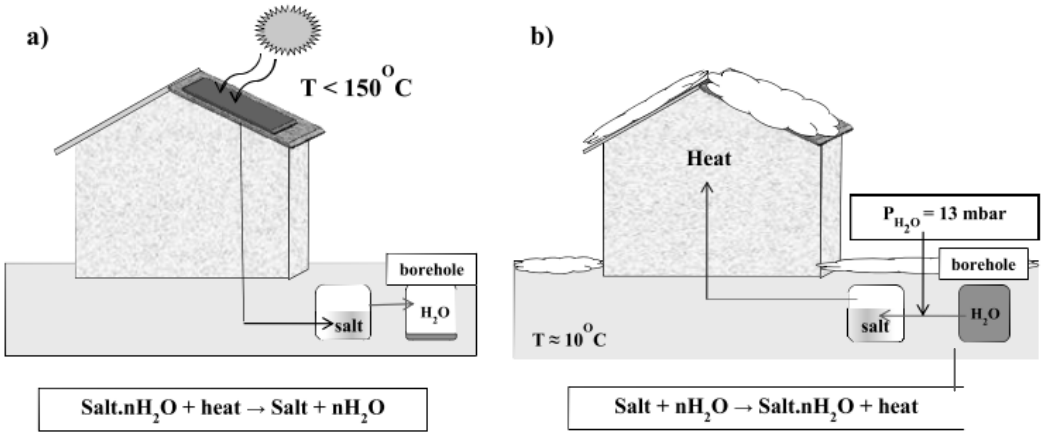

Figure 1: Representation of application of seasonal thermochemical storage, where (a) dehydration and (b) hydration reaction [9].

This reverse reaction is possible under specific temperature and partial vapor pressure conditions defined by the van't Hoff equation (eq. 2), where p_{H_2O} is the partial pressure of water vapor (kPa), p^+ is the reference pressure (100 kPa), **R** is the universal gas constant (8.314 J/mol K), v is the stoichiometric factor for each reaction ($v = x - y$), T is the temperature (K), $\Delta_R S^\theta$ (J/mol K) and $\Delta_R H^\theta$ (J/mol K) correspond to the standard entropy and the standard enthalpy of the reaction, respectively.

$$\ln\left(\frac{p_{H_2O}}{p^+}\right) = \frac{\Delta_R S^\theta}{\boldsymbol{Rv}} - \frac{\Delta_R H^\theta}{\boldsymbol{RvT}} \quad \text{(eq. 2)}$$

Although TCS has advantages over sensible and latent heat storage, its level of maturity is still in a preliminary stage, and a great research effort still needed to make it a suitable alternative. One critical aspect is the technical complexity of TCS systems that results in higher investment costs in comparison with latent and sensible heat storage systems [10]. Since the storage material represents a significant fraction of the total investment costs (up to 30 %), the study of industrial wastes used as a medium of storage has been urged [11] and summarized in Figure 2.

Miro et al [12] and Ushak et al [13] recommend the use of non-metallic industry by-products as SHS (NaCl) and LHS (Bischofite) materials (see Figure 2). Recently, Mamani et al. [14] showed that bischofite based by-product is also a promising TCM. The characterization of synthetic inorganic double salt hydrates similar to those that can be found as wastes show that Astrakanite [15] and Potassium Carnallite [15,16] have potential to be used as TCM, while Lithium Carnallite [15] and Kainite [17] not recommended to apply as TES materials under the conditions performed in the respective studies.

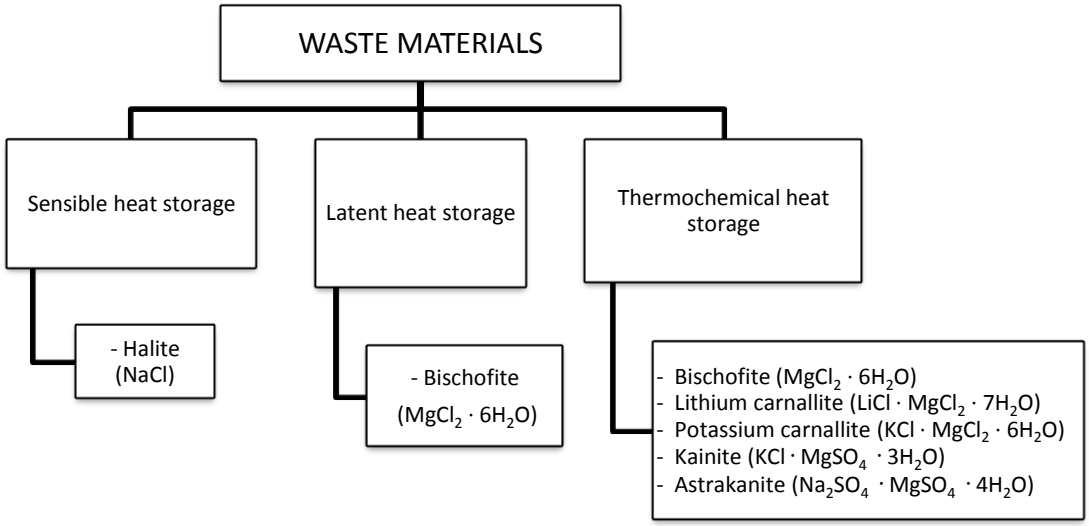

Figure 2: Summary of industrial waste and by-products based on inorganic salts studied as thermal energy storage material.

As it is possible to observe from the review of recent studies (see Figure 2), all of them are based on synthetic materials or by-products obtained in industrial processes. There are no studies that use real natural wastes, without any additional treatment, as possible TES materials based on inorganic salts.

This paper is the first application-oriented study approaching natural waste material suitability as a TCM, which contributes to developing novel low-cost thermochemical materials and their application for seasonal heat storage. The aim of this study is to focus on the thermodynamic characterization of potassium carnallite-waste and the optimization of the operating conditions for its use as TCM. Not only the reversibility and cycle stability of the dehydration-hydration reactions

are evaluated, but also the technical parameters, such as energy storage density and material costs. The results are comparable and competitive with materials reported as the most promising TCM.

2.Materials and methods

2.1. Material selection

The first studies using synthetic $KCl{\cdot}MgCl_2{\cdot}6H_2O$ (99 wt%, where wt% means weight percent, defined as the percent of a component in the mixture) [18,19] described thermal decomposition in two dehydration steps (eq.3 and 4). The release of water from the solid takes place with incongruent melting at 167.5 °C in experiments performed using sealed crucibles and under conditions of the partial pressure of water vapor close to 100 kPa [20].

$$KCl{\cdot}MgCl_2{\cdot}6H_2O(s) \leftrightarrow KCl{\cdot}MgCl_2{\cdot}2H_2O(s) + 4\ H_2O(g) \quad \text{(eq.3)}$$

$$KCl{\cdot}MgCl_2{\cdot}2H_2O(s) \leftrightarrow KCl{\cdot}MgCl_2(s) + 2\ H_2O(g) \quad \text{(eq.4)}$$

In addition to the second step of dehydration reaction (eq.4), the partial elimination of gaseous HCl (product of an irreversible secondary hydrolysis reaction) is detected (eq.5), which compromises the rehydration of anhydrous phase (or minor hydrate). Likewise, HCl is corrosive for the equipment in which it is contained and harmful to human health.

$$2\ KCl{\cdot}MgCl_2{\cdot}2H_2O\ (s) \rightarrow KCl{\cdot}MgCl_2\ (s) + 2\ H_2O\ (g) + KMg\ (OH)_2Cl\ (s) + 2HCl\ (g) \quad \text{(eq.5)}$$

The first application of potassium carnallite as TCM was proposed in [15,16] using synthetic material, with a high concentration of potassium carnallite (~76 wt% $KCl_2{\cdot}MgCl_2{\cdot}6H_2O$, 15.06 wt% $MgCl_2{\cdot}6H_2O$). The results of dehydration of potassium carnallite described it as a promising material for thermochemical storage, at application temperatures below 200 °C. The experiments were performed in an inert atmosphere of N_2 in order to avoid the release of HCl [15]. In the most recent study, the maximum application temperature was limited to 150 °C in a humid atmosphere (p_{H2O} = 25 kPa), in order to get stable chemical reversibility over cycles. Another critical factor identified in those studies was the duration of hydration and dehydration isothermal steps, showing that shorter periods of exposure at high temperatures (150 °C) reduces the degradation of the material over cycles. Therefore, the duration of dehydration isotherms was limited to <20 min. Following the reaction shown in eq.3, the same study reports stability of the enthalpy of reaction through the cycles, with approximate values to 120 kJ/mol $KCl_2{\cdot}MgCl_2{\cdot}6H_2O$ [16]. The operational conditions of thermochemical dehydration and hydration reactions are summarized in Table 1.

Table 1: Operating conditions of dehydration and hydration reactions for synthetic $KCl{\cdot}MgCl_2{\cdot}6H_2O$.

Reactions	Heating rate (K/min)	ϑ (°C)	ΔH_D (kJ/mol)	p_{H2O} (kPa)	Ref.
Dehydration reactions	0.5	84.2	189.68	0	[15]
$KCl{\cdot}MgCl_2{\cdot}6H_2O$ ➔ $KCl{\cdot}MgCl_2{\cdot}2H_2O + 4H_2O$					
$KCl{\cdot}MgCl_2{\cdot}2H_2O$ ➔ $KCl{\cdot}MgCl_2{\cdot}H_2O + H_2O$	0.5	127.1	67.93	0	[15]
Hydration reaction					

$KCl{\cdot}MgCl_2{\cdot}2\,H_2O + 4H_2O \rightarrow KCl{\cdot}MgCl_2{\cdot}6H_2O$	5	100	120	25	[16]

Based on these studies reported previously, synthetic potassium carnallite is a promising TCM, having adequate thermodynamic properties and significant stable chemical reversibility below 150 °C. Nevertheless, for a matter of applicability it is necessary not only to have a material with the characteristics just mentioned but also with high availability and low prices.

In northern Chile, about 1.8 million tons per year of potassium carnallite waste (75 wt% > $KCl{\cdot}MgCl_2{\cdot}6H_2O$) precipitates during the brine concentration process from Salar de Atacama [21,22]. On the basis that this material meets all the requirements mentioned above, 5 kg of natural carnallite-waste provided by the company Albemarle (Antofagasta region, Chile) was used for this study. The sample was homogenized by manual mixing and subjected to drying at 40 °C for approximately 12 hours to eliminate environmental humidity, due to the hygroscopicity of the salt.

2.2. Chemical characterization

-X-ray diffraction (XRD)

Analysis of X-ray diffraction was performed on X-ray diffractometer SIEMENS model D5000 (40 kV, 30 mA); radiation of Cu K α1 (λ = 1.5406 Å); Vertical Bragg–Brentano; Scan Range: 3–70° 2θ; Step Size:0.0201 2θ; StepTime:1.0 s. The powdered sample was positioned on a flat plate sample holder after sample powdering in an agate mortar. The identification of crystallographic phases was carried out using PDF-2 and TOPAS programs.

-Chemical analysis

Approximately 20 g of carnallite was used for the chemical analysis. The methods used to determine chemical composition were: atomic absorption spectrophotometry with direct aspiration (Varian Spectra 220 fs atomic absorption spectrometer) for quantification of K, Mg, Ca, Li, Na; volumetric titration with $AgNO_3$ for chloride identification and volumetric titration with $BaCl_2$ for the identification of sulphate.

-Morphology and composition analysis

A scanning electron microscope (SEM) Jeol, Model JSM6360LV was used for analyzing the morphology and composition of the sample, coupled to an energy dispersive X-ray spectrometer (EDX) Inca Oxford. The measurements were performed under low vacuum, electron beam of 20 kV, working distance of 10 mm, spot size 60 mm, and backscattered electron signal.

2.3. Thermal behavior of carnallite

The thermal stability and reversible dehydration/hydration reaction of carnallite-waste were performed under different operating conditions as follow:

2.3.1 Dehydration reaction

- Thermal behavior of material

The dynamic dehydration was measured with a METTLER TOLEDO TGA-DSC STARe thermogravimetric TG and DSC analyses. The dynamic method used was from room temperature up to 300 °C at 1 K/min. The nitrogen flow rate was set to 25.0 mL/min. For this analysis, a sample amount between 10-20 mg in a 70 µL platinum crucible with an unsealed lid was used to know the change of weight and heat flow at high temperatures.

- Determination of gaseous products by thermogravimetric –mass spectroscopy (TG-MS)

The thermal decomposition and mass loss curves were recorded by Thermogravimetric analysis (NETZSCH STA 449 C Jupiter). A thermogravimetric sample carrier with a thermocouple type S and an accuracy of ± 1 K was used. The measurements were performed from room temperature (25 °C) to 1100 °C performing dynamic experiments with a heating rate of 10 K/min using nitrogen as protective gas with a volume flow of 50 N-mL /min. The sample mass was surrounded by a constant gas flow of 100 N-mL/min nitrogen. The accuracy of the balance was ± 0.1 µg. In order to analyze the generated gases, a Mass spectrometer (NETZSCH QMS 403 C Aëolos) was coupled to the TG analyzer. Sample mass of about ~30 mg was measured in open Al_2O_3 crucibles.

- Determination of solid products by HT-XRD

The X-Ray diffraction was performed at room temperature and high-temperature; 50 °C, 130 °C and 170 °C, with PANalytical X'Pert Pro MPD equipment coupled with Anton Paar 1200 HTK oven. In this study, the following measurement conditions were used: 45kVx40 mA; static air atmosphere, heating/cooling rate of 1 K/min, radiation of Cu Kα1 (λ=1.5406 Å); Scan. Range: 10–80° in 2θ; Step Size: 0.013°. The powdered samples were positioned on a flat plate alumina sample holder after sample powdering. Based on experimental XRD patterns the identification of crystallographic phases has been performed by searching in ICDD PDF-2 (version 2004), and through the search- match of the crystalline structures data, using X'pert HighScore.

2.3.2 Hydration reaction

- STA–MHG Reversibility of Reaction

The investigation of reaction reversibility was carried out using a simultaneous thermal analyzer (NETZSCH STA 449 F3 Jupiter). Equipped with a differential scanning calorimetric and thermogravimetric (DSC-TG) sample holder with a thermocouple Type P and an accuracy of ±1 K was used. The accuracy of the balance was ±0.1 µg. The equipment was coupled to a Modular Humidity Generator (ProUmid MHG-32). Nitrogen was used as protective and purges gas with a volume flow for both of 20 N-mL/min, and as the atmosphere surrounding the sample kept it inert using 100 N-mL/min of only nitrogen flow or nitrogen flow and water vapor. Finally, liquid

nitrogen was used to support the controlled cooling process and the amount of mass used was ~ 10 mg. in an open system of platinum crucible.

The chemical reversibility was calculated as a percentage of weight gained during hydration divided by the weight lost during dehydration, according to the following eq. 6:

$$\%\, rev = \frac{weight\ recovered}{weight\ lost} x\ 100 \qquad \text{(eq.6)}$$

The operating conditions, namely the temperature and humidity programs, used to evaluate the sample reversibility, were taken from [16], where the maximum partial water vapor pressure was set to 30 kPa (38% RH). However, conditions determined as the most adequate, close to the theoretical thermodynamic equilibrium, consisted in the partial pressure of water vapor of 25 kPa (31.6 %RH) for the dehydration-hydration reactions, in the temperature range of 100 °C to 150 °C, setting isothermal durations of 10 and 20 min, respectively. The heating/cooling rates were set to 5 K/min over 15 cycles (see Table 2).

Table 2: Heat storage operating conditions of experiments.

	Dehydration					**Hydration**				
Step conditions	[a]		[b]		[c]		[d]		[e]	-
Experiment	$\vartheta_{initial}$ (°C)	ϑ_{De} (°C)	$p_{H2O,\ Dehy}$ (kPa)	HR (K/min)	$t_{iso,\ De}$ (min)	ϑ_{Hy} (°C)	$p_{H2O,\ Hy}$ (kPa)	CR (K/min)	$t_{iso,\ Hy}$ (min)	N° Cycles
1	40	150	25	5	15	100	25	-5	20	15
2	40	130	1.3	1	60	40	1.3	-1	180	5
3	40	110	1.3	1	15	40	1.3	-1	180	5
4	40	110	4.0	1	15	40	1.3	-1	180	5
5	40	110	4.0	1	15	40	1.3	-1	180	20
6	40	110	4.0	1	15	40	1.3	-1	360	10

During the experimental verification and validation of theoretical thermodynamic equilibrium, is important to set the limits of the operating conditions for using this material [23,24]; especially, when working with hygroscopic or deliquescent materials, which cannot be exposed to relative humidity above the critical level at certain temperatures [25].

The experiments 2-6 were designed to evaluate the material for seasonal heat storage applications. They reproduce the partial pressure of water vapor and temperatures that are characteristic of summer and winter (Figure 3, Table 2). These conditions should be suitable as indicated by the van't Hoff plot for synthetic carnallite [16] (Figure 4). Hydration temperatures were set to 40 °C (which

corresponds to the minimum temperature for water heating) and dehydration temperatures were set to 110 ºC and to 130 °C (which are easily reached by solar collector systems). The water vapor partial pressure conditions varied between 1.3 (10.9 %RH) and 4.0 kPa (35 %RH) for the release and recovery of 4 moles of water (eq.3).

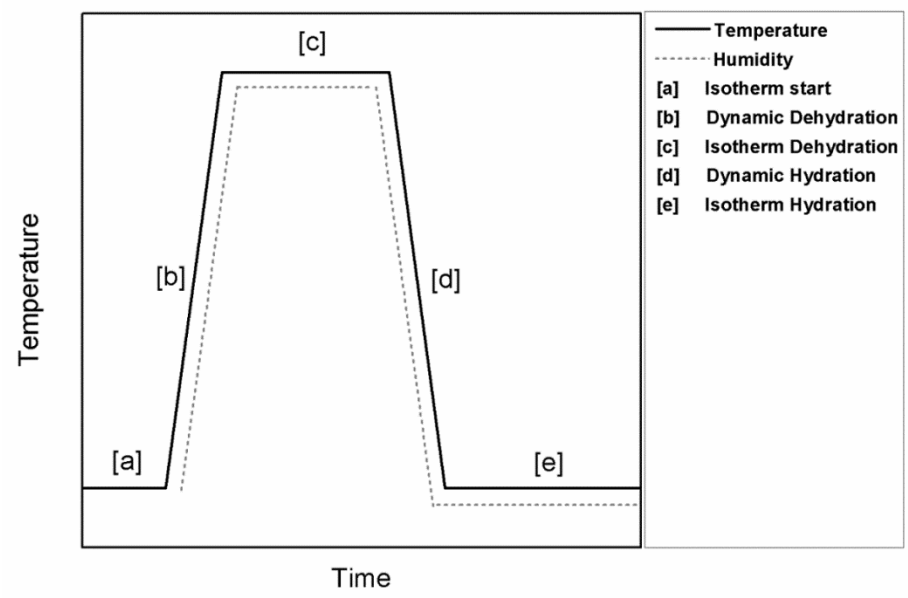

Figure 3: Experimental protocols of dehydration and hydration reactions study.

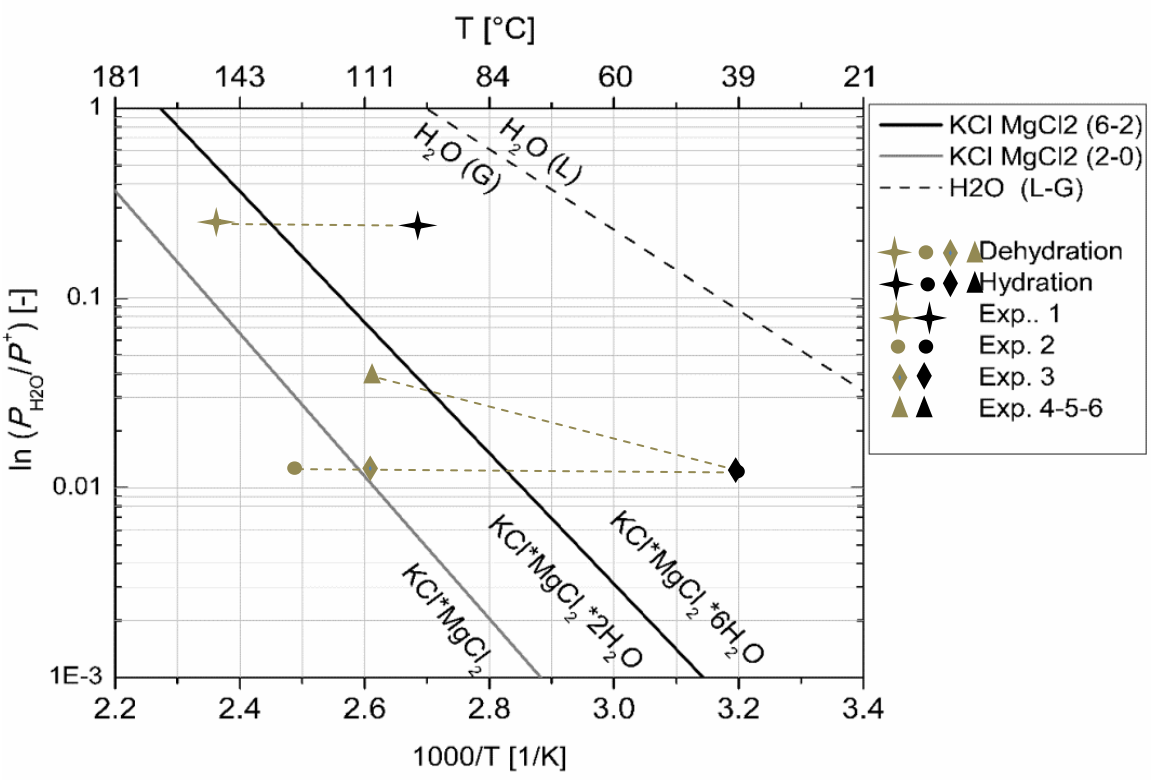

Figure 4: Van't Hoff plot of $KCl{\cdot}MgCl_2{\cdot}6H_2O$ (carnallite). Experimental temperature and humidity programs of hydration and dehydration (dashed line paths delimited by the markers).

-Analysis of products after the cycles

Products obtained from experiments 5 and 6 were analyzed at room temperature using XRD (PANalytical X'Pert Pro MPD, 45kVx40 mA; static air atmosphere, radiation of Cu Kα1 (λ = 1.5418 Å); Scan. Range: 10–80° in 2θ; Step Size: 0.013° and a measuring time of 75 seconds per step) with the objective of identifying the phases of solid products that have been formed during hydrolysis reaction, which explains the material decomposition and the loss of reversibility.

2.4. Energy storage density and energy cost

-Enthalpy of the reaction

The enthalpies of the hydration and dehydration of carnallite-waste were obtained from the differential scanning calorimetric curves (NETZSCH STA 449 F3 Jupiter) using the Software NETZSCH-Proteus –Thermal Analysis which integrates the specific power delivered to the samples (mW/mg) over time. The endothermal and exothermal behaviors were determined based on the tendencies of the DSC signal peaks (upwards or downwards respectively) for 10 reaction cycles.

-Energy storage density

In addition, the amount of energy in Gigajoules (GJ) that can be stored in 1 m^3 (*esd*) was calculated as the product of the dehydration reaction enthalpy and density for the studied salt hydrate.

The density of solid sample was determined pycnometrically [26] at 60 °C with n-dodecane as a displacement liquid and the temperature was controlled with an oven Thermo Scientific, Thermolyne F48020-D8.

-Energy cost

Based on the results of energy storage density for carnallite-waste, the volume (m^3) of material necessary to store 8 GJ of energy needed to cover the heat demand of a passive solar house of 110 m^2 [9,27] was determined and compared with the most promising materials for seasonal heat storage.

3. Results and discussion

3.1. Chemical characterization

-X- ray diffraction

Crystalline phases present in the sample of carnallite-waste were determined using the XRD analysis. Figure 5 shows a XRD pattern with the compounds identified in the waste material: potassium carnallite ($KCl{\cdot}MgCl_2{\cdot}6H_2O$), silvite (KCl), sodium chloride (NaCl) and calcium sulfate ($CaSO_4$), minerals previously identified in the Salar de Atacama [28].

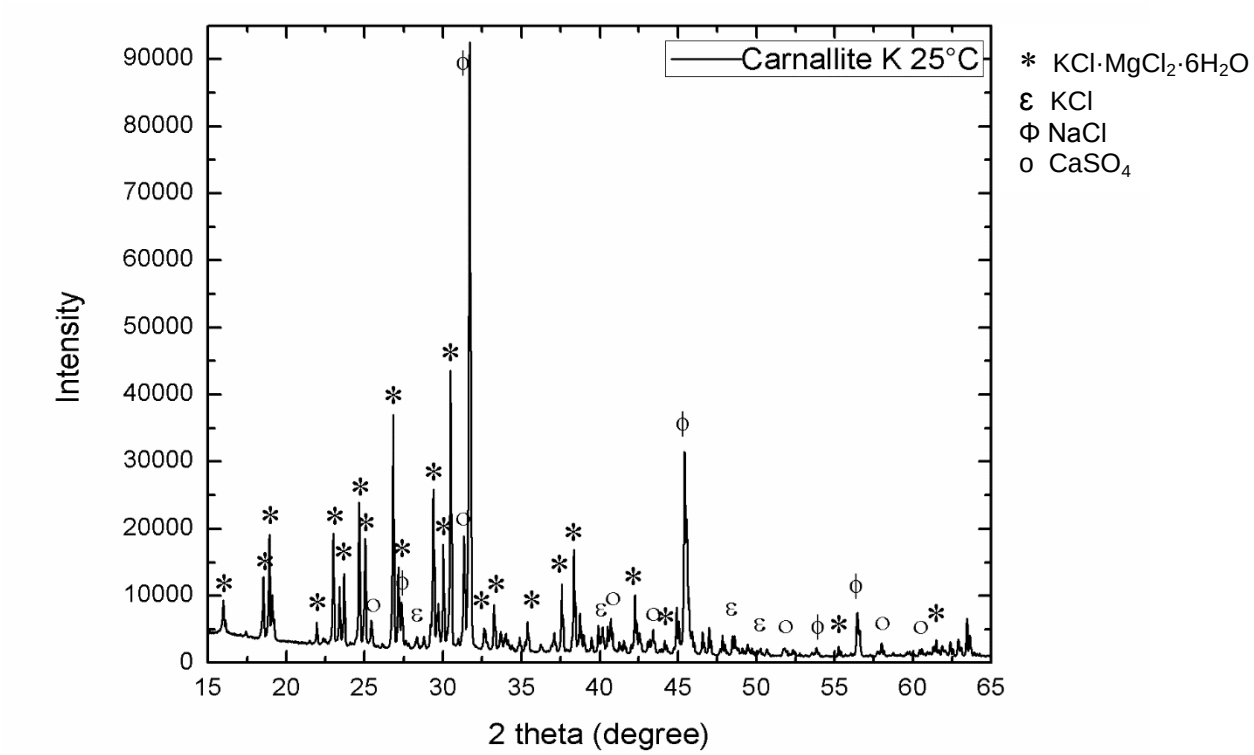

Figure 5: XRD pattern of potassium carnallite waste at 25 °C.

-Chemical analysis

In accordance with the identification of crystalline phases by XRD, an elemental analysis allowed quantifying the concentration of each compound. The chemical elements present in carnallite-waste

are shown in Table 3. It can be seen that the material contains mostly potassium, sodium, magnesium, and chloride. Also, calcium, lithium, and sulfate in smaller quantities.

Table 3: Carnallite-waste chemical analysis.

Elements	**Composition of waste (wt%)**
Lithium, Li	0.14
Sodium, Na	**8.37**
Potassium, K	**10.41**
Magnesium, Mg	**5.94**
Calcium, Ca	0.36
Chloride, Cl	**41.32**
Sulfate, SO_4	1.26
Moisture	0.83
Crystallization water	31.37

The mineralization results are shown in Figure 6 which indicates that potassium carnallite $KCl{\cdot}MgCl_2{\cdot}6H_2O$ (73.54 wt%) is the main component and impurities are sodium chloride (23.04 wt%), calcium sulphate (1.66 wt%) and potassium chloride (1.76 wt%).

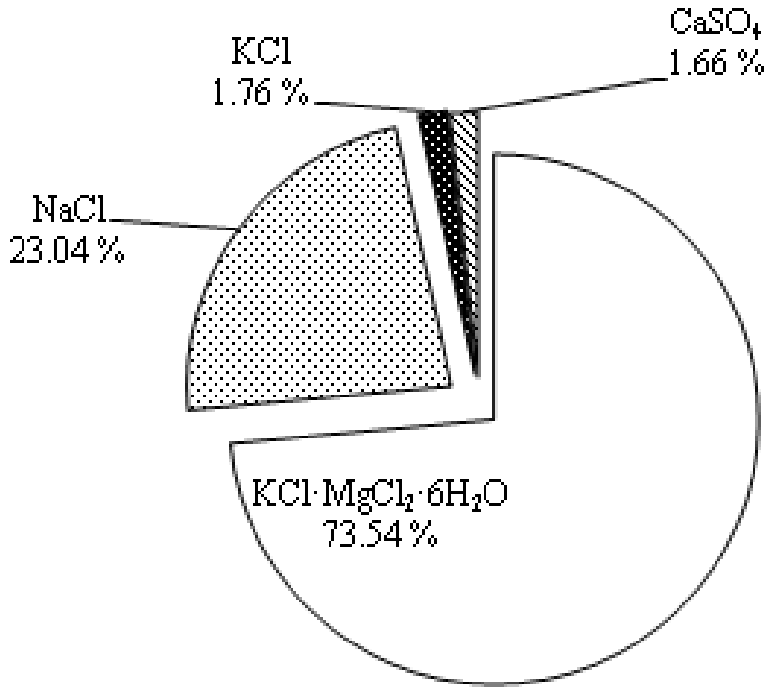

Figure 6: Mineralization of potassium carnallite waste.

The impurities can have a positive or negative effect on the thermal behavior. Previous studies focused on another group of compounds, such as metal hydroxides ($Ca(OH)_2$ and $Mg(OH)_2$), showed that the dehydration temperatures of these materials can be reduced by adding KCl and NaCl in low concentrations (7 wt.%). Furthermore, their thermal decomposition was also reduced [29]. In another study using the mixture of $CaCl_2$ with KCl (2:1), the thermal conductivity, the cyclic stability and the release and capture of water molecules during dehydration and hydration of $CaCl_2$ were improved. It was found that KCl decreases the coalescence and consequently the agglomeration of $CaCl_2$ particles, facilitating the capture and release of water in each reaction [30]. However, a decrease in reaction enthalpy was observed in both studies. Additionally, another single salt widely studied as TCM is $CaSO_4$. This material has hygroscopic properties and is normally found as $CaSO_4 \cdot 0.5H_2O$. Dehydration temperatures of 150 °C and hydration temperatures of 60 and 100 °C have been previously reported as well as problems of agglomeration (reaction shown in eq. 7) [31].

$$CaSO_4\,(s) + 0.5H_2O(g) \leftrightarrow CaSO_4 \cdot 0.5\,H_2O(s) + 16.8\,kJ/mol \qquad \text{(eq.7)}$$

Since potassium carnallite-waste contains NaCl and KCl, they could act as a matrix that reduces particle agglomeration over cycles, thus better reversibility and cyclic stability are expected. Nevertheless, the presence of $CaSO_4$, even in lower concentrations, could increase the agglomeration of carnallite-waste particles. However, if 110 °C temperature is not exceeded, the dehydration reaction of $CaSO_4 \cdot 0.5H_2O$ should not take place.

-Morphology and composition analysis

Morphology of the carnallite-waste particles and the analysis of impurities are shown in Figures 7 and 8.

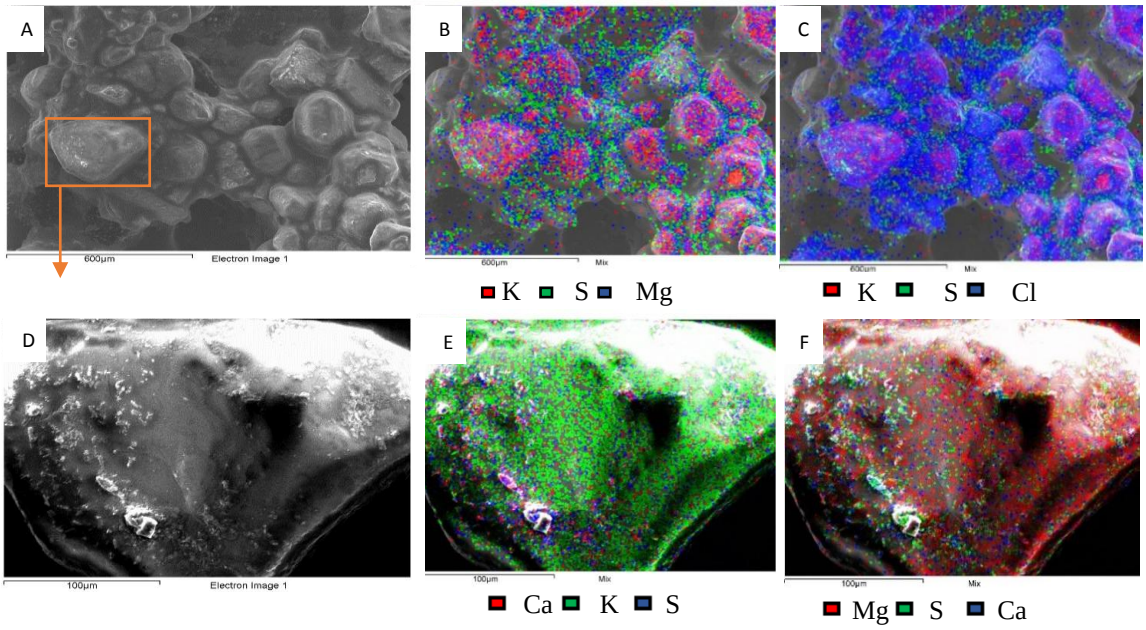

Figure 7: Morphology of carnallite-waste particles using SEM-EDX.

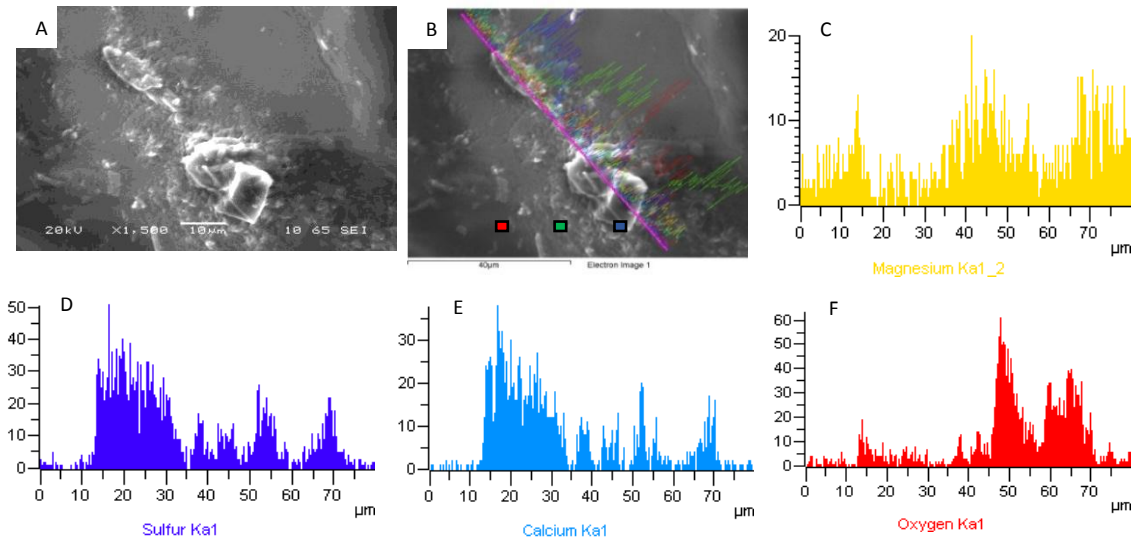

Figure 8: Analysis of impurities adhered to carnallite (see online color version for full interpretation).

Figure 7a (70X magnification) shows the morphology of the carnallite phase, which is not well defined, due to the high hygroscopicity of material. The particle size is less than 500 µm. Figures 7b and c show the presence of Potassium - K (red), Sulfur - S (green), Magnesium - Mg and Chlorine – Cl (Blue) and the interaction of these forming the compound $KCl{\cdot}MgCl_2{\cdot}6H_2O$ (purple). Figures 7d-f (300X magnification), demonstrate a carnallite particle with traces of an impurity containing Ca and S, which would correspond to $CaSO_4$, previously identified by XRD (Figure 6). The analysis at 1500X magnification (Figures 8 a-f) shows the interaction between sulfur (S), calcium (Ca) and oxygen (O) for the formation of $CaSO_4$.

3.2. Dehydration reaction

- Thermal stability

Dehydration of carnallite-waste was studied through the mass loss by increasing the temperature at controlled heating rates of 1 K/min. The results are shown in figure 9, where three steps of dehydration process (endothermic) can be identified. The first is the least sharp among the three steps and corresponds to the evaporation of water adsorbed from the environment (0.13 wt%, below 51 °C). The second step begins at 102.43 °C (ϑ_{onset}) and continues until 136 °C, losing 20.75 wt %,

which corresponds to 4.35 mol of H_2O. Finally, the third step, ranges from 165 °C to 173 °C, losing 9.88 wt% (2.1 mol H_2O).

Between 102 °C and 173 °C the experimental mass loss observed was 30.63 wt%, which exceeds the stoichiometric crystalline water content of the sample (28.73 wt%). This indicates that not only the dehydration reaction took place, but also an irreversible decomposition reaction of the material, e.g. hydrolysis. In other words, HCl was released and a solid products of hydrochloride KMgOHCl and magnesia MgO were formed [20,32]. The energy involved in the second and third dehydration steps were 631.95 kJ/kg and 325.65 kJ/kg, respectively.

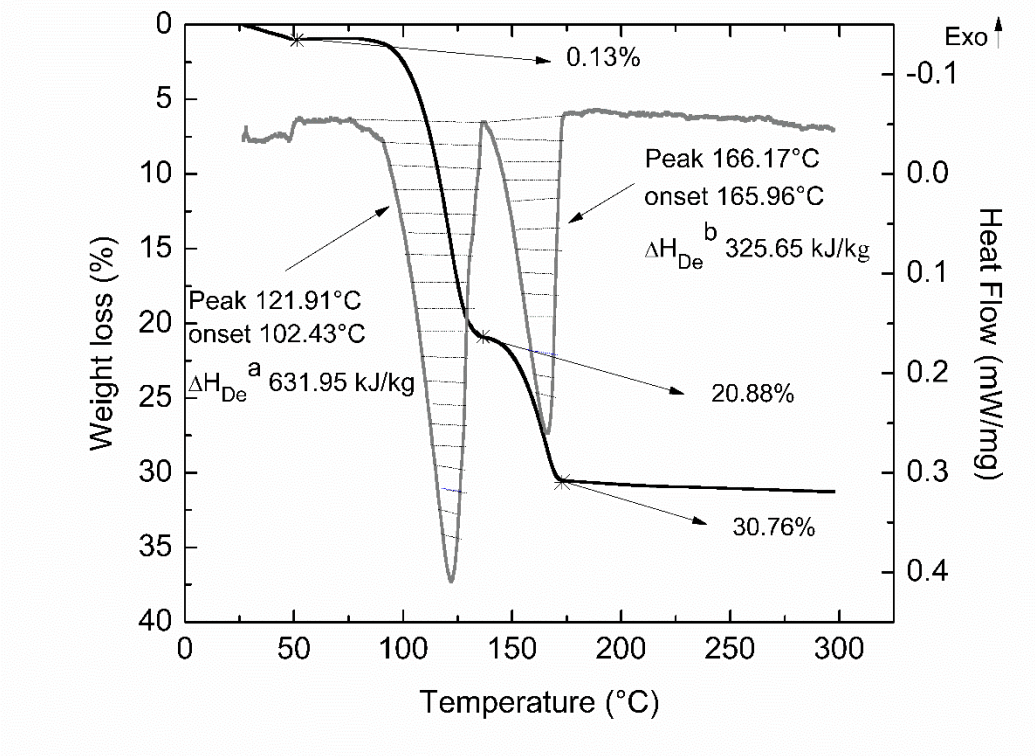

Figure 9: Dehydration of carnallite-waste at 1 K/min using TGA-DSC.

Comparing the results of carnallite-waste mass loss percentages with studies performed using synthetic carnallite [16], it is important to point out that the temperatures of dehydration stages are lower for carnallite waste. It should be noted that lowering dehydration temperature will decrease the energy input of the waste-carnallite system. In addition, the final mass loss observed was 10 wt% lower for carnallite-waste than for synthetic carnallite. These differences are associated with the impurities present in each material, which decrease their purity down to 76.53 wt% and 73.54 wt% for synthetic carnallite and for carnallite-waste, respectively. Synthetic carnallite contains 15.05 wt% of magnesium chloride hexahydrate, which is dehydrated along with synthetic carnallite [16]. In contrast, carnallite-waste contains impurities that are not dehydrated/reactive, so that the mass loss would correspond only to the dehydration of carnallite-waste.

-Determination of gaseous products by thermogravimetric – mass spectroscopy (TG-MS)

The release of HCl indicates the start of hydrolysis reaction (eq.5), which is a disadvantage for a thermochemical material. Gaseous products produced by heating the carnallite-waste to 600 °C were studied by means of TG-MS (Figure 10).

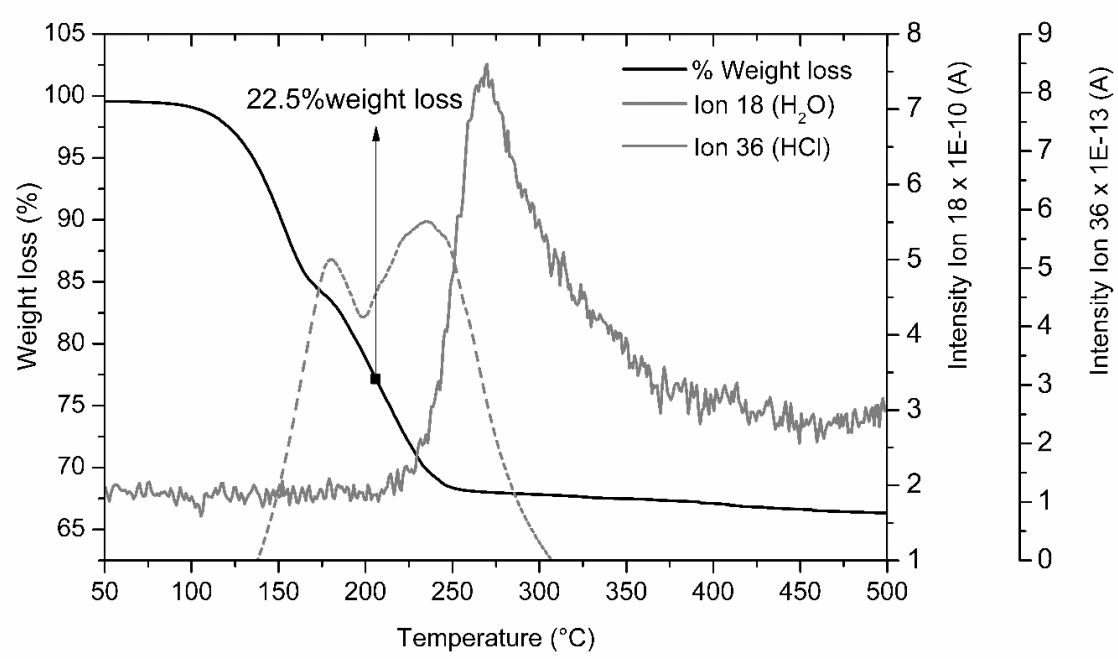

Figure 10: TG-MS curve of thermal decomposition of carnallite-waste.

Figure 10 shows the mass signal of 18 g/mol (dashed line), which confirms the release of water in two dehydration steps in the temperature range of 130 °C to 280 °C. In addition, a weak mass signal of 36 g/mol (gray line) is observed starting at 200 °C, indicating the release of HCl. The release of HCl coincides with the end of the second dehydration step, demonstrating that the hydrolysis reaction occurs together with the dehydration reaction of $KCl{\cdot}MgCl_2{\cdot}2H_2O$, releasing HCl gas as a product. This has been also previously reported by Emons et al. [18,19] and Araten [32]. It was further determined that the hydrolysis reaction begins when the mass loss of carnallite-waste is 22.5 wt%, which corresponds to the loss of the fifth mole of water.

The hydrolysis reaction is detrimental to thermochemical storage applications for various reasons: it reduces the reaction reversibility by breaking down the material gradually during the cycles; it is highly corrosive for metals and toxic for human health. Thus, for carnallite-waste to be suitable as thermochemical storage material, it is necessary to limit its dehydration only until the loss of the fourth mole of water, that is, up to a maximum mass loss of 19 wt%.

- Determination of solid products by HT-XRD

To determine the crystalline phases that are present during the dehydration process of carnallite-waste, the analysis of X-ray diffraction at three different temperatures was carried out. The XRD pattern at 50 °C was used as a reference, that is, before the dehydration beginning. The other two experiments were carried out at 130 °C and 170 °C when the first and the second dehydration steps were completed. The XRD patterns obtained are shown in Figure 11, and the crystalline phases identified are also shown in Table 4.

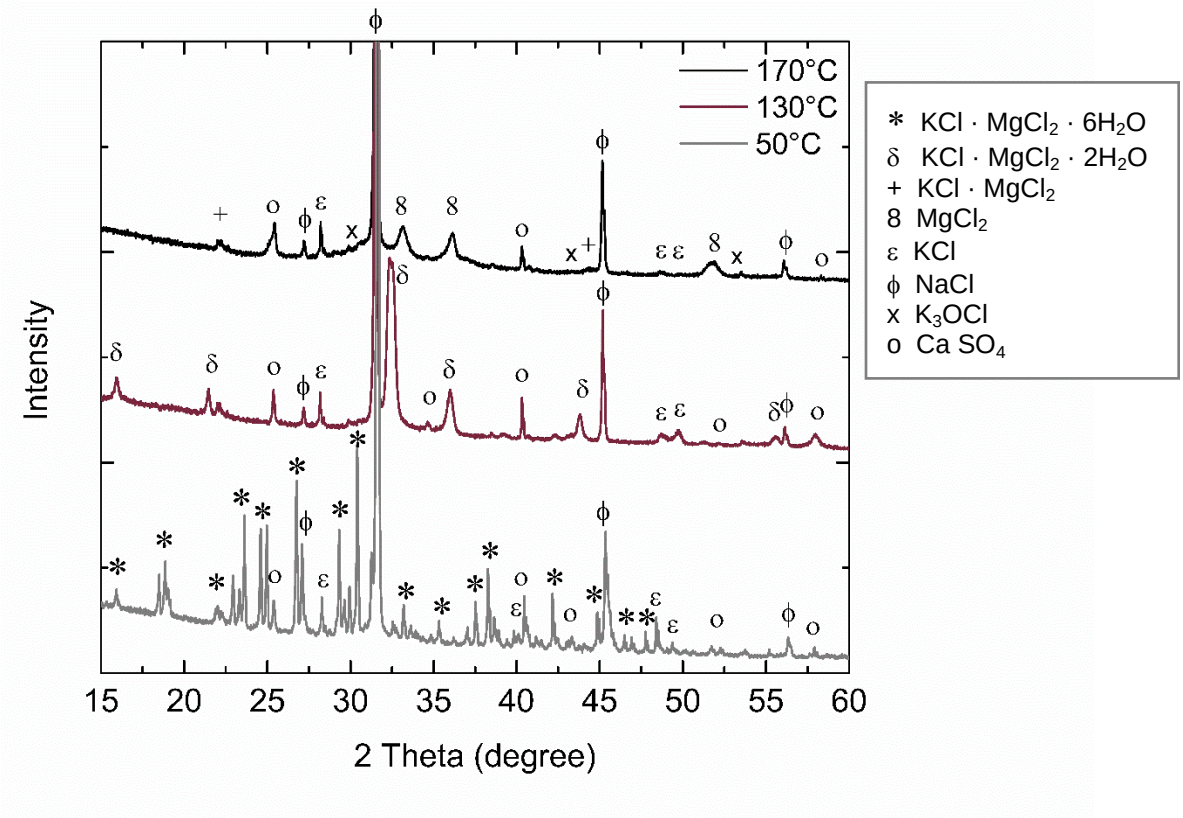

Figure 11: Carnallite diffraction pattern at 50 °C, 130 °C and 170 °C.

Table 4: Identification of products of carnallite-waste thermal decomposition based on XRD.

Solid products of thermal decomposition of carnallite-waste		
50 °C	**130 °C**	**170 °C**
$KCl{\cdot}MgCl_2{\cdot}6H_2O$	$KCl{\cdot}MgCl_2{\cdot}2H_2O$	$KCl{\cdot}MgCl_2$
NaCl	NaCl	NaCl

KCl	KCl	KCl
$CaSO_4$	$CaSO_4$	$CaSO_4$
		$MgCl_2K_3OCl$

According to these results, the first step of dehydration was completed at 130 °C and the main product corresponds to $KCl{\cdot}MgCl_2{\cdot}2H_2O$. This agrees with the results of TG-MS where the loss of approximately 4 moles of water is observed. The absence of hydroxychlorides indicates that the hydrolysis reaction has not occurred. Upon completion of the second dehydration step at 170 °C, potassium carnallite anhydride $KCl{\cdot}MgCl_2$ is identified, indicating the complete dehydration of the salt. This dehydration along with the decomposition of $KCl{\cdot}MgCl_2{\cdot}2H_2O$ in the second step, plus the identification of potassium oxychloride K_3OCl, could indicate that the hydrolysis reaction has occurred between 130 ° C and 170 °C. On the other hand, at 170 ºC $MgCl_2$ is also identified, which denotes that a part of potassium carnallite is possibly dissociated. Also, the appearance of an amorphous phase is observed, which is evidenced by the base line of XRD pattern and the loss of peaks. The impurities of NaCl, KCl and $CaSO_4$ were identified for all studied temperatures.

3.3. Hydration reaction

- *STA–MHG Reversibility of Reaction*

The TG results from Figure 12 show 15 cycles of dehydration/hydration reaction of carnallite-waste (eq. 3), under pressure and temperature conditions close to the theoretical equilibrium (25 kPa and 150 °C - 100 °C). In the first cycle, 22 wt% (4.62 mol H_2O) mass loss and 14 wt% (3.03 mol H_2O) mass gain are observed, which corresponds to 65.5 % of chemical reversibility. However, this chemical reversibility is progressively reduced through the cycles, reaching only 2.8 % at the 15^{th} cycle.

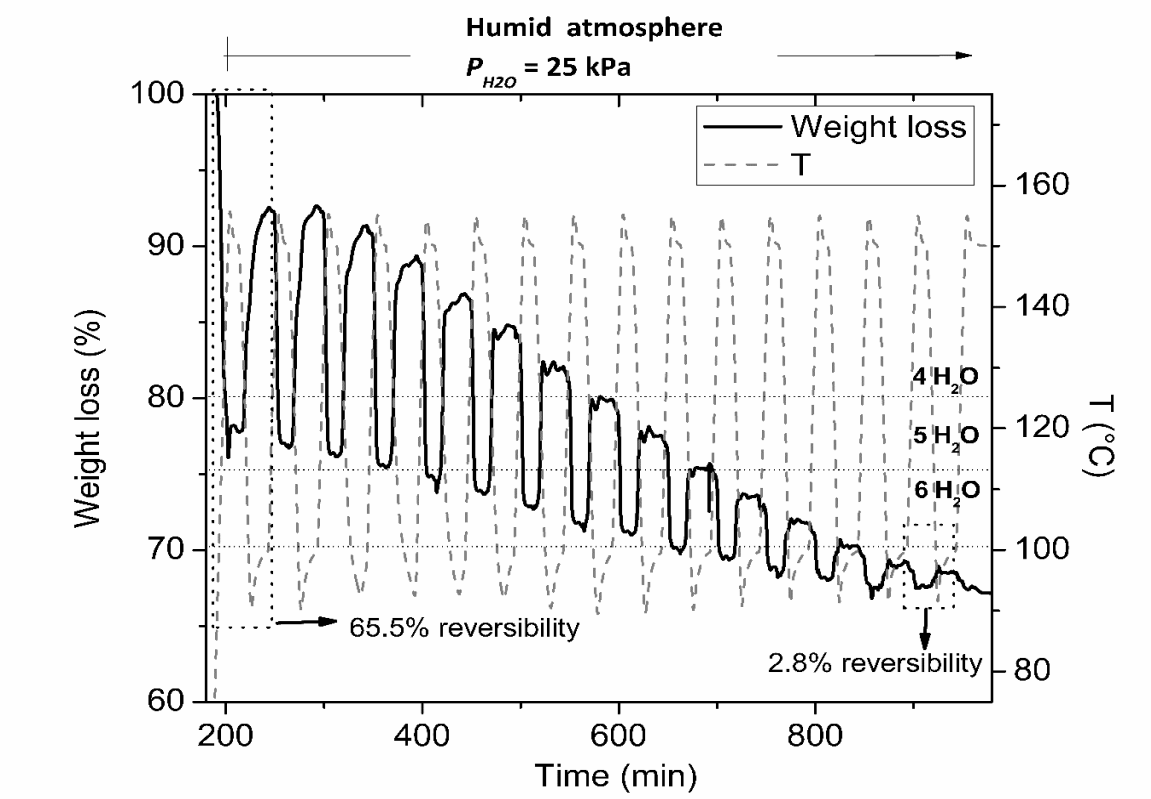

Figure 12: STA-MHG measurement of dehydration/hydration of carnallite waste for 15 cycles, 25 kPa and 150 °C – 100 °C range.

The reduction of the chemical reversibility degree defines a poor cyclic stability of the reaction under the listed conditions, which could be associated with the decomposition of $KCl{\cdot}MgCl_2{\cdot}2H_2O$ during the second dehydration step. This gradual decomposition is identified as a negative slope on the dehydration baseline (Figure 12), in which $KCl{\cdot}MgCl_2{\cdot}6\ H_2O$ loses a larger amount of mass during dehydration than it gains during hydration through the cycles. In other words, during the first dehydration, 22 wt% (4.62 mol H_2O) of mass is lost, this means that the reactions shown in eq. 4 and eq. 5 are partially taking place. Furthermore, in the following cycles the mass loss increases to 31.4 wt%, this exceeds the maximum mass loss possible, where the 2.8 wt% extra mass loss corresponds to gaseous HCl (product of the hydrolysis reaction).

The decomposition of $KCl{\cdot}MgCl_2{\cdot}2H_2O$ increases with each cycle and the concentration of rehydrated $KCl{\cdot}MgCl_2{\cdot}6H_2O$ ("active" material) decreases (see Figure 13). Moreover, the concentration of inactive material increases in the same proportion due to the irreversible decomposition.

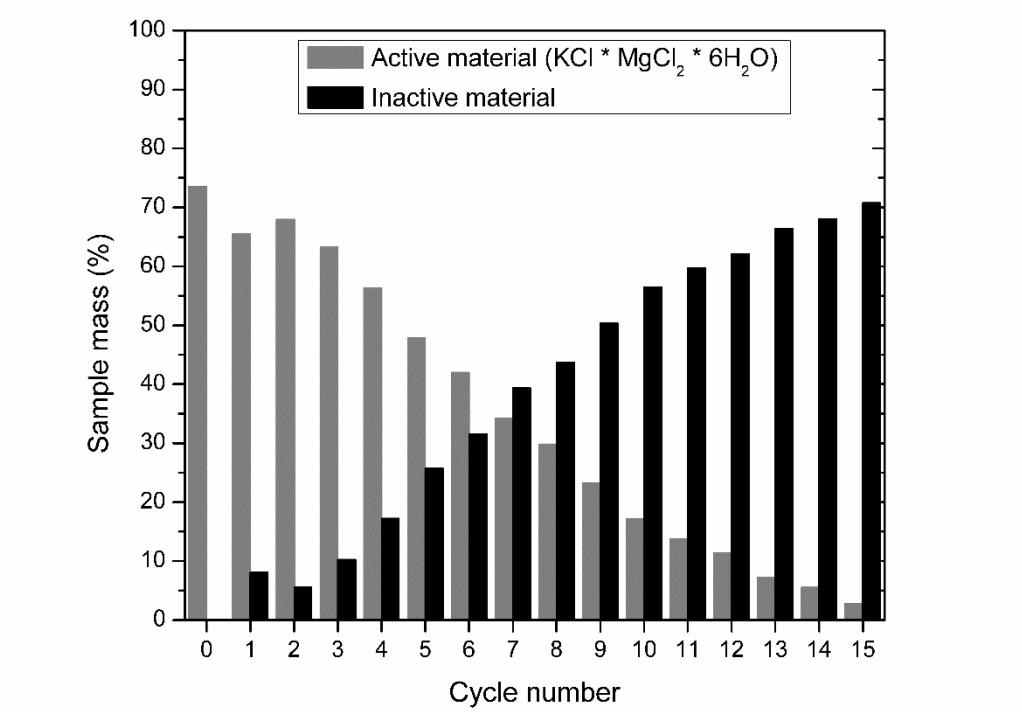

Figure 13: Products of 15 cycles of dehydration and hydration reactions; $KCl{\cdot}MgCl_2{\cdot}6H_2O$ and inactive material.

Comparing carnallite-waste and synthetic carnallite it can be seen that loss of chemical reversibility and decomposition takes place in a greater proportion for carnallite-waste (Figure 14). This could be explained by the presence of different impurities in the composition of both materials [33]. The carnallite-waste impurities cause a faster decomposition at 150 °C than that of synthetic carnallite, as a consequence, the reaction reversibility is reduced through the cycles.

Additionally, the reduction of the chemical reversibility degree could be associated with the agglomeration of the samples. Usually, the salt hydrate particles show agglomeration under high water vapor pressures, decreasing this way a complete chemical conversion of the material through several cycles [30]. However, this aspect must be further investigated on a larger scale than used in this study.

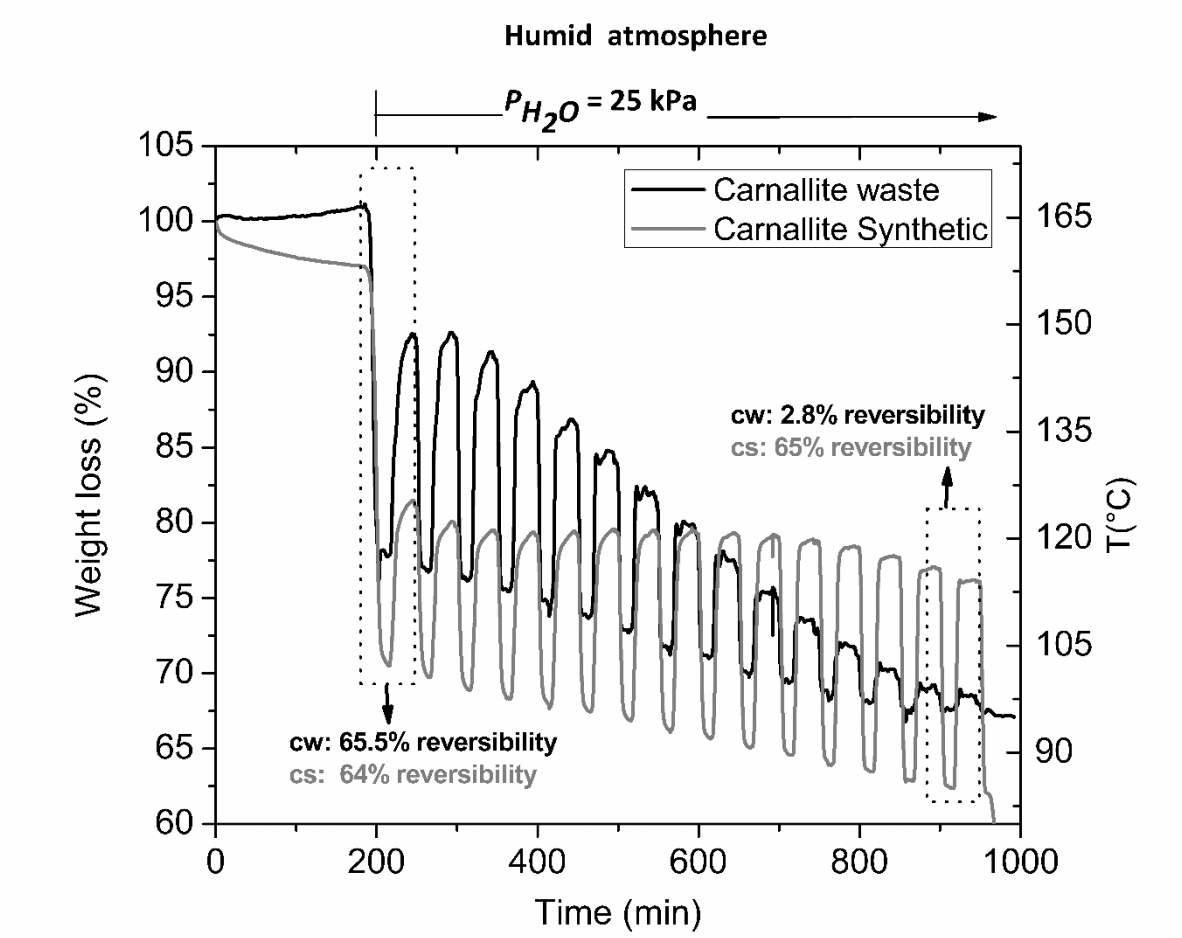

Figure 14: Comparison of dehydration /hydration cycles reaction for synthetic sample [16] and carnallite-waste.

Due to the decomposition of carnallite-waste at high temperatures and partial pressure of water vapor, further experiments were performed reducing the maximum temperatures from 150°C either to 110 °C or to130 °C, and the maximum p_{H2O} from 25 kPa to 4.0 kPa. The hydration was carried out at 40 °C and p_{H2O}= 1.3 kPa (see experiments 2-6, Table 2). The results of experiment 2 (five reaction cycles) are shown in Figure 15. As can be seen, the chemical reversibility of 95 % is achieved in the first cycle, which gradually decreases in the following cycles to 79.4 % (5^{th} cycle). Besides, as expected and according to the van't Hoff plot (Figure 4), the appearance of the second stage of dehydration during the isotherm at 130 °C is observed. This second step reaction gets sharper from the second cycle onwards, indicating that the hydrolysis reaction of $KCl{\cdot}MgCl_2{\cdot}2H_2O$ (eq. 4 and 5) and a progressive decomposition of the sample took place and thus the overall chemical reversibility is reduced. As mentioned before, this can be identified on the negative slope of the baseline of the TG curves.

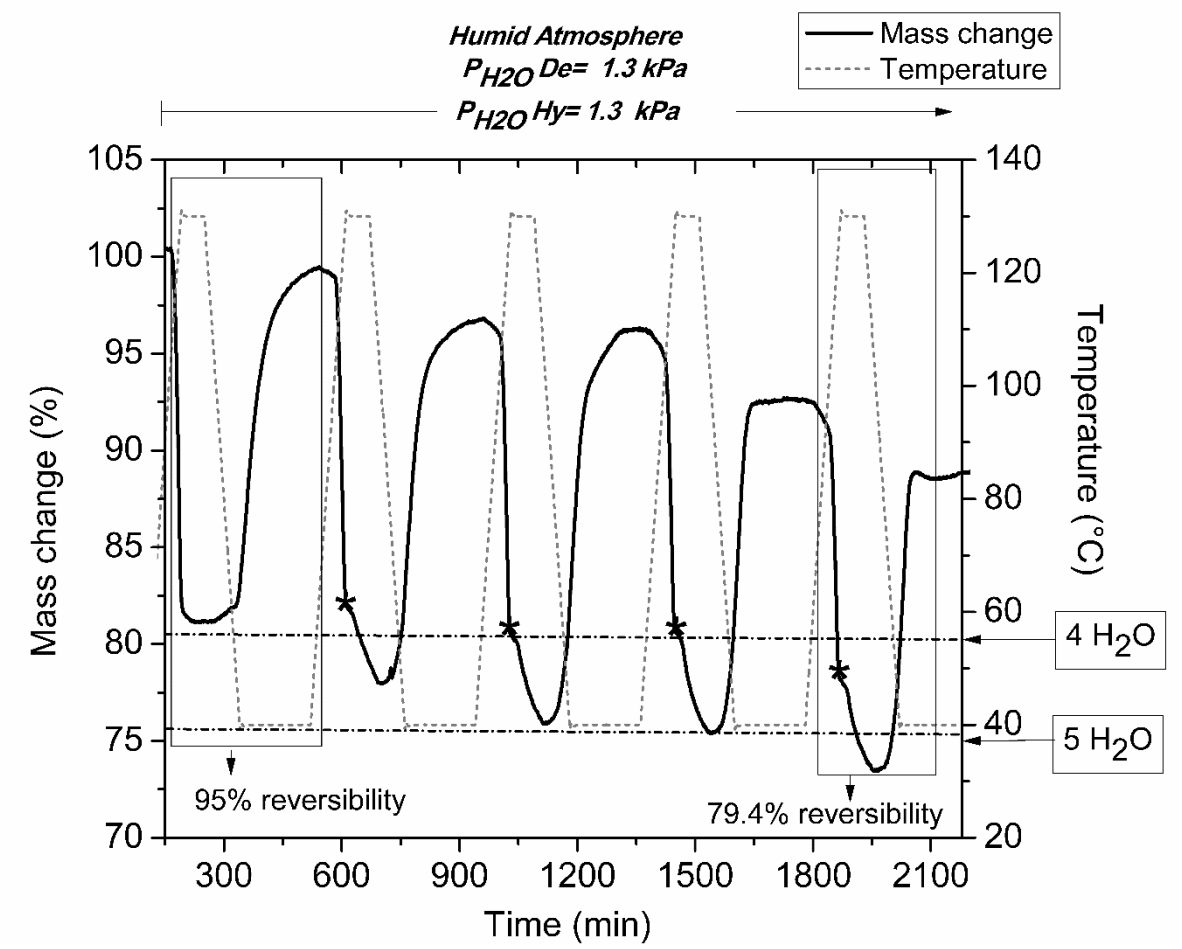

Figure 15: Results of reversibility of carnallite-waste under operating conditions for seasonal heat storage (experiment 2).

Experiment 3 from Table 2 focused on preventing the second dehydration step by decreasing the dehydration temperature from 130 °C to 110 °C, in addition to decreasing the duration time of the isotherm from 30 min to 15 min. Results are shown in Figure 16, demonstrating that the second step of dehydration does not happen. Despite, the chemical conversion of the first cycle is 93.9 %, in the fifth cycle, a reduction of chemical reversibility to 75 % is observed without significant changes in the baseline. Therefore, there is other factor in addition to the temperature that influences the reaction reversibility. Hence, it was decided to reproduce the conditions of seasonal partial pressures in summer (4.0 kPa) and in winter (1.3 kPa) with greater fidelity (experiment 4). The results are shown in Figure 17. Clearly, the reaction reversibility improves in each cycle, the conversion in the first cycle is 89 % and in the fifth cycle is 92.5 %, without significant changes in the baseline that indicate decomposition of the material.

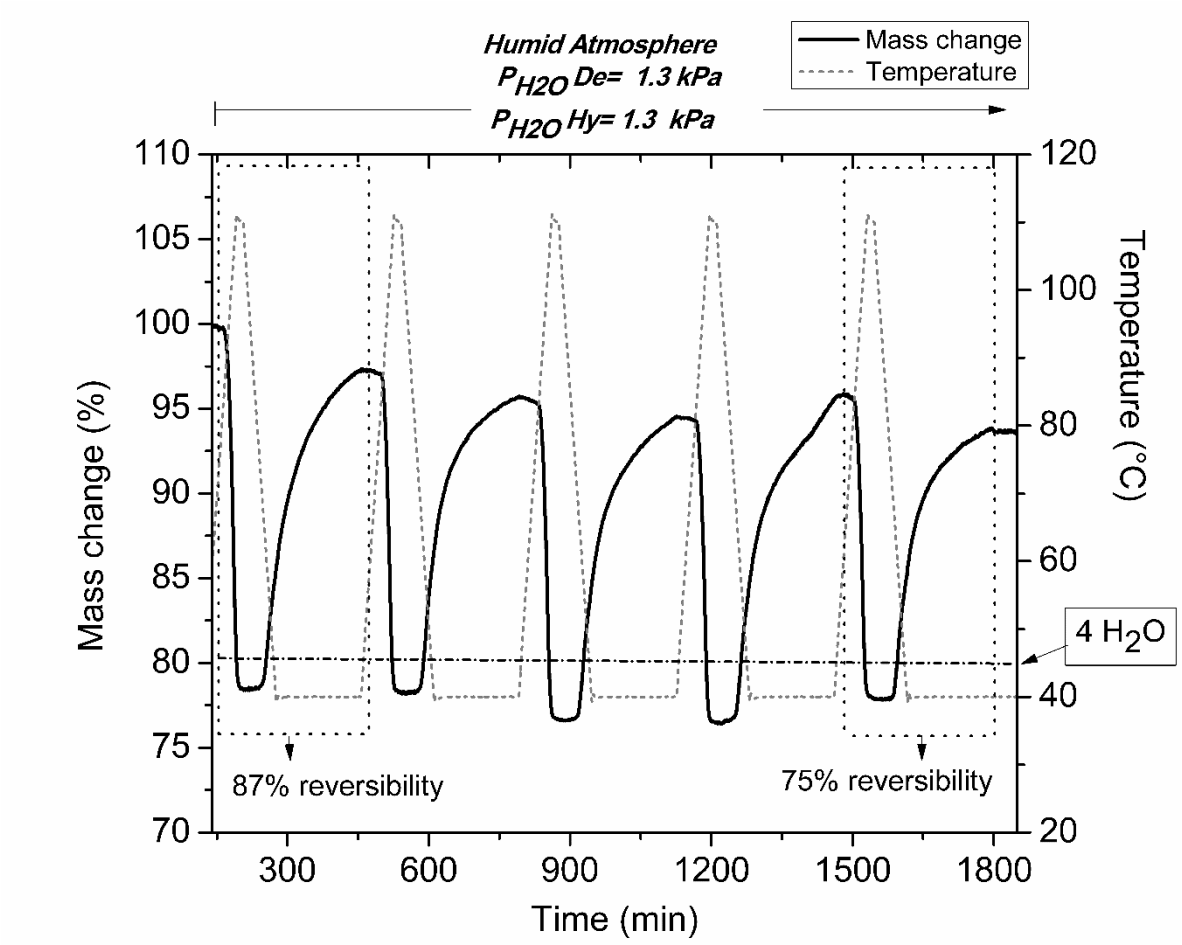

Figure 16: Optimization of the dehydration temperature reaction of carnallite waste under seasonal conditions (Experiment 3).

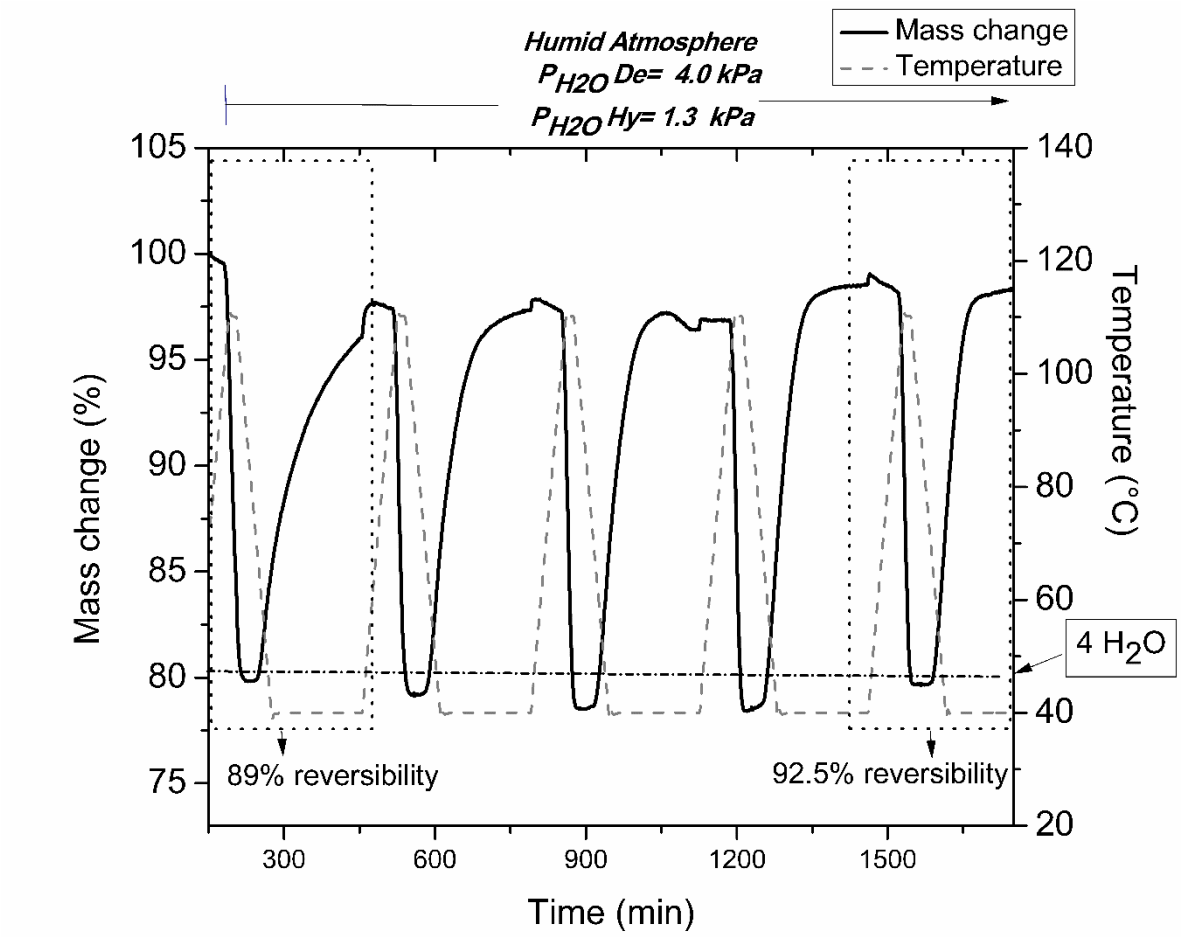

Figure 17: Optimization of dehydration reaction of carnallite waste under seasonal conditions (Experiment 4).

Experiment 5 (see Table 2) was carried out to evaluate cyclic stability for 20 cycles (20 years of seasonal application). Results are shown in Figure 18, where the chemical reversibility is stable in the first five cycles but decreases down to 87 % and 67.1 % after 10 and 20 reaction cycles, respectively. In addition, a negative slope in the baseline is observed, which indicates the possible material decomposition in each cycle. However, under these operating conditions, the mass loss of 19 wt% corresponding to the maximum mass loss of the first step of the reaction, is exceeded only in the last cycle (20.9 wt%). Therefore, the loss of chemical reversibility could not be associated with the decomposition by hydrolysis.

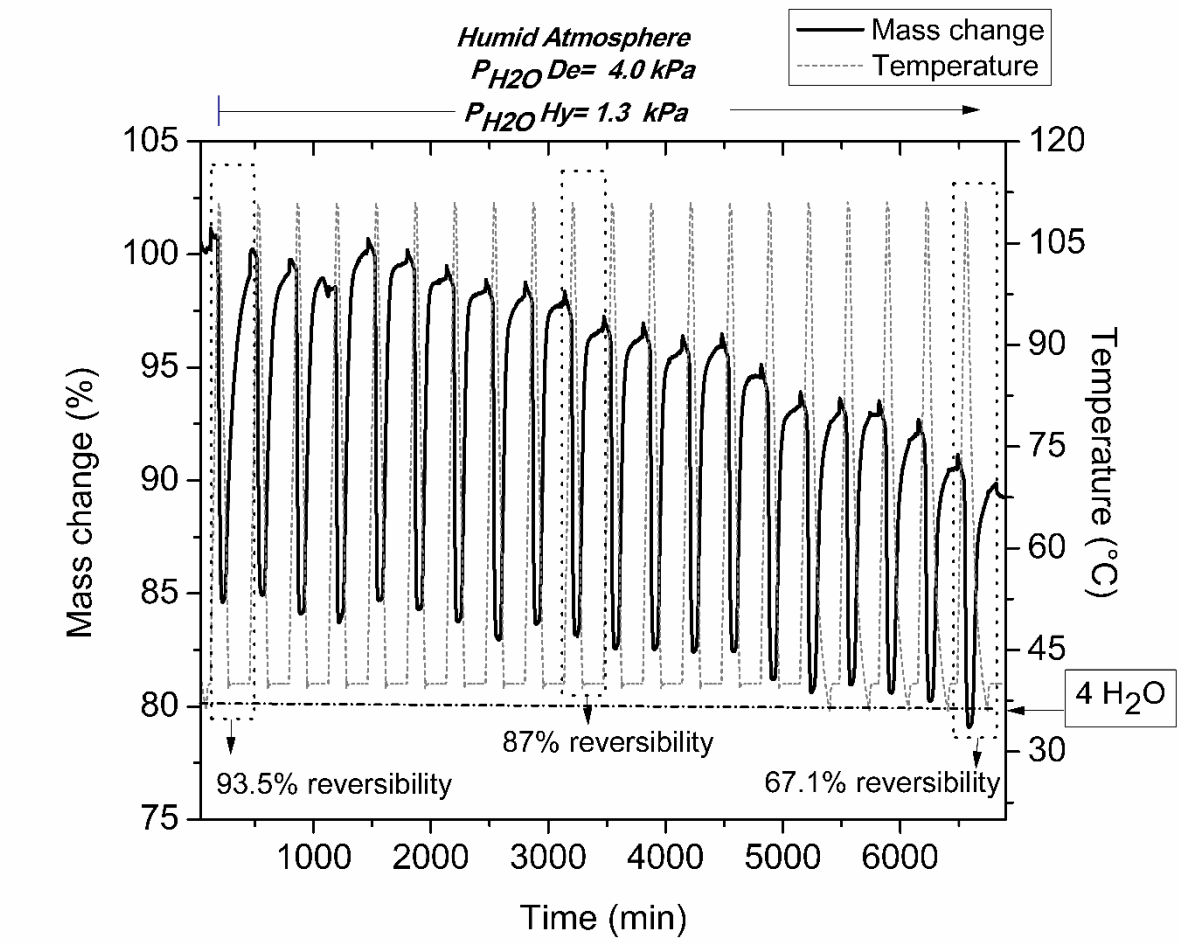

Figure 18: Cycle stability of carnallite waste under seasonal conditions (Experiment 5).

In order to improve the cyclic stability of carnallite-waste, long-term hydration reactions described in Table 2 were carried out (experiment 6). In this case, the pressure and temperature conditions of experiment 5 were maintained, but the water vapor partial pressure change was increased during dehydration at rates of 57 Pa/min and 39 Pa/min, for the first cycle and from the second cycle onwards, respectively. Furthermore, the hydration isothermal duration was doubled from 180 to 360 minutes to reach the equilibrium during the hydration step in all cycles. Under these conditions, the results showed (see Figure 19) a more stable behavior through the cycles. Furthermore, a greater mass loss is observed during dehydration steps and, a greater mass gain is reached during hydration in each cycle, achieving a conversion of 87.2 % in the tenth cycle. However, this conversion degree does not differ from the result obtained in the tenth cycle for the material under the conditions of experiment 5 (87 % in the tenth cycle). Therefore, the decrease of chemical reversibility under seasonal dehydration (ϑ_{De} = 110 °C and $p_{H2O,\ De}$ = 4.0 kPa) and hydration conditions (ϑ_{Hy} = 40 °C and $p_{H2O,\ Hy}$ = 1.3 kPa) is not attributed to changes in the operational parameters of temperature and pressure. Finally, it is necessary to highlight the hydration temperature (ϑ_{Hy}) is close to 40 °C. This value is suitable for seasonal heat applications, in which the heating of houses and water for domestic use is required [34].

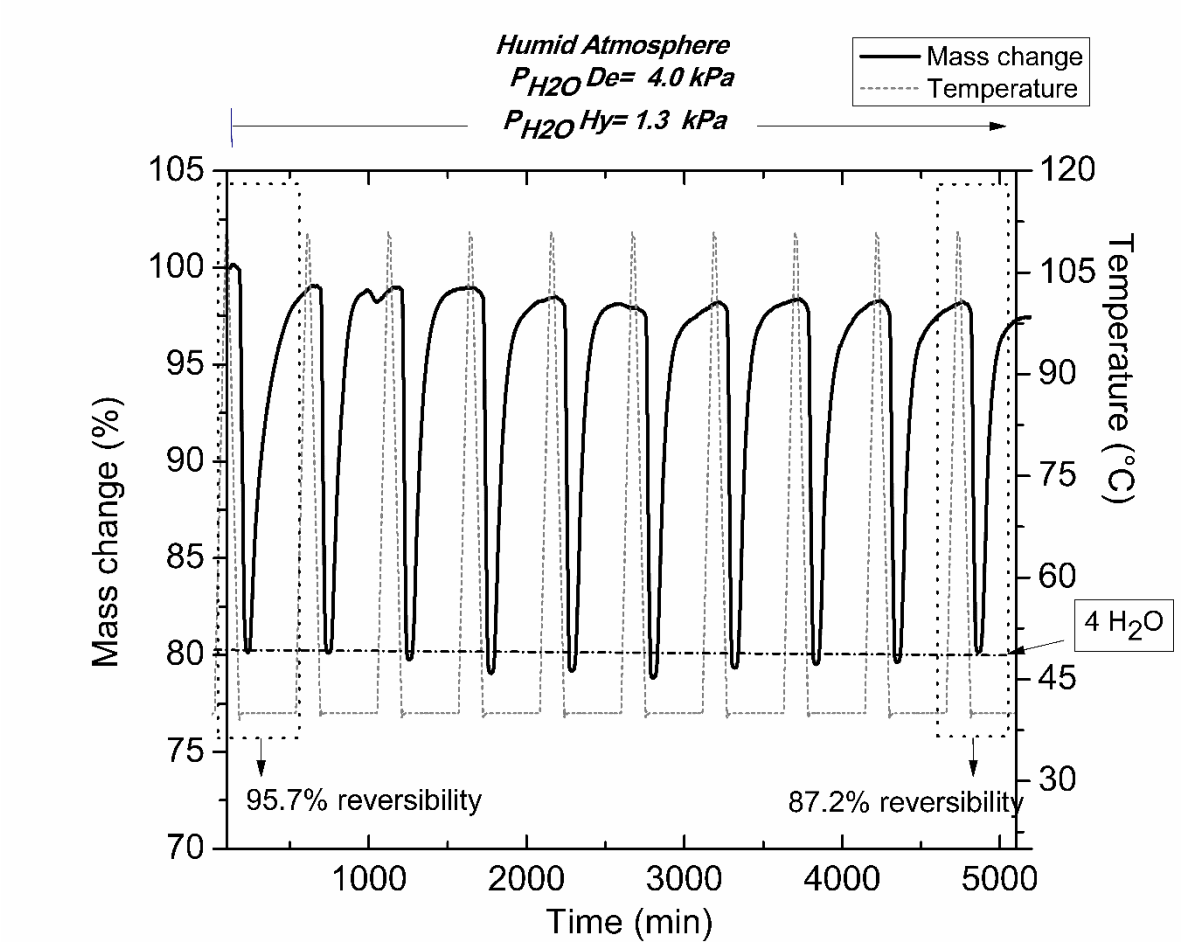

Figure 19: Dehydration/hydration of carnallite waste for 10 cycles at long time (6 hours) of hydration (Experiment 6).

-XRD of the products of 10 and 20 reaction cycles

To discard the material decomposition after 10 and 20 cycles (experiments 5 and 6), the products of these experiments were analyzed by XRD. The results are shown in Figure 20, where crystalline phases corresponding to hydrolysis products were not identified. Therefore, the material decomposition by hydrolysis reaction cannot be detected with the methods used in this study. Moreover, the XRD pattern of 20 cycles-product showed less intense peaks than those of 10 cycles-product, meaning the loss of crystallinity of carnallite-waste through the cycles. As a consequence, not only the sample reactivity drops progressively but also the complexity of the material increases. In other words, the cycles of dehydration-hydration could result in a physical change of the sample, from a crystalline solid into a semi-crystalline or amorphous solid [35], i.e. the incorporation of water molecules during hydration would decrease, as agglomeration increases and therefore the particle sizes, making more difficult the diffusivity of water vapor through the sample.

Agglomeration due to the loss of crystallinity of hydrated materials is an important aspect to consider during the scale-up process. Not only because this issue could increase with the increase of the sample scale, but also because it could jeopardize the potential use of salt hydrates for TCS systems. Still, proposing the use of industrial waste remains as a great advantage, as the material costs practically do not have a significant influence on the total investment cost of the system, giving the possibility of replacing the medium of storage every 10 cycles (10 years).

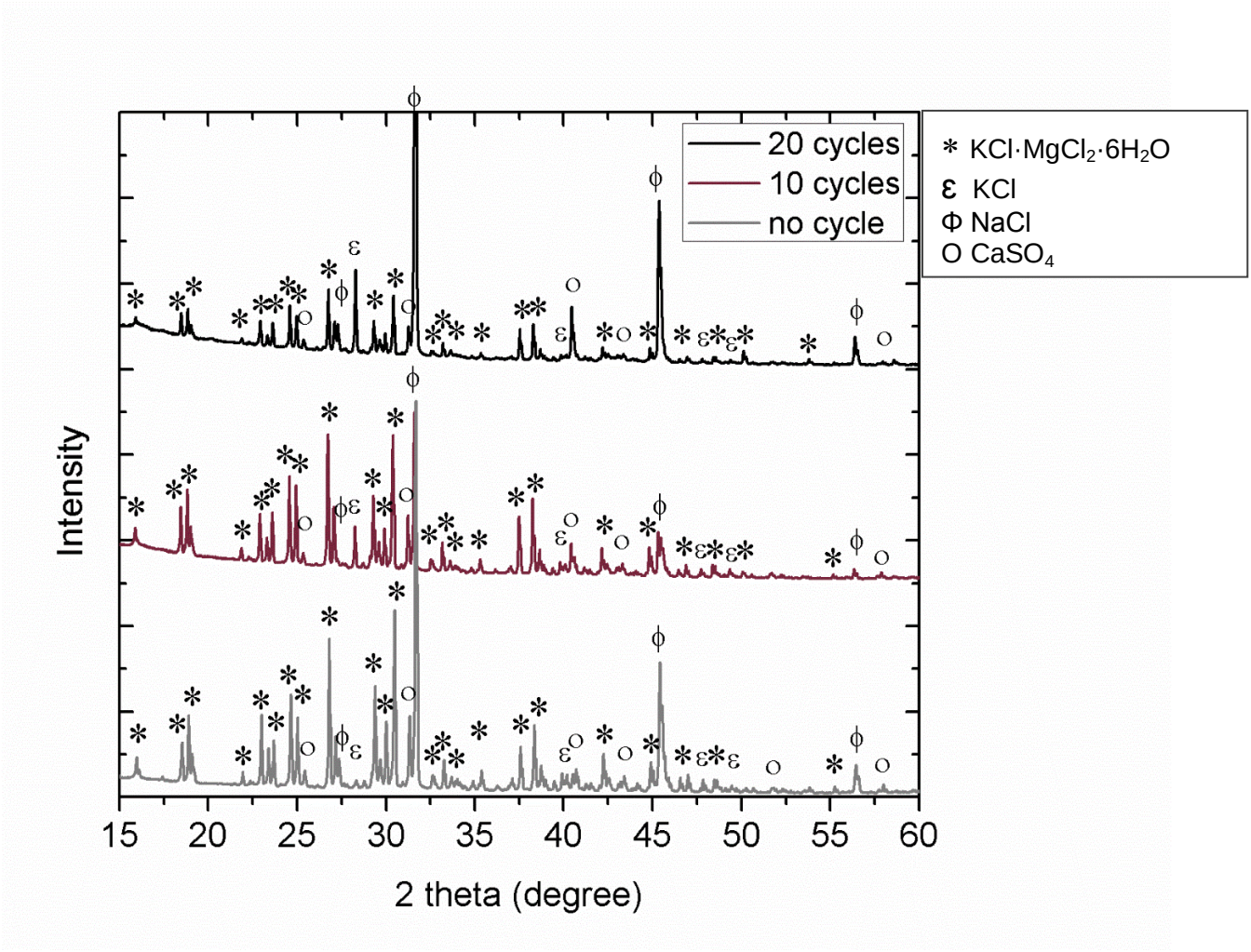

Figure 20: Potassium carnallite XRD pattern before cycling and after 10, 20 cycles at room temperature.

4. Potential application of carnallite-waste material

4.1 Evaluation of energy storage density

According to literature [36], a TCM should have energy storage density (*esd*) equal to or greater than 1.3 GJ/m^3 to be considered suitable for seasonal heat storage applications at temperatures below 120 °C. In order to establish the potential of carnallite, the *esd* was calculated for each cycle, based on reaction enthalpy changes (ΔH) (see Figure 21) and the density (1.7103 kg/m^3 at 28.8 °C), and summarized in Table 5.

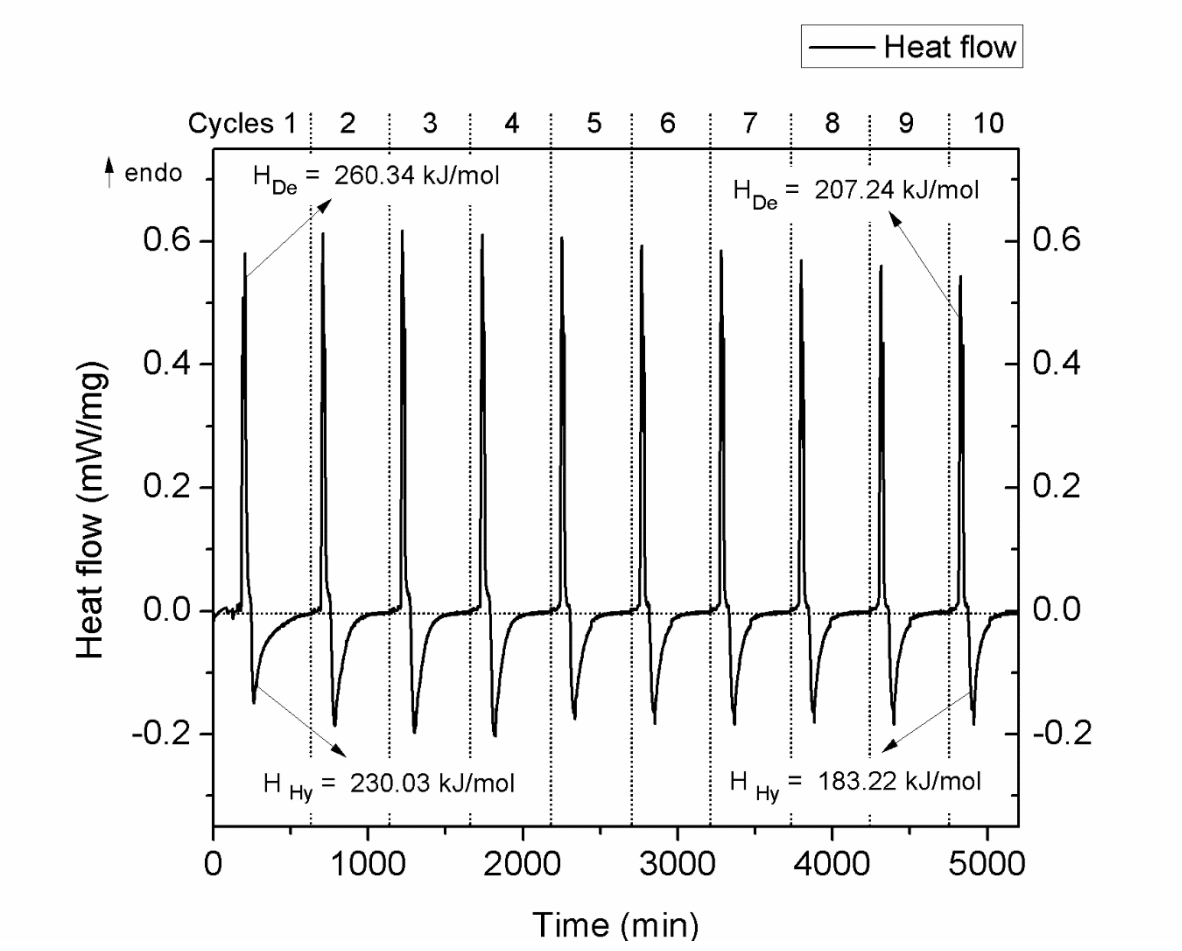

Figure 21: Enthalpies of dehydration/ hydration from experiment 6.

Table 5: Energy storage density estimated for dynamic dehydration of potassium carnallite.

PM:277.6 g/mol		ρ[28.8 °C]=1.7103 [kg/m^3]		
Cycle	**ΔH_{De} [kJ/mol H_2O]**	***esd*$_{De}$ [GJ/m^3]**	**ΔH_{Hy} [kJ/mol H_2O]**	***esd*$_{Hy}$ [GJ/m^3]**
1	59.85	1.604	52.88	1.417
2	57.03	1.528	52.73	1.413
3	58.35	1.564	54.20	1.453
4	56.10	1.504	52.76	1.414
5	49.89	1.337	46.40	1.243
6	48.84	1.309	44.85	1.202
7	48.48	1.299	45.16	1.210
8	48.24	1.293	41.57	1.114
9	47.77	1.280	42.04	1.127
10	47.64	1.277	42.12	1.129

It can be seen in Table 5, that the esd_{Hy} of carnallite-waste in the first four cycles is close to 1.4 GJ/m^3 and is larger than those reported in scientific papers [36]. Also, it can be observed that from the fifth cycle onwards the esd_{Hy} decreases to 1.129 GJ/m^3 in cycle 10 because decreasing of the chemical reversibility of the sample (see Figure 19).

In this way, in a practical application, carnallite storage material must be replaced every 10 years. It should be mentioned that this would not increase the investment costs significantly, since carnallite-waste is a natural waste without any commercial cost nor environmental impact.

4.2 Evaluation of potential for seasonal heat storage applications

The esd_{Hy} and the price per mega Joule of energy stored of carnallite-waste were compared among salt hydrates that have been previously reported as promising for seasonal heat storage applications (Table 6). The esd_{Hy} of carnallite-waste corresponds to the calculated at the tenth cycle (1.129 GJ/m^3). The values of esd_{Hy} were directly correlated with the material volume needed to store 8 GJ of energy, considered as the required energy capacity to supply the heat demands of a common house during the six months of cold seasons [9,36]. Even though the largest storage volume corresponds to carnallite-waste, the material costs, practically "0", leads to a storage material price of 0 €/MJ. Therefore, the use of this waste material improves the potential of developing sustainable technologies to store/generate heat.

Table 6. Comparison of *esd* and energy cost for waste sample of potassium carnallite and most promising TCM, candidates for seasonal heat storage [32].

Materials	Highest and lowest hydrate	N° H_2O moles in reaction	$_{Hy}$ *esd* (GJ/m^3) open system	Volume material (m^3) for 8 GJ	Price (€/MJ)
***KCl·MgCl$_2$ (waste)**	6 – 2	4.36	1.129	7.1	0
$MgCl_2$	6 – 2	3	1.93	4.1	0.14
LiCl	1 – 0	1	2.08	3.8	35.53
K_2CO_3	1.5 – 0	1.5	1.30	6.2	1.67
$CuCl_2$	2 – 0	2	1.74	4.6	4.33

*Experimental result after 10 cycles reactions.

4. Conclusions

Overall, the chemical characterization of carnallite-waste, determined its composition as 73.5 wt% of $KCl{\cdot}MgCl_2{\cdot}6H_2O$, mixed with the main impurity of 23.04 wt% NaCl. This material, in the operating conditions close to equilibrium (at p_{H2O} =25 kPa), showed lower cyclic stability compared to the synthetic material. As a result, lower reversibility of rehydration is observed in each cycle. To improve the cyclic stability of carnallite-waste, the operating conditions of dehydration were experimentally optimized to 110 °C, p_{H2O} = 4.0 kPa and the operating conditions of hydration to 40 °C and p_{H2O} =1.3 kPa. Thereby, greater reaction reversibility in each cycle and no sign of material decomposition by hydrolysis were achieved. During the thermodynamic characterization of the reactive system and following the van't Hoff plot, a temperature decrease of 20K and the increase of the water vapor pressure of dehydration prevented the material from decomposing by hydrolysis reaction. Likewise, an increase of the hydration isothermal time allowed to attain reversibility loss of only 8.5 % during ten cycles (10 years of application). This reversibility loss is associated with the loss of the material crystalline structure when subjected to constant hydration cycles, allowing the agglomeration of particles. Hereby it can be stated that the partial loss of reversibility of hydration of this carnallite-waste is produced due to the decomposition through hydrolysis, loss of crystalline structure and agglomeration of the particles when cycled more than 5 times.

However, after ten cycles the loss of reversibility is still low enough not to compromise its potential application in seasonal heat storage. In addition, the energy storage density determined during the tenth hydration cycle was 1.129 GJ/m^3, a value that is comparable and competitive with materials such as K_2CO_3 and $MgCl_2$, reported as promising for seasonal thermochemical storage applications.

Finally, it is important to note that this is a waste material, so it has no commercial value and its use contributes to the reuse of industrial waste for sustainable applications.

5. Declaration of interest: none

6. Acknowledgments

Verónica Mamani thanks CONICYT for her doctorate scholarship CONICYT No. 21150145, Svetlana Ushak thanks financial support of CONICYT/FONDAP Nº 15110019 SERC-Chile,

CONICYT/PCI/REDES N°170131 and CONICYT/FONDECYT REGULAR N° 1170675 projects. Andrea Gutierrez would like to thank DAAD for her DLR/DAAD Postdoctoral fellowship. University of Barcelona and Diopma group thank the funding by the Spanish Government (RTI2018-093849-B-C32), and the Catalan Government for the quality accreditation (2017 SGR 118).

7. References

[1] Kalaiselvan and Parameshwaran, Energy and energy management, Thermal Energy Storage Technologies for Sustainability 2014; Chapter 1: 1-19.

[2] BP Statistical Review of World Energy; 2015. bp.com/statistical review (accessed on May 2016).

[3] P. Pardo, A. Deydiera, Z. Anxionnaz-Minvielle, S. Rougé, M.Cabassud, P.Cognet. A review on high temperature thermochemical heat energy storage. Renewable and Sustainable Energy Reviews 2014; 32:591–610.

[4] N'T soukpoe KE, Liu H, Le Pierrès N, Luo L. A review on long-term sorption solar energy storage. Renewable Sustainable Energy Rev 2009; 13:2385–96.

[5] Juan Wu, Xin feng Long, Research progress of solar thermochemical energy storage, Int. J. Energy Res. 2015; 39: 869–888.

[6] T. Yan, R. Z. Wang, T. X. Li, L.W. Wang, Ishugah T. Fred, A review of promising candidate reactions for chemical heat storage, Renewable and Sustainable Energy Reviews 2015; 43:13–31.

[7] Kokouvi Edem N'Tsoukpoe, Thomas Schmidt, Holger Urs Rammelberg, Beatriz Amanda Watts, Wolfgang K.L. Ruck. A systematic multi-step creening of numerous salt hydrates for low temperature thermochemical energy storage. Applied Energy 2014; 124: 1–16.

[8] Claire J. Ferchaud, Robbert A.A. Scherpenborg, Herbert A. Zondag and Robert de Boer. Thermochemical seasonal solar heat storage in salt hydrates for residential applications - Influence of the water vapor pressure on the desorption kinetics of MgSO4.7H2O. Energy Procedia 2014; 57: 2436 – 2440.

[9] C.J. Ferchaud, H.A. Zondag, A. Rubino, R. de Boer. Seasonal Sorption Heat Storage – Research on Thermochemical Materials and Storage Performance. ECN-M--12-070 Conference 2012.

[10]Devrim Aydin, Sean P. Casey, Saffa Riffat. The latest advancements on thermochemical heat storage systems. Renewable and Sustainable Energy Reviews 2015; 41: 356–367.

[11] Gutierrez Andrea, Miró Laia, Gil Antoni, Rodríguez-Aseguinolaza Javier, Barreneche Camila. Advances in the valorization of waste and by-product materials as thermal energy storage (TES) materials. Renewable and Sustainable Energy Reviews 2016; 59: 763–783.

[12] Miró L, Navarro ME, Suresh P, Gil A, Fernández AI, Cabeza LF. Experimental characterization of a solid industrial by-product as material for high temperature sensible thermal energy storage (TES). Appl Energy 2014; 113:1261–8.

[13] Svetlana Ushak, Andrea Gutierrez, Hector Galleguillos, Angel G. Fernandez, Luisa F. Cabeza, Mario Grágeda. Thermophysical characterization of a by-product from the non-metallic industry as inorganic PCM Solar Energy Materials & Solar Cells 2015; 132: 385 –391.

[14] V. Mamani, A. Gutiérrez, S. Ushak. Development of low-cost inorganic salt hydrate as a thermochemical energy storage material. Solar Energy Materials and Solar Cells 2018; 176: 346–356.

[15] Andrea Gutierrez, Svetlana Ushak, Veronica Mamani, Pedro Vargas, Camila Barreneche, Luisa F. Cabeza, Mario Grágeda, Characterization of wastes based on inorganic double salt

hydrates as potential thermal energy storage materials, Sol. Energy Mater. Sol. Cells 2017;170:149-159.
[16] Andrea Gutierrez, Svetlana Ushak, Marc Linder. High Carnallite-Bearing Material for Thermochemical Energy Storage: Thermophysical Characterization. *ACS Sustainable Chem. Eng.*, 2018; 6 (5): 6135–6145.
[17] S. Ushak, A. Gutierrez, E. Flores, H. Galleguillos, M.Grageda., Development of Thermal Energy Storage Materials from Waste-Process Salts. Energy Procedia 2014; 57: 627-632.
[18] H.-H. Emons. Mechanism and kinetics of formation and decomposition of carnallitic double salts. Journal of Thermal Analysis 1988; 33: 113-120
[19] Emons, H.-H.; Naumann, R.; Pohl, T.; Voigt, H. Thermoanalytical investigations on the decomposition of double salts: I. the decomposition of carnallite. J. Therm. Anal. 574 Calorim. 1984; 29: 571-579.
[20] H.-H. Emons and Th. Fanghiinel. Thermal decomposition of carnallite ($KCl.MgCl_2 .6H_2O$)-comparison of experimental results and phase equilibria. Journal of Thermal Analysis. 1989; 35: 2161-2167.
[21] Boletín informativo del ministerio de energía, http://www.energia.gob.cl/energias-renovables (2016).
[22] Los hitos del 2014, ELECTRICIDAD, La revista energética de Chile, (2015).
[23] Korotkov, J. A.; Mikhkailov, E. F.; Andreevm, G. A.; Eltsov, B. I.; Plyakov, J. A.; Shestakov, B. G.; Kechina, G. D. Method of dehydrating carnallite. United States Patent Nr. 4,224,291, 1980.
[24] Meir Elam, Sara Ben-Ari, Nestor Leiderman. Carnallite having reduced moisture absorption and method of producing it. Patent WO2001083401A1 (2001).
[25] Bushra Khalid. Effect of Temperature and Humidity on Salt Mine Environment. Pakistan Journal of Meteorology 2010; 7:1-13.
[26] A. Minevich, Y. Marcus, L. Ben-Dor,] Densities of solid and molten salts hydrates and their mixtures and viscosities of the molten salts, Journal of Chemical & Engineering Data 2004; 48: 1451-1455.
[27] Nathaly Romero. Engineer undergraduate thesis, avalaible in spanish: Consumo de energía a nivel residencial en Chile y análisis de eficiencia energética en calefacción. Memoria de ingeniero civil. Universidad de Chile, 2011.
[28] Pedro Pavlovic. The industry of lithium in Chile. Available in spanish in journal: Ingenieros, Revista de Colegio de Ingenieros en Chile, 2014, 02: 30-35
[29] Shkatulov, Alexandr Aristov, Yuri. Modification of magnesium and calcium hydroxides with salts: An efficient way to advanced materials for storage of middle temperature heat. Energy 2015; 85: 667-676.
[30] Korhammer Kathrin, Druske Mona Maria, Fopah-Lele Armand, Rammelberg Holger Urs, Wegscheider Nina, Opel Oliver Thomas Osterland, Wolfgang Ruck. Sorption and thermal characterization of composite materials based on chlorides for thermal energy storage. Applied Energy 2016; 162: 1462–1472.
[31] Hongyu Huang, Jun Li, Huhetaoli, Yugo Osaka, Chenguang Wang, Noriyuki Kobayashi, Zhaohong He, and Lisheng Deng. Porous-Resin-Supported Calcium Sulfate Materials for Thermal Energy Storage. Energy Technol. 2016; 4: 1401 – 1408.

[32] Araten, David Ashboren. Carnallite Decomposition into Magnesia, Hydrochloric Acid and Potassium Chloride: A 'Thermal Analysis Study; Formation of Pure Periclase. J. appl. Chem. Biotechnol 1973; 23: 77-86.
[33] Danny Müller, Christian Knoll, Georg Gravogl, Werner Artner, Jan M. Welch, Elisabeth Eitenberger, Gernot Friedbacher, Manfred Schreiner, Michael Harasek, Klaudia Hradil, Andreas Werner, Ronald Miletich, Peter Weinberger. Tuning the performance of MgO for thermochemical energy storage by T dehydration – From fundamentals to phase impurities. Applied Energy 2019; 253: 113562.
[34] Elisa Guelpa, Vittorio Verda. Thermal energy storage in district heating and cooling systems: A review. Applied Energy 2019; 252: 113474.
[35] Xavier Fontanet. Estudio de Na_2S como material de almacenamiento termoquímico. Memoria ingeniería de materiales. Escuela técnica superior de ingeniería industrial de Barcelona, 2013.
[36] P.A.J. Donkers, L.C. Sögütoglu, H.P. Huinink, H.R. Fischer, O.C.G. Adan. A review of salt hydrates for seasonal heat storage in domestic applications. Applied Energy 2017; 199: 45–68.

INDUSTRIAL CARNALLITE-WASTE FOR THERMOCHEMICAL ENERGY STORAGE APPLICATION

V. Mamani [1], A. Gutiérrez[2], A. I. Fernández[3], S. Ushak [1]*

1 Department of Chemical Engineering and Mineral Processing and Center for Advanced Study of Lithium and Industrial Minerals (CELiMIN), Universidad de Antofagasta, Campus Coloso, Av. Universidad de Antofagasta 02800, Antofagasta, Chile

[2] German Aerospace Center – DLR e. V., Institute of Engineering Thermodynamics, Pfaffenwaldring 38, 70569 Stuttgart, Germany

[3] Department of Materials Science and Physical Chemistry, Universitat de Barcelona, Martí i Franqués 1, 08028 Barcelona, Spain

Corresponding author e-mail: svetlana.ushak@uantof.cl

Abstract

The key to successful development and implementation of thermochemical storage systems is the identification of high energy density and low-cost storage materials. In this work, an industrial waste based on a double salt hydrate, coming from non-metallic mining was studied for thermochemical storage applications. Initially, chemical characterization was performed and determined that carnallite-waste material consists of 73.54 wt% of $KCl{\cdot}MgCl_2{\cdot}6H_2O$ and impurities such as NaCl (23.04 wt%), KCl (1.76 wt%) and $CaSO_4$ (1.66 wt%). Using thermal analyses methods, the operating conditions such as temperatures and partial pressures, were optimized for seasonal thermochemical storage applications to P_{Hy} = 1.3 kPa and ϑ_{Hy} = 40 °C, and to P_{De} = 4.0 kPa and ϑ_{De} = 110 °C. Under these conditions, the reaction reversibility over 10 cycles (10 years) was significantly high, with only 8.5% decrease in chemical reversibility. Furthermore, the duration of dehydration and hydration isotherms was optimized to 15 and 360 minutes, respectively. Finally, 1.129 GJ/m^3 energy storage density was calculated after the tenth cycle of hydration/dehydration for this material. Hence 7.1 m^3 of carnallite was estimated to meet the demand of 8 GJ of energy for an average household during the six months of cold seasons. These results are comparable and competitive with an energy storage density of materials such as K_2CO_3 and $MgCl_2$, reported as promising for seasonal thermochemical storage applications. It should be noted that carnallite-waste material has no commercial value so far and its use contributes to developing sustainable low-cost thermochemical energy storage systems.

Keywords: thermochemical storage energy; potassium magnesium chloride hexahydrate; carnallite-waste material; doble inorganic salt; dehydration and hydration reaction; seasonal heat storage.

1. Introduction

Population growth in the last decades has brought a great industrial activity increase, which as a consequence, has also increased greenhouse gas emissions. Thereby, nowadays one of the greatest challenges that countries face in order to maintain sustainable economic development and to reduce dependence on conventional energy sources is to increase energy efficiency based on renewable sources and thermal energy storage (TES) systems [1,2]. The principle of TES is based on storing heat while the energy source is available, and use it later for heating/cooling applications or the generation of other types of energy e. g. electric [3]. The heat can come from different sources such

as industrial waste heat, solar energy, etc. Applications vary from domestic to industrial level depending on the temperature level [4]. The heat storage mechanisms can be sensible heat storage (SHS), latent heat storage (LHS) and thermochemical storage (TCS). TCS has the highest energy storage density in terms of medium of storage (~ 0.92 – 3.56 GJ/m^3), which is from 5 to 10 times higher compared to LHS (0.15-0.37 GJ/m^3) and SHS (0.033 - 0.4 GJ/m^3), respectively [3,4]. In addition, TCS systems reviewed in [5], use thermochemical materials (TCM) that store and release heat through reversible chemical reactions with practically no heat losses over time [6]. This characteristic is especially attractive for long-term TES applications such as seasonal heat storage, using for example salt hydrates, summarized in [7]. In this case, the heat is stored and released through a reversible reaction of dehydration and hydration (See eq.1) [8]. On the one hand, during summer the system is charged by means of material dehydration, flowing hot air heated by solar collectors, at maximum temperatures of 150 °C. On the other hand, during winter the discharging process is carried out, flowing humid air (e.g. p_{H2O} ~ 1.3 kPa, ϑ_{SAT} = 10°C) through the partially hydrated or totally anhydrous powder. Lastly, this discharge process, release the stored heat through the exothermic hydration reaction [9] (Figure 1).

$$M \cdot xH_2O_{(s)} + \Delta_R H \;\leftrightarrow\; M \cdot yH_2O_{(S)} + (x-y)H_2O_{(g)} \qquad \text{(eq. 1)}$$

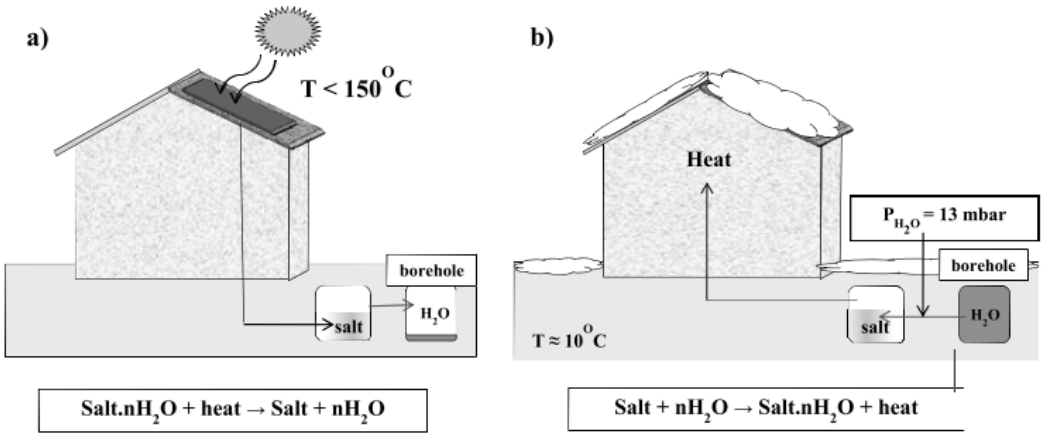

Figure 1: Representation of application of seasonal thermochemical storage, where (a) dehydration and (b) hydration reaction [9].

This reverse reaction is possible under specific temperature and partial vapor pressure conditions defined by the van't Hoff equation (eq. 2), where p_{H_2O} is the partial pressure of water vapor (kPa), p^+ is the reference pressure (100 kPa), **R** is the universal gas constant (8.314 J/mol K), v is the stoichiometric factor for each reaction ($v = x - y$), T is the temperature (K), $\Delta_R S^\theta$ (J/mol K) and $\Delta_R H^\theta$ (J/mol K) correspond to the standard entropy and the standard enthalpy of the reaction, respectively.

$$\ln\left(\frac{p_{H_2O}}{p^+}\right) = \frac{\Delta_R S^\theta}{\boldsymbol{Rv}} - \frac{\Delta_R H^\theta}{\boldsymbol{RvT}} \qquad \text{(eq. 2)}$$

Although TCS has advantages over sensible and latent heat storage, its level of maturity is still in a preliminary stage, and a great research effort still needed to make it a suitable alternative. One

critical aspect is the technical complexity of TCS systems that results in higher investment costs in comparison with latent and sensible heat storage systems [10]. Since the storage material represents a significant fraction of the total investment costs (up to 30 %), the study of industrial wastes used as a medium of storage has been urged [11] and summarized in Figure 2.

Miro et al [12] and Ushak et al [13] recommend the use of non-metallic industry by-products as SHS (NaCl) and LHS (Bischofite) materials (see Figure 2). Recently, Mamani et al. [14] showed that bischofite based by-product is also a promising TCM. The characterization of synthetic inorganic double salt hydrates similar to those that can be found as wastes show that Astrakanite [15] and Potassium Carnallite [15,16] have potential to be used as TCM, while Lithium Carnallite [15] and Kainite [17] not recommended to apply as TES materials under the conditions performed in the respective studies.

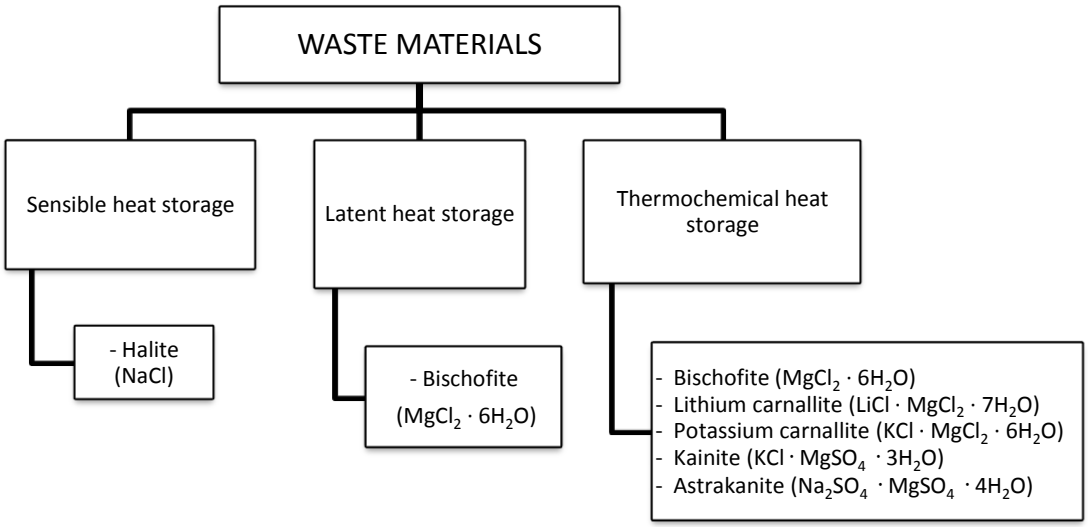

Figure 2: Summary of industrial waste and by-products based on inorganic salts studied as thermal energy storage material.

As it is possible to observe from the review of recent studies (see Figure 2), all of them are based on synthetic materials or by-products obtained in industrial processes. There are no studies that use real natural wastes, without any additional treatment, as possible TES materials based on inorganic salts.

This paper is the first application-oriented study approaching natural waste material suitability as a TCM, which contributes to developing novel low-cost thermochemical materials and their application for seasonal heat storage. The aim of this study is to focus on the thermodynamic characterization of potassium carnallite-waste and the optimization of the operating conditions for its use as TCM. Not only the reversibility and cycle stability of the dehydration-hydration reactions are evaluated, but also the technical parameters, such as energy storage density and material costs. The results are comparable and competitive with materials reported as the most promising TCM.

2.Materials and methods

2.1. Material selection

The first studies using synthetic $KCl{\cdot}MgCl_2{\cdot}6H_2O$ (99 wt%, where wt% means weight percent, defined as the percent of a component in the mixture) [18,19] described thermal decomposition in two dehydration steps (eq.3 and 4). The release of water from the solid takes place with incongruent melting at 167.5 °C in experiments performed using sealed crucibles and under conditions of the partial pressure of water vapor close to 100 kPa [20].

$$KCl{\cdot}MgCl_2{\cdot}6H_2O(s) \leftrightarrow KCl{\cdot}MgCl_2{\cdot}2H_2O(s) + 4\ H_2O(g) \quad \text{(eq.3)}$$

$$KCl{\cdot}MgCl_2{\cdot}2H_2O(s) \leftrightarrow KCl{\cdot}MgCl_2(s) + 2\ H_2O(g) \quad \text{(eq.4)}$$

In addition to the second step of dehydration reaction (eq.4), the partial elimination of gaseous HCl (product of an irreversible secondary hydrolysis reaction) is detected (eq.5), which compromises the rehydration of anhydrous phase (or minor hydrate). Likewise, HCl is corrosive for the equipment in which it is contained and harmful to human health.

$$2\ KCl{\cdot}MgCl_2{\cdot}2H_2O\ (s) \rightarrow KCl{\cdot}MgCl_2\ (s) + 2\ H_2O\ (g) + KMg\ (OH)_2Cl\ (s) + 2HCl\ (g) \quad \text{(eq.5)}$$

The first application of potassium carnallite as TCM was proposed in [15,16] using synthetic material, with a high concentration of potassium carnallite (~76 wt% $KCl{\cdot}MgCl_2{\cdot}6H_2O$, 15.06 wt% $MgCl_2{\cdot}6H_2O$). The results of dehydration of potassium carnallite described it as a promising material for thermochemical storage, at application temperatures below 200 °C. The experiments were performed in an inert atmosphere of N_2 in order to avoid the release of HCl [15]. In the most recent study, the maximum application temperature was limited to 150 °C in a humid atmosphere (p_{H2O} = 25 kPa), in order to get stable chemical reversibility over cycles. Another critical factor identified in those studies was the duration of hydration and dehydration isothermal steps, showing that shorter periods of exposure at high temperatures (150 °C) reduces the degradation of the material over cycles. Therefore, the duration of dehydration isotherms was limited to <20 min. Following the reaction shown in eq.3, the same study reports stability of the enthalpy of reaction through the cycles, with approximate values to 120 kJ/mol $KCl{\cdot}MgCl_2{\cdot}6H_2O$ [16]. The operational conditions of thermochemical dehydration and hydration reactions are summarized in Table 1.

Table 1: Operating conditions of dehydration and hydration reactions for synthetic $KCl{\cdot}MgCl_2{\cdot}6H_2O$.

Reactions	Heating rate (K/min)	ϑ (°C)	ΔH_D (kJ/mol)	p_{H2O} (kPa)	Ref.
Dehydration reactions	0.5	84.2	189.68	0	[15]
$KCl{\cdot}MgCl_2{\cdot}6H_2O$ ➔ $KCl{\cdot}MgCl_2{\cdot}2H_2O + 4H_2O$					
$KCl{\cdot}MgCl_2{\cdot}2H_2O$ ➔ $KCl{\cdot}MgCl_2{\cdot}H_2O + H_2O$	0.5	127.1	67.93	0	[15]
Hydration reaction					
$KCl{\cdot}MgCl_2{\cdot}2\ H_2O + 4H_2O$ ➔ $KCl{\cdot}MgCl_2{\cdot}6H_2O$	5	100	120	25	[16]

Based on these studies reported previously, synthetic potassium carnallite is a promising TCM, having adequate thermodynamic properties and significant stable chemical reversibility below

150 °C. Nevertheless, for a matter of applicability it is necessary not only to have a material with the characteristics just mentioned but also with high availability and low prices.

In northern Chile, about 1.8 million tons per year of potassium carnallite waste (75 wt% > $KCl{\cdot}MgCl_2{\cdot}6H_2O$) precipitates during the brine concentration process from Salar de Atacama [21,22]. On the basis that this material meets all the requirements mentioned above, 5 kg of natural carnallite-waste provided by the company Albemarle (Antofagasta region, Chile) was used for this study. The sample was homogenized by manual mixing and subjected to drying at 40 °C for approximately 12 hours to eliminate environmental humidity, due to the hygroscopicity of the salt.

2.2. Chemical characterization

-X-ray diffraction (XRD)

Analysis of X-ray diffraction was performed on X-ray diffractometer SIEMENS model D5000 (40 kV, 30 mA); radiation of Cu K α1 (λ = 1.5406 Å); Vertical Bragg–Brentano; Scan Range: 3–70° 2θ; Step Size:0.0201 2θ; StepTime:1.0 s. The powdered sample was positioned on a flat plate sample holder after sample powdering in an agate mortar. The identification of crystallographic phases was carried out using PDF-2 and TOPAS programs.

-Chemical analysis

Approximately 20 g of carnallite was used for the chemical analysis. The methods used to determine chemical composition were: atomic absorption spectrophotometry with direct aspiration (Varian Spectra 220 fs atomic absorption spectrometer) for quantification of K, Mg, Ca, Li, Na; volumetric titration with $AgNO_3$ for chloride identification and volumetric titration with $BaCl_2$ for the identification of sulphate.

-Morphology and composition analysis

A scanning electron microscope (SEM) Jeol, Model JSM6360LV was used for analyzing the morphology and composition of the sample, coupled to an energy dispersive X-ray spectrometer (EDX) Inca Oxford. The measurements were performed under low vacuum, electron beam of 20 kV, working distance of 10 mm, spot size 60 mm, and backscattered electron signal.

2.3. Thermal behavior of carnallite

The thermal stability and reversible dehydration/hydration reaction of carnallite-waste were performed under different operating conditions as follow:

2.3.1 Dehydration reaction

- *Thermal behavior of material*

The dynamic dehydration was measured with a METTLER TOLEDO TGA-DSC STARe thermogravimetric TG and DSC analyses. The dynamic method used was from room temperature up to 300 °C at 1 K/min. The nitrogen flow rate was set to 25.0 mL/min. For this analysis, a sample amount between 10-20 mg in a 70 μL platinum crucible with an unsealed lid was used to know the change of weight and heat flow at high temperatures.

- *Determination of gaseous products by thermogravimetric –mass spectroscopy (TG-MS)*

The thermal decomposition and mass loss curves were recorded by Thermogravimetric analysis (NETZSCH STA 449 C Jupiter). A thermogravimetric sample carrier with a thermocouple type S and an accuracy of ± 1 K was used. The measurements were performed from room temperature (25 °C) to 1100 °C performing dynamic experiments with a heating rate of 10 K/min using nitrogen as protective gas with a volume flow of 50 N-mL /min. The sample mass was surrounded by a constant gas flow of 100 N-mL/min nitrogen. The accuracy of the balance was ± 0.1 μg. In order to analyze the generated gases, a Mass spectrometer (NETZSCH QMS 403 C Aëolos) was coupled to the TG analyzer. Sample mass of about ~30 mg was measured in open Al_2O_3 crucibles.

- *Determination of solid products by HT-XRD*

The X-Ray diffraction was performed at room temperature and high-temperature; 50 °C, 130 °C and 170 °C, with PANalytical X'Pert Pro MPD equipment coupled with Anton Paar 1200 HTK oven. In this study, the following measurement conditions were used: 45kVx40 mA; static air atmosphere, heating/cooling rate of 1 K/min, radiation of Cu Kα1 (λ=1.5406 Å); Scan. Range: 10–80° in 2θ; Step Size: 0.013°. The powdered samples were positioned on a flat plate alumina sample holder after sample powdering. Based on experimental XRD patterns the identification of crystallographic phases has been performed by searching in ICDD PDF-2 (version 2004), and through the search- match of the crystalline structures data, using X'pert HighScore.

2.3.2 Hydration reaction

- *STA–MHG Reversibility of Reaction*

The investigation of reaction reversibility was carried out using a simultaneous thermal analyzer (NETZSCH STA 449 F3 Jupiter). Equipped with a differential scanning calorimetric and thermogravimetric (DSC-TG) sample holder with a thermocouple Type P and an accuracy of ±1 K was used. The accuracy of the balance was ±0.1 μg. The equipment was coupled to a Modular Humidity Generator (ProUmid MHG-32). Nitrogen was used as protective and purges gas with a volume flow for both of 20 N-mL/min, and as the atmosphere surrounding the sample kept it inert using 100 N-mL/min of only nitrogen flow or nitrogen flow and water vapor. Finally, liquid nitrogen was used to support the controlled cooling process and the amount of mass used was ~ 10 mg. in an open system of platinum crucible.

The chemical reversibility was calculated as a percentage of weight gained during hydration divided by the weight lost during dehydration, according to the following eq. 6:

$$\%\, rev = \frac{weight\ recovered}{weight\ lost} x\ 100 \qquad \text{(eq.6)}$$

The operating conditions, namely the temperature and humidity programs, used to evaluate the sample reversibility, were taken from [16], where the maximum partial water vapor pressure was set to 30 kPa (38% RH). However, conditions determined as the most adequate, close to the theoretical thermodynamic equilibrium, consisted in the partial pressure of water vapor of 25 kPa (31.6 %RH) for the dehydration-hydration reactions, in the temperature range of 100 °C to 150 °C, setting isothermal durations of 10 and 20 min, respectively. The heating/cooling rates were set to 5 K/min over 15 cycles (see Table 2).

Table 2: Heat storage operating conditions of experiments.

	Dehydration					**Hydration**				
Step conditions	[a]		[b]		[c]	[d]			[e]	-
Experiment	$\vartheta_{initial}$ (°C)	ϑ_{De} (°C)	$p_{H2O,\ Dehy}$ (kPa)	HR (K/min)	$t_{iso,\ De}$ (min)	ϑ_{Hy} (°C)	$p_{H2O,\ Hy}$ (kPa)	CR (K/min)	$t_{iso,\ Hy}$ (min)	N° Cycles
1	40	150	25	5	15	100	25	-5	20	15
2	40	130	1.3	1	60	40	1.3	-1	180	5
3	40	110	1.3	1	15	40	1.3	-1	180	5
4	40	110	4.0	1	15	40	1.3	-1	180	5
5	40	110	4.0	1	15	40	1.3	-1	180	20
6	40	110	4.0	1	15	40	1.3	-1	360	10

During the experimental verification and validation of theoretical thermodynamic equilibrium, is important to set the limits of the operating conditions for using this material [23,24]; especially, when working with hygroscopic or deliquescent materials, which cannot be exposed to relative humidity above the critical level at certain temperatures [25].

The experiments 2-6 were designed to evaluate the material for seasonal heat storage applications. They reproduce the partial pressure of water vapor and temperatures that are characteristic of summer and winter (Figure 3, Table 2). These conditions should be suitable as indicated by the van't Hoff plot for synthetic carnallite [16] (Figure 4). Hydration temperatures were set to 40 °C (which corresponds to the minimum temperature for water heating) and dehydration temperatures were set to 110 ºC and to 130 °C (which are easily reached by solar collector systems). The water vapor partial pressure conditions varied between 1.3 (10.9 %RH) and 4.0 kPa (35 %RH) for the release and recovery of 4 moles of water (eq.3).

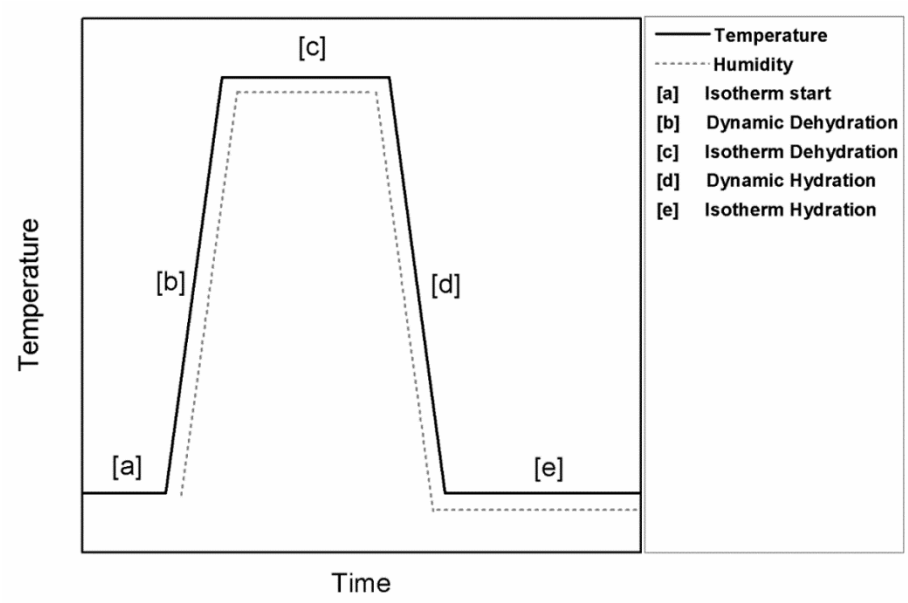

Figure 3: Experimental protocols of dehydration and hydration reactions study.

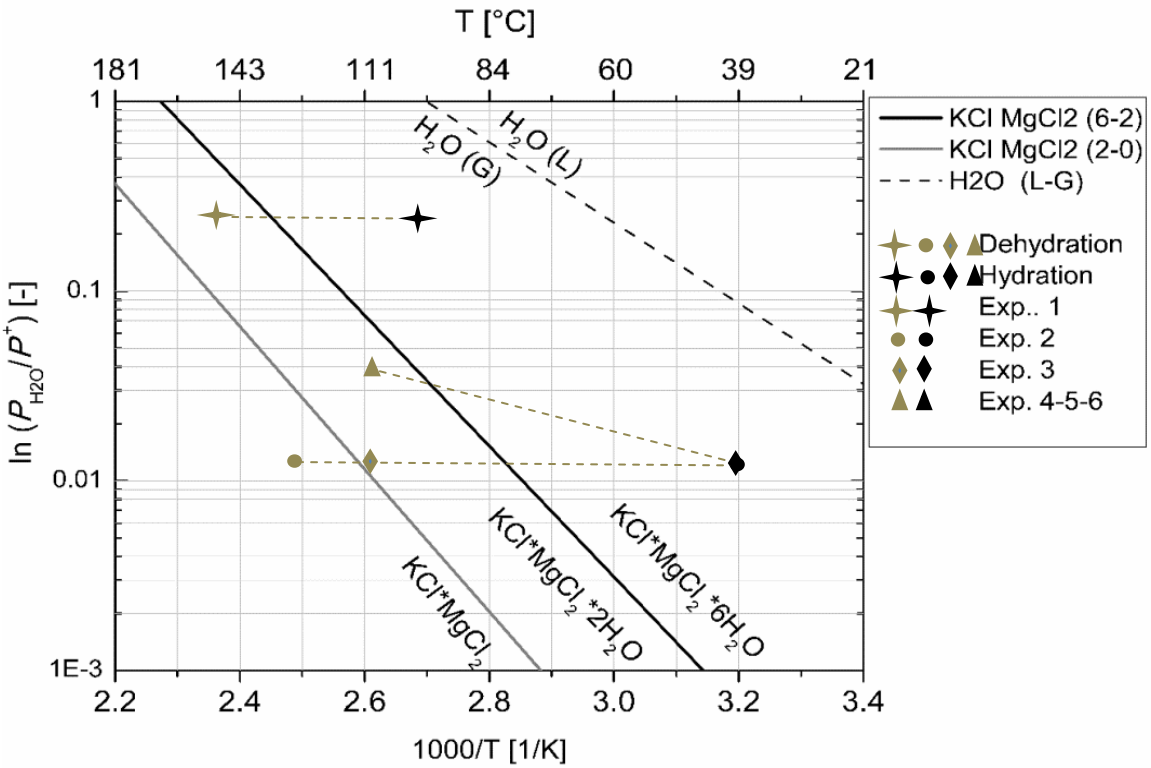

Figure 4: Van't Hoff plot of $KCl{\cdot}MgCl_2{\cdot}6H_2O$ (carnallite). Experimental temperature and humidity programs of hydration and dehydration (dashed line paths delimited by the markers).

-Analysis of products after the cycles

Products obtained from experiments 5 and 6 were analyzed at room temperature using XRD (PANalytical X'Pert Pro MPD, 45kVx40 mA; static air atmosphere, radiation of Cu Kα1 (λ = 1.5418 Å); Scan. Range: 10–80° in 2θ; Step Size: 0.013° and a measuring time of 75 seconds per step) with the objective of identifying the phases of solid products that have been formed during hydrolysis reaction, which explains the material decomposition and the loss of reversibility.

2.4. Energy storage density and energy cost

-Enthalpy of the reaction

The enthalpies of the hydration and dehydration of carnallite-waste were obtained from the differential scanning calorimetric curves (NETZSCH STA 449 F3 Jupiter) using the Software NETZSCH-Proteus –Thermal Analysis which integrates the specific power delivered to the samples (mW/mg) over time. The endothermal and exothermal behaviors were determined based on the tendencies of the DSC signal peaks (upwards or downwards respectively) for 10 reaction cycles.

-Energy storage density

In addition, the amount of energy in Gigajoules (GJ) that can be stored in 1 m^3 (*esd*) was calculated as the product of the dehydration reaction enthalpy and density for the studied salt hydrate.

The density of solid sample was determined pycnometrically [26] at 60 °C with n-dodecane as a displacement liquid and the temperature was controlled with an oven Thermo Scientific, Thermolyne F48020-D8.

-Energy cost

Based on the results of energy storage density for carnallite-waste, the volume (m^3) of material necessary to store 8 GJ of energy needed to cover the heat demand of a passive solar house of 110 m^2 [9,27] was determined and compared with the most promising materials for seasonal heat storage.

3. Results and discussion

3.1. Chemical characterization

-X- ray diffraction

Crystalline phases present in the sample of carnallite-waste were determined using the XRD analysis. Figure 5 shows a XRD pattern with the compounds identified in the waste material: potassium carnallite ($KCl{\cdot}MgCl_2{\cdot}6H_2O$), silvite (KCl), sodium chloride (NaCl) and calcium sulfate ($CaSO_4$), minerals previously identified in the Salar de Atacama [28].

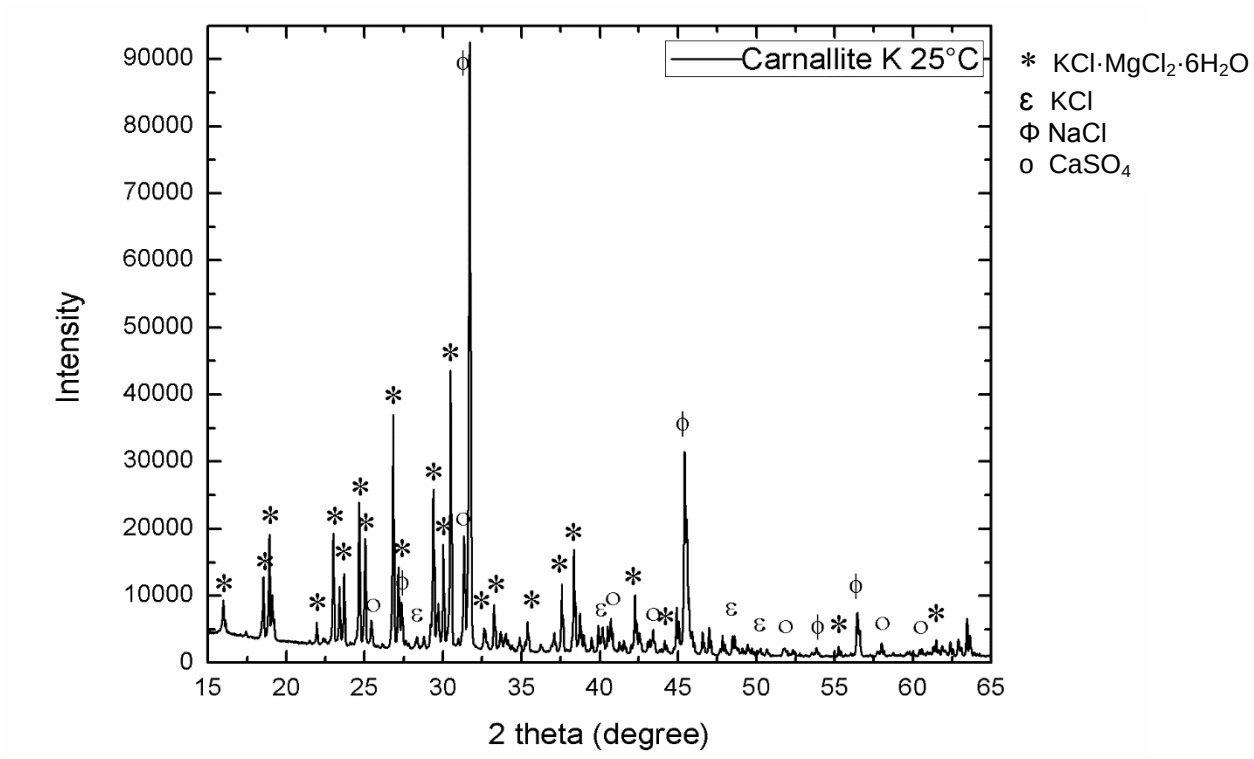

Figure 5: XRD pattern of potassium carnallite waste at 25 °C.

-Chemical analysis

In accordance with the identification of crystalline phases by XRD, an elemental analysis allowed quantifying the concentration of each compound. The chemical elements present in carnallite-waste are shown in Table 3. It can be seen that the material contains mostly potassium, sodium, magnesium, and chloride. Also, calcium, lithium, and sulfate in smaller quantities.

Table 3: Carnallite-waste chemical analysis.

Elements	**Composition of waste (wt%)**
Lithium, Li	0.14
Sodium, Na	**8.37**
Potassium, K	**10.41**
Magnesium, Mg	**5.94**
Calcium, Ca	0.36
Chloride, Cl	**41.32**
Sulfate, SO_4	1.26
Moisture	0.83
Crystallization water	31.37

The mineralization results are shown in Figure 6 which indicates that potassium carnallite $KCl{\cdot}MgCl_2{\cdot}6H_2O$ (73.54 wt%) is the main component and impurities are sodium chloride (23.04 wt%), calcium sulphate (1.66 wt%) and potassium chloride (1.76 wt%).

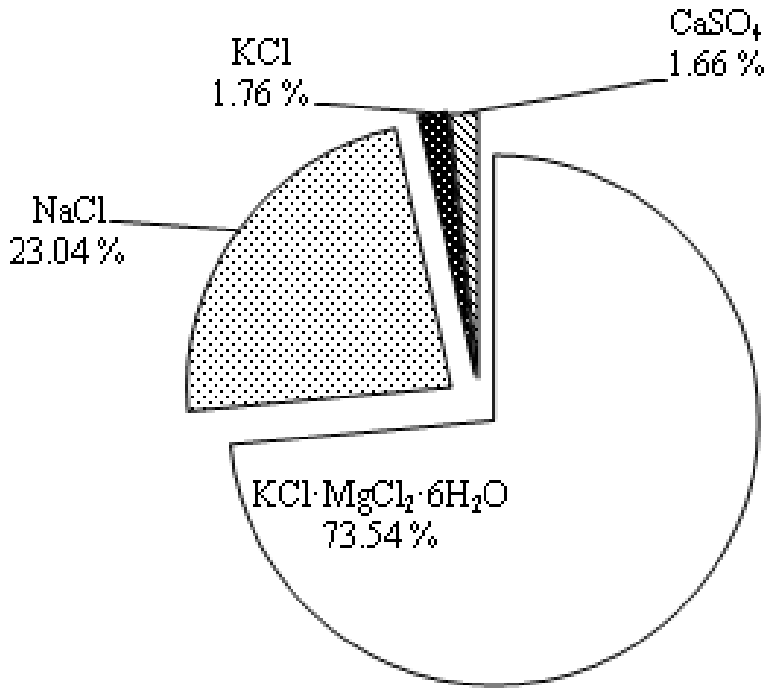

Figure 6: Mineralization of potassium carnallite waste.

The impurities can have a positive or negative effect on the thermal behavior. Previous studies focused on another group of compounds, such as metal hydroxides ($Ca(OH)_2$ and $Mg(OH)_2$), showed that the dehydration temperatures of these materials can be reduced by adding KCl and NaCl in low concentrations (7 wt.%). Furthermore, their thermal decomposition was also reduced [29]. In another study using the mixture of $CaCl_2$ with KCl (2:1), the thermal conductivity, the cyclic stability and the release and capture of water molecules during dehydration and hydration of $CaCl_2$ were improved. It was found that KCl decreases the coalescence and consequently the

agglomeration of $CaCl_2$ particles, facilitating the capture and release of water in each reaction [30]. However, a decrease in reaction enthalpy was observed in both studies. Additionally, another single salt widely studied as TCM is $CaSO_4$. This material has hygroscopic properties and is normally found as $CaSO_4 \cdot 0.5H_2O$. Dehydration temperatures of 150 °C and hydration temperatures of 60 and 100 °C have been previously reported as well as problems of agglomeration (reaction shown in eq. 7) [31].

$$CaSO_4\,(s) + 0.5H_2O(g) \leftrightarrow CaSO_4 \cdot 0.5\,H_2O(s) + 16.8\,kJ/mol \qquad (eq.7)$$

Since potassium carnallite-waste contains NaCl and KCl, they could act as a matrix that reduces particle agglomeration over cycles, thus better reversibility and cyclic stability are expected. Nevertheless, the presence of $CaSO_4$, even in lower concentrations, could increase the agglomeration of carnallite-waste particles. However, if 110 °C temperature is not exceeded, the dehydration reaction of $CaSO_4 \cdot 0.5H_2O$ should not take place.

-Morphology and composition analysis

Morphology of the carnallite-waste particles and the analysis of impurities are shown in Figures 7 and 8.

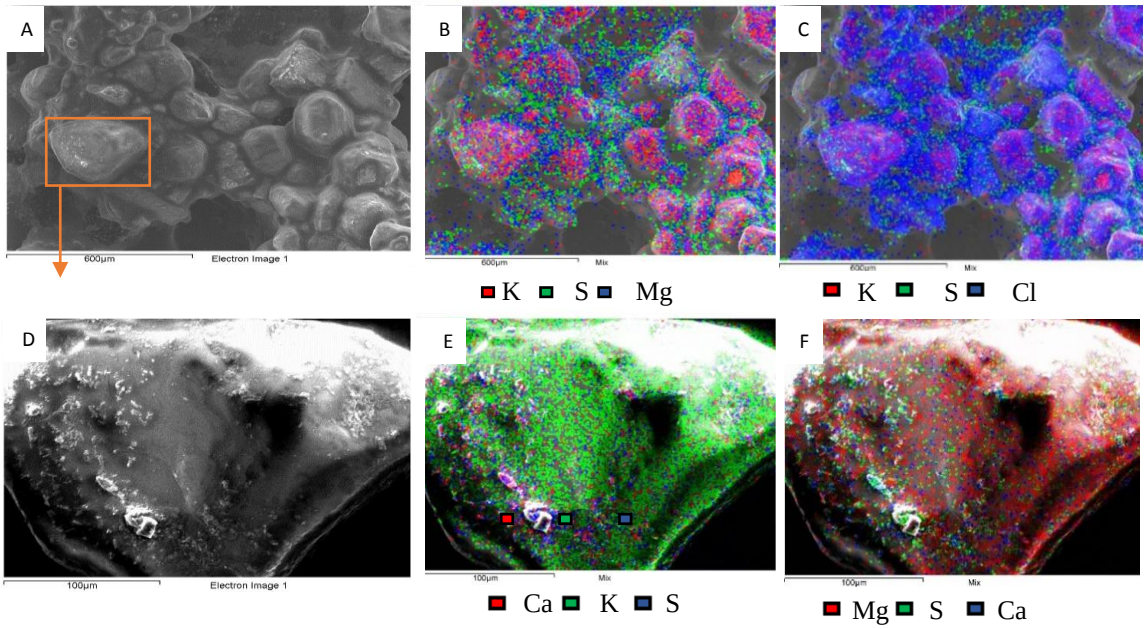

Figure 7: Morphology of carnallite-waste particles using SEM-EDX.

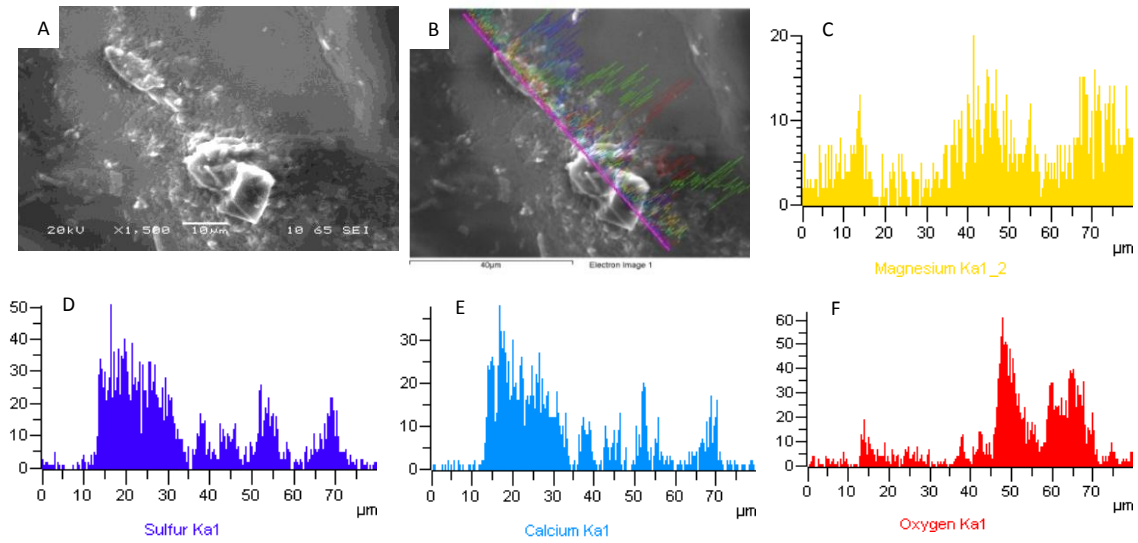

Figure 8: Analysis of impurities adhered to carnallite (see online color version for full interpretation).

Figure 7a (70X magnification) shows the morphology of the carnallite phase, which is not well defined, due to the high hygroscopicity of material. The particle size is less than 500 µm. Figures 7b and c show the presence of Potassium - K (red), Sulfur - S (green), Magnesium - Mg and Chlorine – Cl (Blue) and the interaction of these forming the compound $KCl{\cdot}MgCl_2{\cdot}6H_2O$ (purple). Figures 7d-f (300X magnification), demonstrate a carnallite particle with traces of an impurity containing Ca and S, which would correspond to $CaSO_4$, previously identified by XRD (Figure 6). The analysis at 1500X magnification (Figures 8 a-f) shows the interaction between sulfur (S), calcium (Ca) and oxygen (O) for the formation of $CaSO_4$.

3.2. Dehydration reaction

- Thermal stability

Dehydration of carnallite-waste was studied through the mass loss by increasing the temperature at controlled heating rates of 1 K/min. The results are shown in figure 9, where three steps of dehydration process (endothermic) can be identified. The first is the least sharp among the three steps and corresponds to the evaporation of water adsorbed from the environment (0.13 wt%, below 51 °C). The second step begins at 102.43 °C (ϑ_{onset}) and continues until 136 °C, losing 20.75 wt %, which corresponds to 4.35 mol of H_2O. Finally, the third step, ranges from 165 °C to 173 °C, losing 9.88 wt% (2.1 mol H_2O).

Between 102 °C and 173 °C the experimental mass loss observed was 30.63 wt%, which exceeds the stoichiometric crystalline water content of the sample (28.73 wt%). This indicates that not only the dehydration reaction took place, but also an irreversible decomposition reaction of the material, e.g. hydrolysis. In other words, HCl was released and a solid products of hydrochloride KMgOHCl

and magnesia MgO were formed [20,32]. The energy involved in the second and third dehydration steps were 631.95 kJ/kg and 325.65 kJ/kg, respectively.

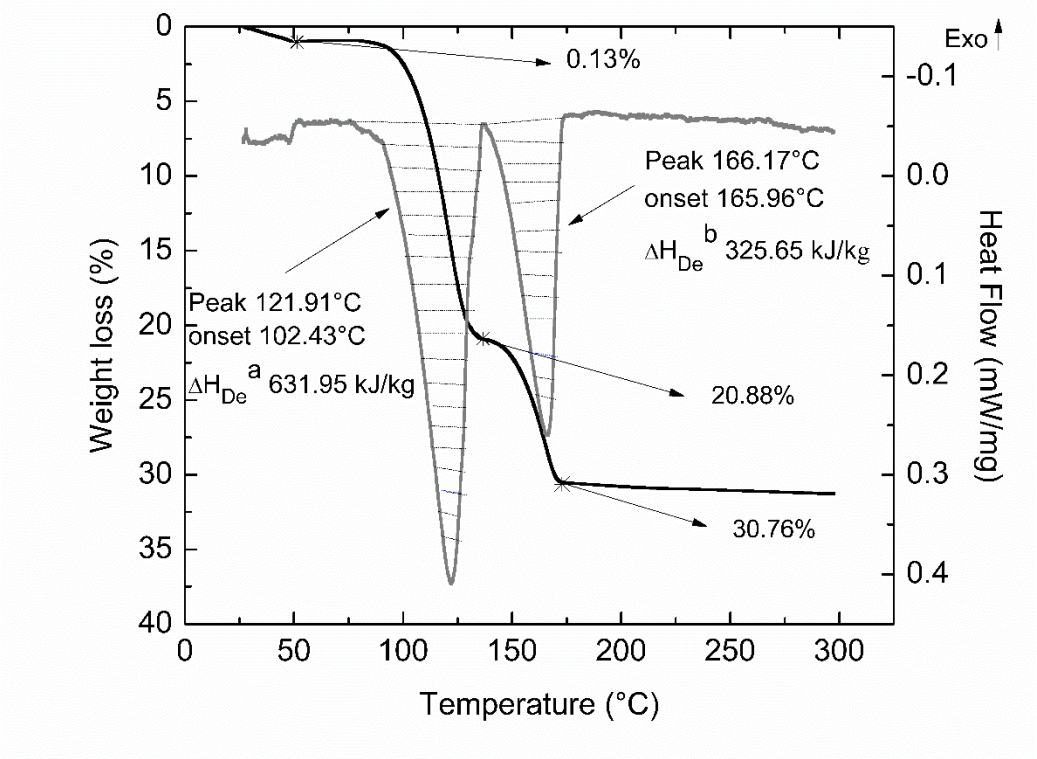

Figure 9: Dehydration of carnallite-waste at 1 K/min using TGA-DSC.

Comparing the results of carnallite-waste mass loss percentages with studies performed using synthetic carnallite [16], it is important to point out that the temperatures of dehydration stages are lower for carnallite waste. It should be noted that lowering dehydration temperature will decrease the energy input of the waste-carnallite system. In addition, the final mass loss observed was 10 wt% lower for carnallite-waste than for synthetic carnallite. These differences are associated with the impurities present in each material, which decrease their purity down to 76.53 wt% and 73.54 wt% for synthetic carnallite and for carnallite-waste, respectively. Synthetic carnallite contains 15.05 wt% of magnesium chloride hexahydrate, which is dehydrated along with synthetic carnallite [16]. In contrast, carnallite-waste contains impurities that are not dehydrated/reactive, so that the mass loss would correspond only to the dehydration of carnallite-waste.

-Determination of gaseous products by thermogravimetric – mass spectroscopy (TG-MS)

The release of HCl indicates the start of hydrolysis reaction (eq.5), which is a disadvantage for a thermochemical material. Gaseous products produced by heating the carnallite-waste to 600 °C were studied by means of TG-MS (Figure 10).

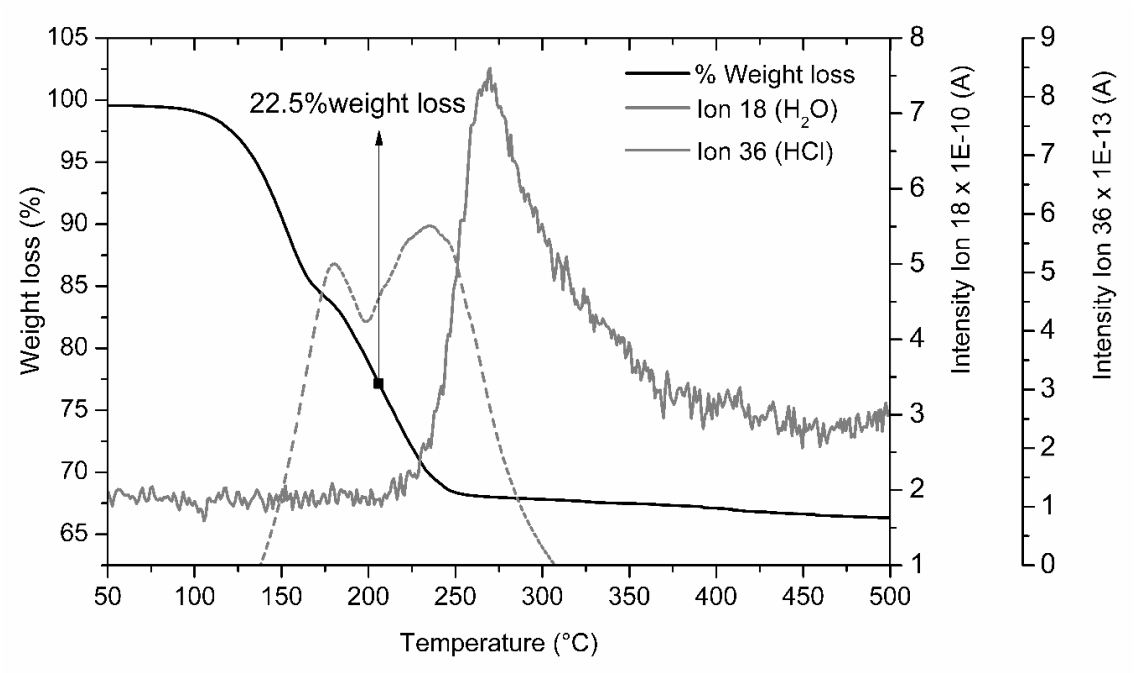

Figure 10: TG-MS curve of thermal decomposition of carnallite-waste.

Figure 10 shows the mass signal of 18 g/mol (dashed line), which confirms the release of water in two dehydration steps in the temperature range of 130 °C to 280 °C. In addition, a weak mass signal of 36 g/mol (gray line) is observed starting at 200 °C, indicating the release of HCl. The release of HCl coincides with the end of the second dehydration step, demonstrating that the hydrolysis reaction occurs together with the dehydration reaction of $KCl{\cdot}MgCl_2{\cdot}2H_2O$, releasing HCl gas as a product. This has been also previously reported by Emons et al. [18,19] and Araten [32]. It was further determined that the hydrolysis reaction begins when the mass loss of carnallite-waste is 22.5 wt%, which corresponds to the loss of the fifth mole of water.

The hydrolysis reaction is detrimental to thermochemical storage applications for various reasons: it reduces the reaction reversibility by breaking down the material gradually during the cycles; it is highly corrosive for metals and toxic for human health. Thus, for carnallite-waste to be suitable as thermochemical storage material, it is necessary to limit its dehydration only until the loss of the fourth mole of water, that is, up to a maximum mass loss of 19 wt%.

- Determination of solid products by HT-XRD

To determine the crystalline phases that are present during the dehydration process of carnallite-waste, the analysis of X-ray diffraction at three different temperatures was carried out. The XRD pattern at 50 °C was used as a reference, that is, before the dehydration beginning. The other two experiments were carried out at 130 °C and 170 °C when the first and the second dehydration steps were completed. The XRD patterns obtained are shown in Figure 11, and the crystalline phases identified are also shown in Table 4.

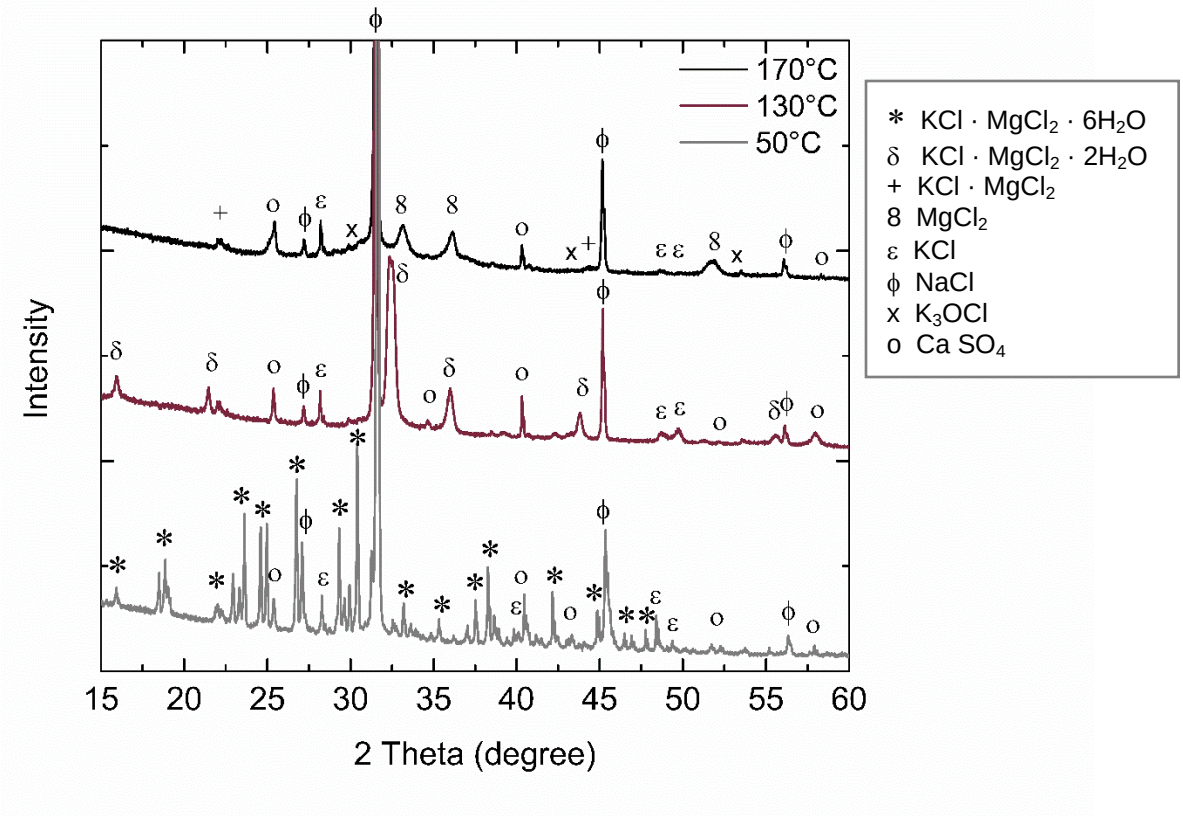

Figure 11: Carnallite diffraction pattern at 50 °C, 130 °C and 170 °C.

Table 4: Identification of products of carnallite-waste thermal decomposition based on XRD.

Solid products of thermal decomposition of carnallite-waste		
50 °C	**130 °C**	**170 °C**
$KCl{\cdot}MgCl_2{\cdot}6H_2O$	$KCl{\cdot}MgCl_2{\cdot}2H_2O$	$KCl{\cdot}MgCl_2$
NaCl	NaCl	NaCl
KCl	KCl	KCl
$CaSO_4$	$CaSO_4$	$CaSO_4$
		$MgCl_2K_3OCl$

According to these results, the first step of dehydration was completed at 130 °C and the main product corresponds to $KCl{\cdot}MgCl_2{\cdot}2H_2O$. This agrees with the results of TG-MS where the loss of approximately 4 moles of water is observed. The absence of hydroxychlorides indicates that the hydrolysis reaction has not occurred. Upon completion of the second dehydration step at 170 °C, potassium carnallite anhydride $KCl{\cdot}MgCl_2$ is identified, indicating the complete dehydration of the salt. This dehydration along with the decomposition of $KCl{\cdot}MgCl_2{\cdot}2H_2O$ in the second step, plus the identification of potassium oxychloride K_3OCl, could indicate that the hydrolysis reaction has occurred between 130 ° C and 170 °C. On the other hand, at 170 ºC $MgCl_2$ is also identified, which denotes that a part of potassium carnallite is possibly dissociated. Also, the appearance of an amorphous phase is observed, which is evidenced by the base line of XRD pattern and the loss of peaks. The impurities of NaCl, KCl and $CaSO_4$ were identified for all studied temperatures.

3.3. Hydration reaction

- *STA–MHG Reversibility of Reaction*

The TG results from Figure 12 show 15 cycles of dehydration/hydration reaction of carnallite-waste (eq. 3), under pressure and temperature conditions close to the theoretical equilibrium (25 kPa and 150 °C - 100 °C). In the first cycle, 22 wt% (4.62 mol H_2O) mass loss and 14 wt% (3.03 mol H_2O) mass gain are observed, which corresponds to 65.5 % of chemical reversibility. However, this chemical reversibility is progressively reduced through the cycles, reaching only 2.8 % at the 15^{th} cycle.

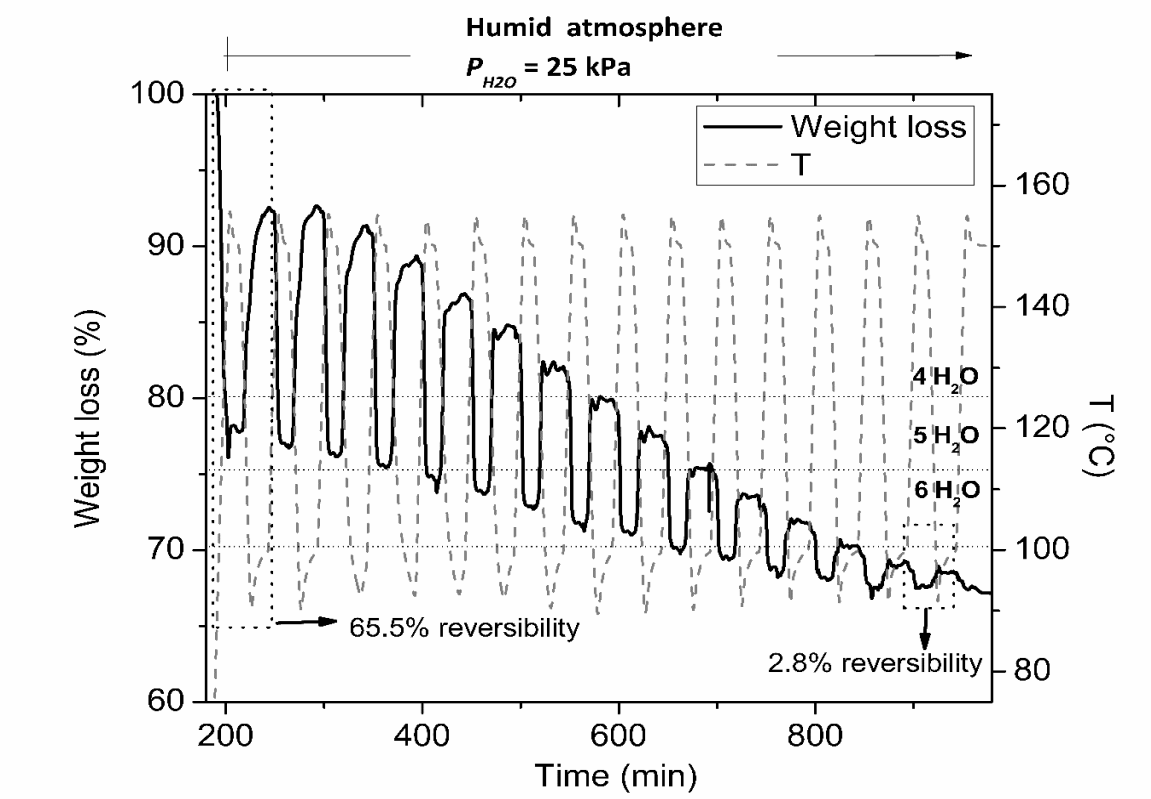

Figure 12: STA-MHG measurement of dehydration/hydration of carnallite waste for 15 cycles, 25 kPa and 150 °C – 100 °C range.

The reduction of the chemical reversibility degree defines a poor cyclic stability of the reaction under the listed conditions, which could be associated with the decomposition of $KCl{\cdot}MgCl_2{\cdot}2H_2O$ during the second dehydration step. This gradual decomposition is identified as a negative slope on the dehydration baseline (Figure 12), in which $KCl{\cdot}MgCl_2{\cdot}6\ H_2O$ loses a larger amount of mass during dehydration than it gains during hydration through the cycles. In other words, during the first dehydration, 22 wt% (4.62 mol H_2O) of mass is lost, this means that the reactions shown in eq. 4 and eq. 5 are partially taking place. Furthermore, in the following cycles the mass loss increases to 31.4 wt%, this exceeds the maximum mass loss possible, where the 2.8 wt% extra mass loss corresponds to gaseous HCl (product of the hydrolysis reaction).

The decomposition of $KCl{\cdot}MgCl_2{\cdot}2H_2O$ increases with each cycle and the concentration of rehydrated $KCl{\cdot}MgCl_2{\cdot}6H_2O$ ("active" material) decreases (see Figure 13). Moreover, the concentration of inactive material increases in the same proportion due to the irreversible decomposition.

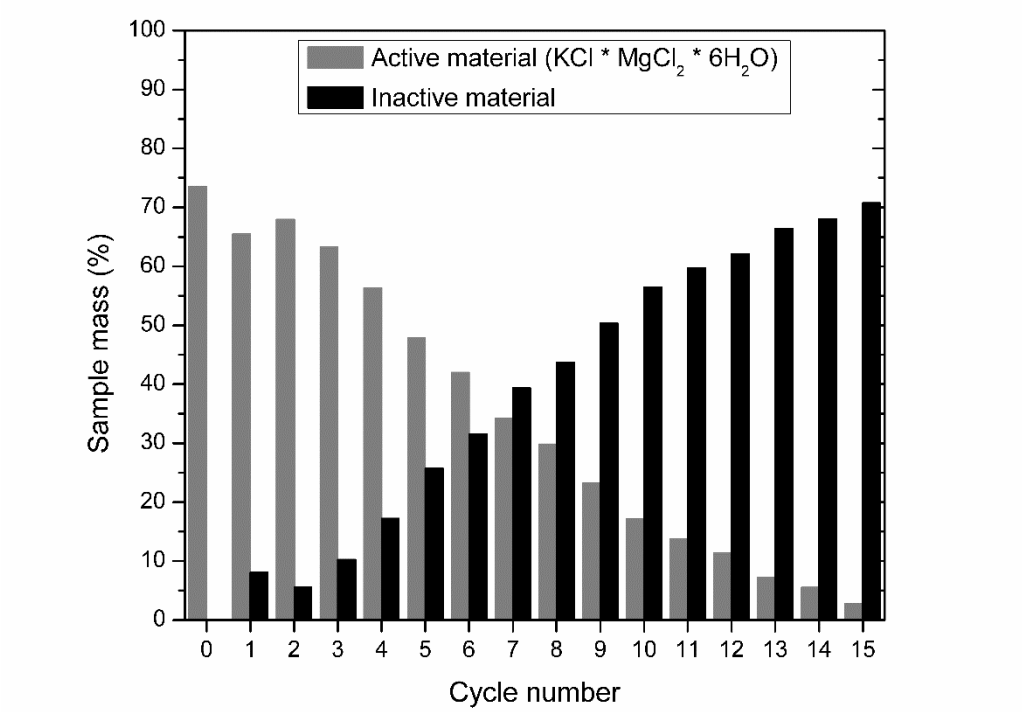

Figure 13: Products of 15 cycles of dehydration and hydration reactions; $KCl{\cdot}MgCl_2{\cdot}6H_2O$ and inactive material.

Comparing carnallite-waste and synthetic carnallite it can be seen that loss of chemical reversibility and decomposition takes place in a greater proportion for carnallite-waste (Figure 14). This could be explained by the presence of different impurities in the composition of both materials [33]. The carnallite-waste impurities cause a faster decomposition at 150 °C than that of synthetic carnallite, as a consequence, the reaction reversibility is reduced through the cycles.

Additionally, the reduction of the chemical reversibility degree could be associated with the agglomeration of the samples. Usually, the salt hydrate particles show agglomeration under high water vapor pressures, decreasing this way a complete chemical conversion of the material through several cycles [30]. However, this aspect must be further investigated on a larger scale than used in this study.

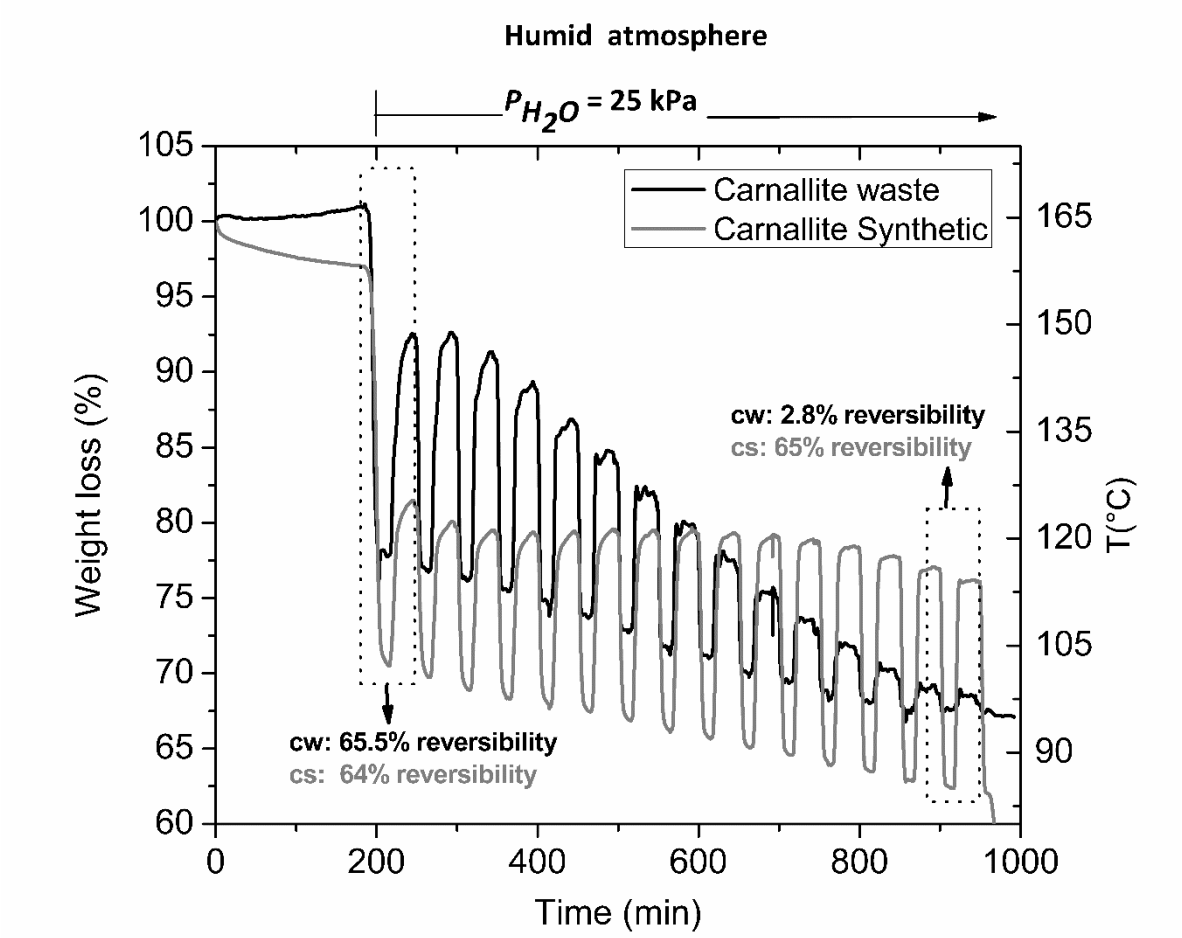

Figure 14: Comparison of dehydration /hydration cycles reaction for synthetic sample [16] and carnallite-waste.

Due to the decomposition of carnallite-waste at high temperatures and partial pressure of water vapor, further experiments were performed reducing the maximum temperatures from 150°C either to 110 °C or to130 °C, and the maximum p_{H2O} from 25 kPa to 4.0 kPa. The hydration was carried out at 40 °C and p_{H2O}= 1.3 kPa (see experiments 2-6, Table 2). The results of experiment 2 (five reaction cycles) are shown in Figure 15. As can be seen, the chemical reversibility of 95 % is achieved in the first cycle, which gradually decreases in the following cycles to 79.4 % (5^{th} cycle). Besides, as expected and according to the van't Hoff plot (Figure 4), the appearance of the second stage of dehydration during the isotherm at 130 °C is observed. This second step reaction gets sharper from the second cycle onwards, indicating that the hydrolysis reaction of $KCl{\cdot}MgCl_2{\cdot}2H_2O$ (eq. 4 and 5) and a progressive decomposition of the sample took place and thus the overall chemical reversibility is reduced. As mentioned before, this can be identified on the negative slope of the baseline of the TG curves.

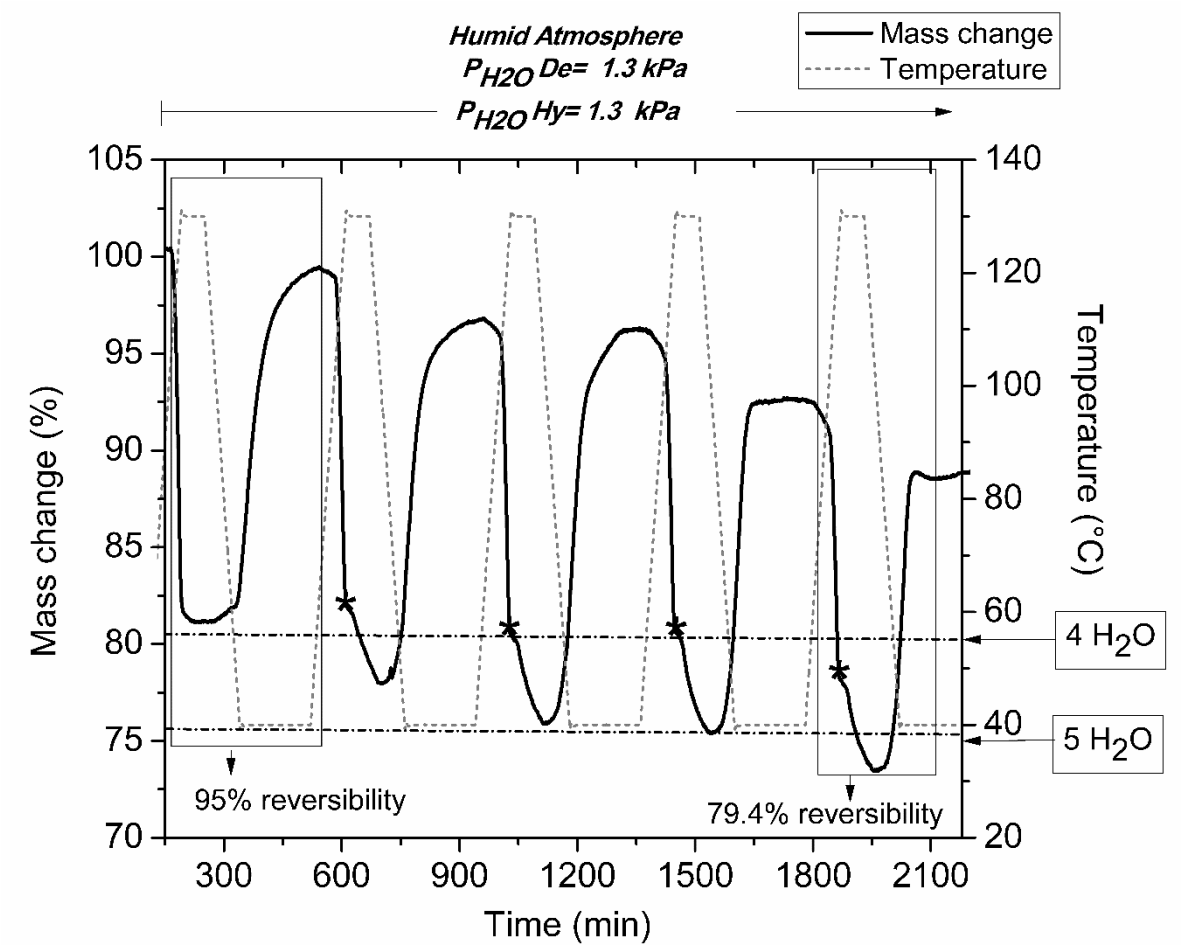

Figure 15: Results of reversibility of carnallite-waste under operating conditions for seasonal heat storage (experiment 2).

Experiment 3 from Table 2 focused on preventing the second dehydration step by decreasing the dehydration temperature from 130 °C to 110 °C, in addition to decreasing the duration time of the isotherm from 30 min to 15 min. Results are shown in Figure 16, demonstrating that the second step of dehydration does not happen. Despite, the chemical conversion of the first cycle is 93.9 %, in the fifth cycle, a reduction of chemical reversibility to 75 % is observed without significant changes in the baseline. Therefore, there is other factor in addition to the temperature that influences the reaction reversibility. Hence, it was decided to reproduce the conditions of seasonal partial pressures in summer (4.0 kPa) and in winter (1.3 kPa) with greater fidelity (experiment 4). The results are shown in Figure 17. Clearly, the reaction reversibility improves in each cycle, the conversion in the first cycle is 89 % and in the fifth cycle is 92.5 %, without significant changes in the baseline that indicate decomposition of the material.

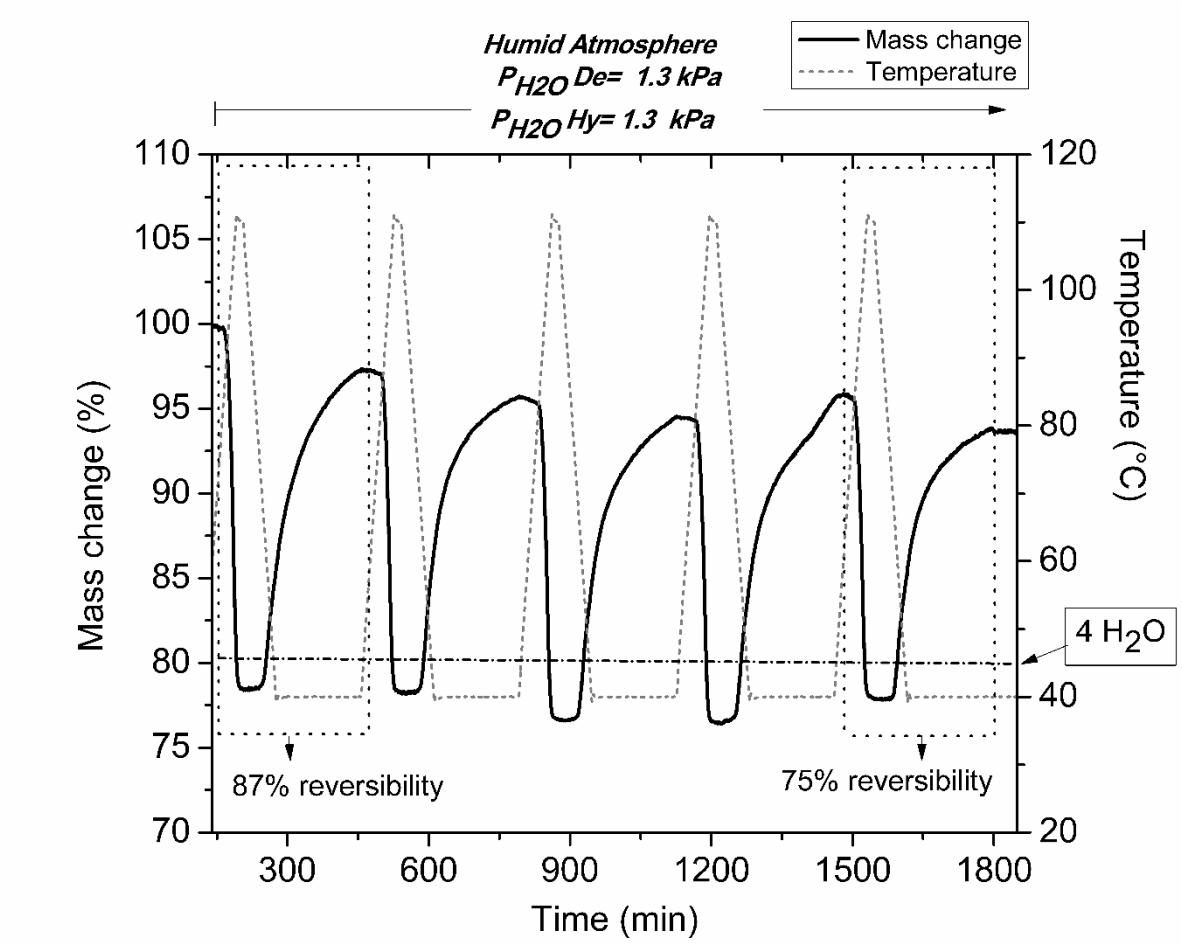

Figure 16: Optimization of the dehydration temperature reaction of carnallite waste under seasonal conditions (Experiment 3).

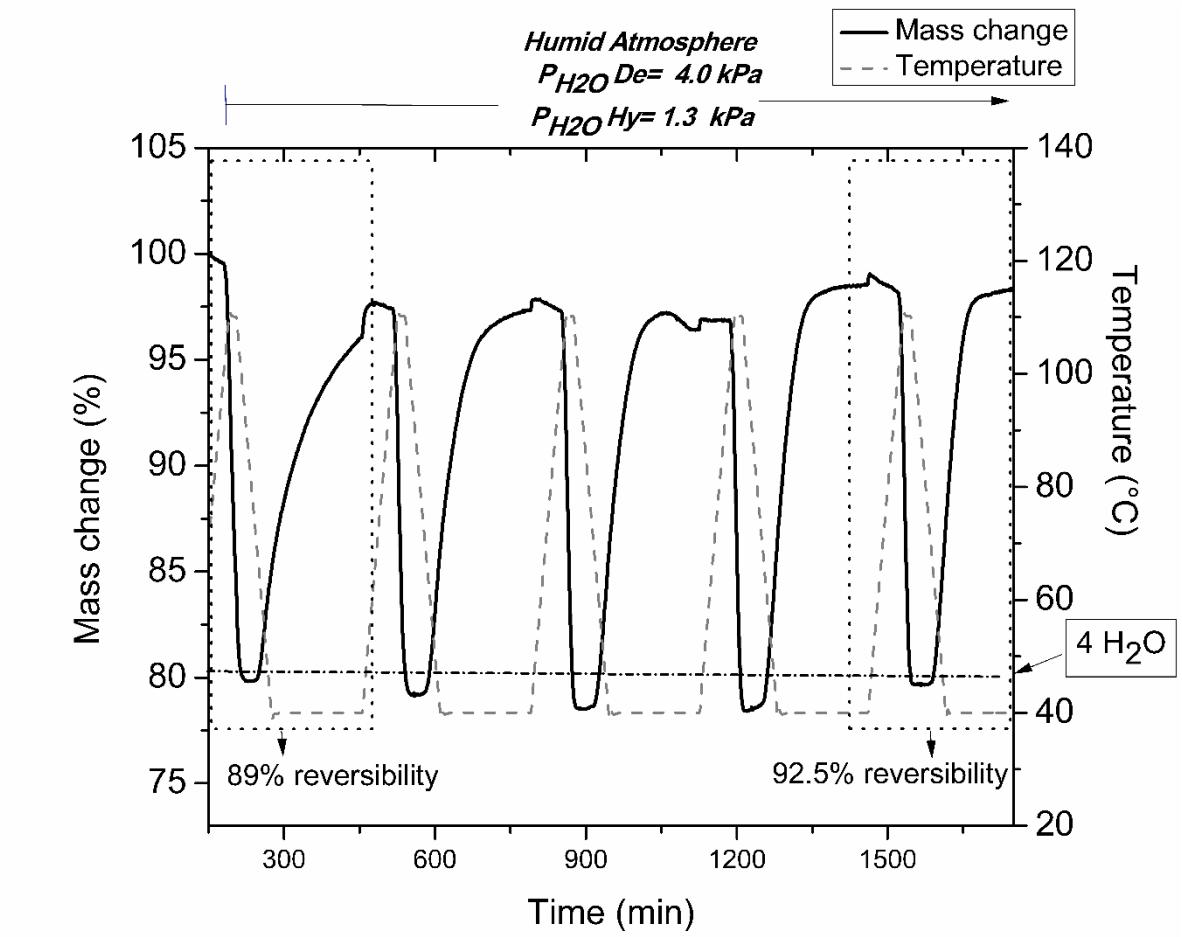

Figure 17: Optimization of dehydration reaction of carnallite waste under seasonal conditions (Experiment 4).

Experiment 5 (see Table 2) was carried out to evaluate cyclic stability for 20 cycles (20 years of seasonal application). Results are shown in Figure 18, where the chemical reversibility is stable in the first five cycles but decreases down to 87 % and 67.1 % after 10 and 20 reaction cycles, respectively. In addition, a negative slope in the baseline is observed, which indicates the possible material decomposition in each cycle. However, under these operating conditions, the mass loss of 19 wt% corresponding to the maximum mass loss of the first step of the reaction, is exceeded only in the last cycle (20.9 wt%). Therefore, the loss of chemical reversibility could not be associated with the decomposition by hydrolysis.

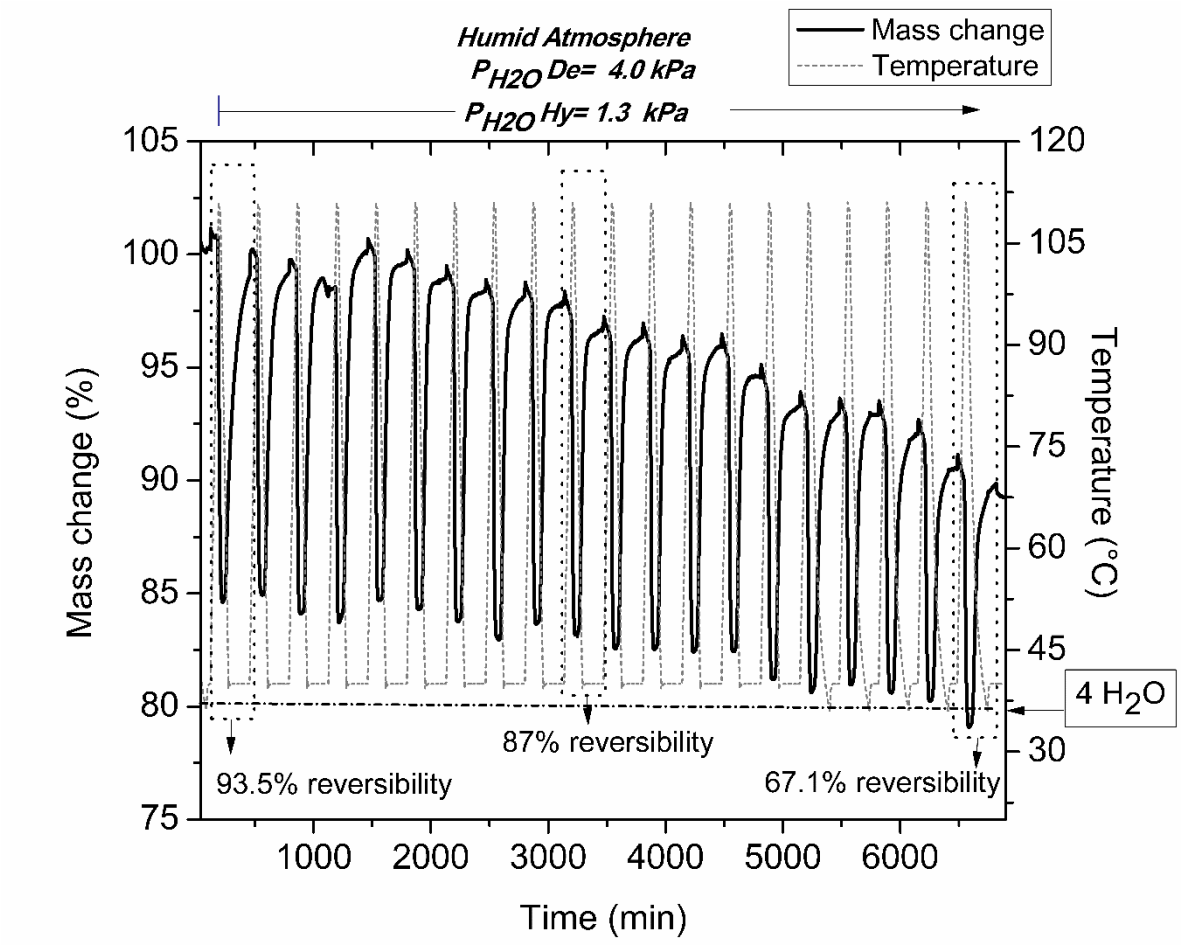

Figure 18: Cycle stability of carnallite waste under seasonal conditions (Experiment 5).

In order to improve the cyclic stability of carnallite-waste, long-term hydration reactions described in Table 2 were carried out (experiment 6). In this case, the pressure and temperature conditions of experiment 5 were maintained, but the water vapor partial pressure change was increased during dehydration at rates of 57 Pa/min and 39 Pa/min, for the first cycle and from the second cycle onwards, respectively. Furthermore, the hydration isothermal duration was doubled from 180 to 360 minutes to reach the equilibrium during the hydration step in all cycles. Under these conditions, the results showed (see Figure 19) a more stable behavior through the cycles. Furthermore, a greater mass loss is observed during dehydration steps and, a greater mass gain is reached during hydration in each cycle, achieving a conversion of 87.2 % in the tenth cycle. However, this conversion degree does not differ from the result obtained in the tenth cycle for the material under the conditions of experiment 5 (87 % in the tenth cycle). Therefore, the decrease of chemical reversibility under seasonal dehydration (ϑ_{De} = 110 °C and $p_{H2O,\ De}$ = 4.0 kPa) and hydration conditions (ϑ_{Hy} = 40 °C and $p_{H2O,\ Hy}$ = 1.3 kPa) is not attributed to changes in the operational parameters of temperature and pressure. Finally, it is necessary to highlight the hydration temperature (ϑ_{Hy}) is close to 40 °C. This value is suitable for seasonal heat applications, in which the heating of houses and water for domestic use is required [34].

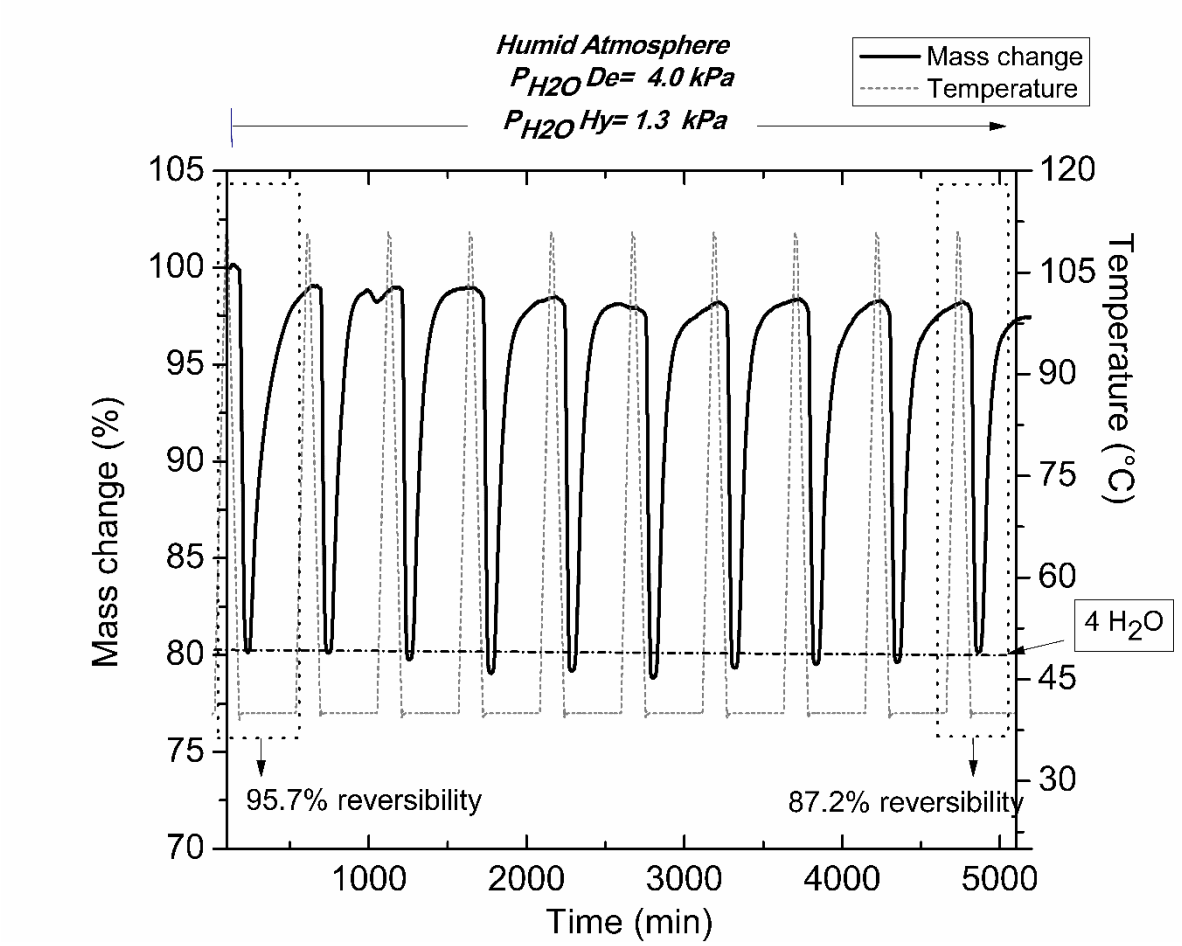

Figure 19: Dehydration/hydration of carnallite waste for 10 cycles at long time (6 hours) of hydration (Experiment 6).

-XRD of the products of 10 and 20 reaction cycles

To discard the material decomposition after 10 and 20 cycles (experiments 5 and 6), the products of these experiments were analyzed by XRD. The results are shown in Figure 20, where crystalline phases corresponding to hydrolysis products were not identified. Therefore, the material decomposition by hydrolysis reaction cannot be detected with the methods used in this study. Moreover, the XRD pattern of 20 cycles-product showed less intense peaks than those of 10 cycles-product, meaning the loss of crystallinity of carnallite-waste through the cycles. As a consequence, not only the sample reactivity drops progressively but also the complexity of the material increases. In other words, the cycles of dehydration-hydration could result in a physical change of the sample, from a crystalline solid into a semi-crystalline or amorphous solid [35], i.e. the incorporation of water molecules during hydration would decrease, as agglomeration increases and therefore the particle sizes, making more difficult the diffusivity of water vapor through the sample.

Agglomeration due to the loss of crystallinity of hydrated materials is an important aspect to consider during the scale-up process. Not only because this issue could increase with the increase of the sample scale, but also because it could jeopardize the potential use of salt hydrates for TCS systems. Still, proposing the use of industrial waste remains as a great advantage, as the material costs practically do not have a significant influence on the total investment cost of the system, giving the possibility of replacing the medium of storage every 10 cycles (10 years).

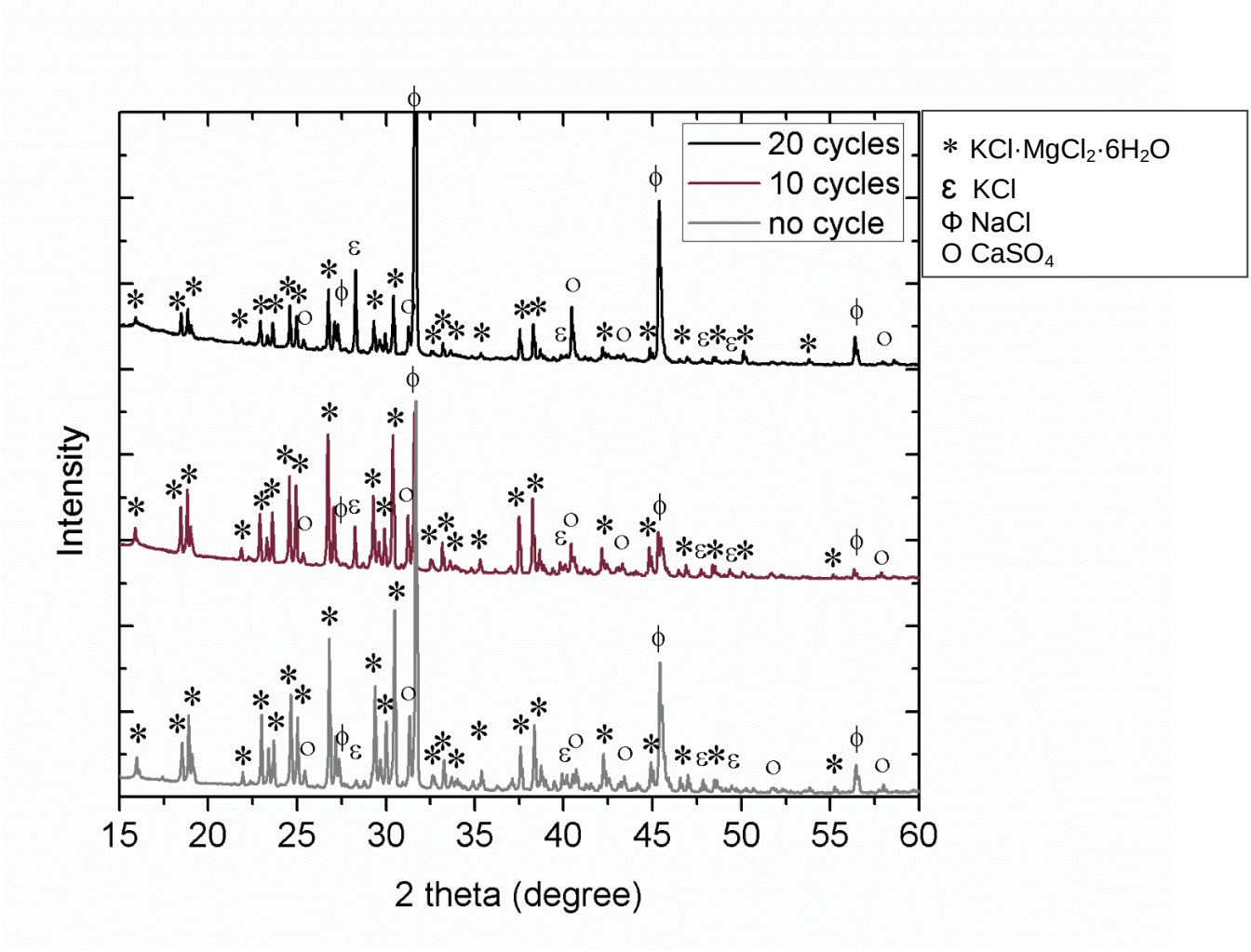

Figure 20: Potassium carnallite XRD pattern before cycling and after 10, 20 cycles at room temperature.

4. Potential application of carnallite-waste material

4.1 Evaluation of energy storage density

According to literature [36], a TCM should have energy storage density (*esd*) equal to or greater than 1.3 GJ/m^3 to be considered suitable for seasonal heat storage applications at temperatures below 120 °C. In order to establish the potential of carnallite, the *esd* was calculated for each cycle, based on reaction enthalpy changes (ΔH) (see Figure 21) and the density (1.7103 kg/m^3 at 28.8 °C), and summarized in Table 5.

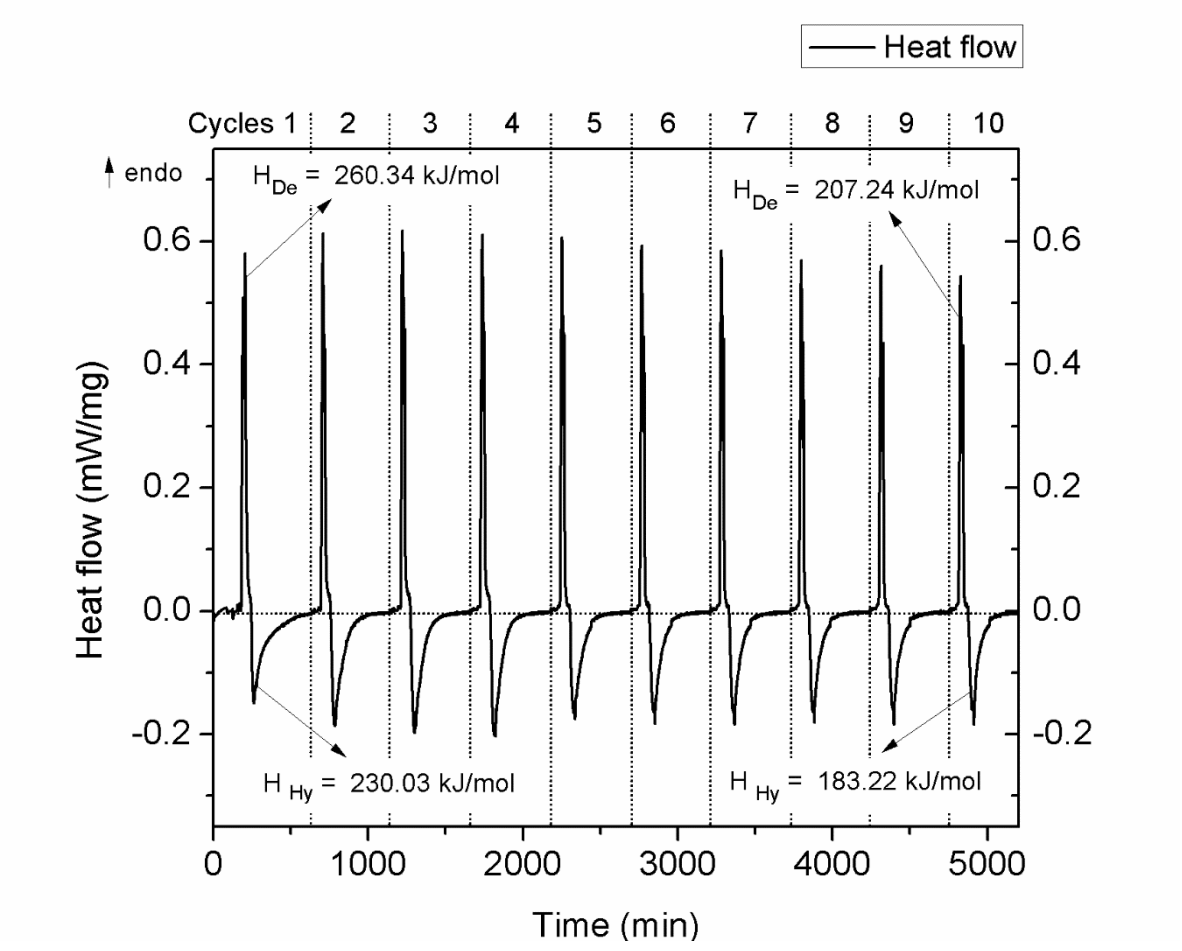

Figure 21: Enthalpies of dehydration/ hydration from experiment 6.

Table 5: Energy storage density estimated for dynamic dehydration of potassium carnallite.

PM:277.6 g/mol		ρ[28.8 °C]=1.7103 [kg/m^3]		
Cycle	**ΔH_{De} [kJ/mol H_2O]**	***esd*$_{De}$ [GJ/m^3]**	**ΔH_{Hy} [kJ/mol H_2O]**	***esd*$_{Hy}$ [GJ/m^3]**
1	59.85	1.604	52.88	1.417
2	57.03	1.528	52.73	1.413
3	58.35	1.564	54.20	1.453
4	56.10	1.504	52.76	1.414
5	49.89	1.337	46.40	1.243
6	48.84	1.309	44.85	1.202
7	48.48	1.299	45.16	1.210
8	48.24	1.293	41.57	1.114
9	47.77	1.280	42.04	1.127
10	47.64	1.277	42.12	1.129

It can be seen in Table 5, that the esd_{Hy} of carnallite-waste in the first four cycles is close to 1.4 GJ/m^3 and is larger than those reported in scientific papers [36]. Also, it can be observed that from the fifth cycle onwards the esd_{Hy} decreases to 1.129 GJ/m^3 in cycle 10 because decreasing of the chemical reversibility of the sample (see Figure 19).

In this way, in a practical application, carnallite storage material must be replaced every 10 years. It should be mentioned that this would not increase the investment costs significantly, since carnallite-waste is a natural waste without any commercial cost nor environmental impact.

4.2 Evaluation of potential for seasonal heat storage applications

The esd_{Hy} and the price per mega Joule of energy stored of carnallite-waste were compared among salt hydrates that have been previously reported as promising for seasonal heat storage applications (Table 6). The esd_{Hy} of carnallite-waste corresponds to the calculated at the tenth cycle (1.129 GJ/m^3). The values of esd_{Hy} were directly correlated with the material volume needed to store 8 GJ of energy, considered as the required energy capacity to supply the heat demands of a common house during the six months of cold seasons [9,36]. Even though the largest storage volume corresponds to carnallite-waste, the material costs, practically "0", leads to a storage material price of 0 €/MJ. Therefore, the use of this waste material improves the potential of developing sustainable technologies to store/generate heat.

Table 6. Comparison of *esd* and energy cost for waste sample of potassium carnallite and most promising TCM, candidates for seasonal heat storage [32].

Materials	Highest and lowest hydrate	N° H_2O moles in reaction	$_{Hy}$ *esd* (GJ/m^3) open system	Volume material (m^3) for 8 GJ	Price (€/MJ)
***KCl·MgCl$_2$ (waste)**	6 – 2	4.36	1.129	7.1	0
$MgCl_2$	6 – 2	3	1.93	4.1	0.14
LiCl	1 – 0	1	2.08	3.8	35.53
K_2CO_3	1.5 – 0	1.5	1.30	6.2	1.67
$CuCl_2$	2 – 0	2	1.74	4.6	4.33

*Experimental result after 10 cycles reactions.

4. Conclusions

Overall, the chemical characterization of carnallite-waste, determined its composition as 73.5 wt% of $KCl{\cdot}MgCl_2{\cdot}6H_2O$, mixed with the main impurity of 23.04 wt% NaCl. This material, in the operating conditions close to equilibrium (at p_{H2O} =25 kPa), showed lower cyclic stability compared to the synthetic material. As a result, lower reversibility of rehydration is observed in each cycle. To improve the cyclic stability of carnallite-waste, the operating conditions of dehydration were experimentally optimized to 110 °C, p_{H2O} = 4.0 kPa and the operating conditions of hydration to 40 °C and p_{H2O} =1.3 kPa. Thereby, greater reaction reversibility in each cycle and no sign of material decomposition by hydrolysis were achieved. During the thermodynamic characterization of the reactive system and following the van't Hoff plot, a temperature decrease of 20K and the increase of the water vapor pressure of dehydration prevented the material from decomposing by hydrolysis reaction. Likewise, an increase of the hydration isothermal time allowed to attain reversibility loss of only 8.5 % during ten cycles (10 years of application). This reversibility loss is associated with the loss of the material crystalline structure when subjected to constant hydration cycles, allowing the agglomeration of particles. Hereby it can be stated that the partial loss of reversibility of hydration of this carnallite-waste is produced due to the decomposition through hydrolysis, loss of crystalline structure and agglomeration of the particles when cycled more than 5 times.

However, after ten cycles the loss of reversibility is still low enough not to compromise its potential application in seasonal heat storage. In addition, the energy storage density determined during the tenth hydration cycle was 1.129 GJ/m^3, a value that is comparable and competitive with materials such as K_2CO_3 and $MgCl_2$, reported as promising for seasonal thermochemical storage applications.

Finally, it is important to note that this is a waste material, so it has no commercial value and its use contributes to the reuse of industrial waste for sustainable applications.

5. Declaration of interest: none

6. Acknowledgments

Verónica Mamani thanks CONICYT for her doctorate scholarship CONICYT No. 21150145, Svetlana Ushak thanks financial support of CONICYT/FONDAP Nº 15110019 SERC-Chile,

CONICYT/PCI/REDES N°170131 and CONICYT/FONDECYT REGULAR N° 1170675 projects. Andrea Gutierrez would like to thank DAAD for her DLR/DAAD Postdoctoral fellowship. University of Barcelona and Diopma group thank the funding by the Spanish Government (RTI2018-093849-B-C32), and the Catalan Government for the quality accreditation (2017 SGR 118).

7. References

[1] Kalaiselvan and Parameshwaran, Energy and energy management, Thermal Energy Storage Technologies for Sustainability 2014; Chapter 1: 1-19.

[2] BP Statistical Review of World Energy; 2015. bp.com/statistical review (accessed on May 2016).

[3] P. Pardo, A. Deydiera, Z. Anxionnaz-Minvielle, S. Rougé, M.Cabassud, P.Cognet. A review on high temperature thermochemical heat energy storage. Renewable and Sustainable Energy Reviews 2014; 32:591–610.

[4] N'T soukpoe KE, Liu H, Le Pierrès N, Luo L. A review on long-term sorption solar energy storage. Renewable Sustainable Energy Rev 2009; 13:2385–96.

[5] Juan Wu, Xin feng Long, Research progress of solar thermochemical energy storage, Int. J. Energy Res. 2015; 39: 869–888.

[6] T. Yan, R. Z. Wang, T. X. Li, L.W. Wang, Ishugah T. Fred, A review of promising candidate reactions for chemical heat storage, Renewable and Sustainable Energy Reviews 2015; 43:13–31.

[7] Kokouvi Edem N'Tsoukpoe, Thomas Schmidt, Holger Urs Rammelberg, Beatriz Amanda Watts, Wolfgang K.L. Ruck. A systematic multi-step creening of numerous salt hydrates for low temperature thermochemical energy storage. Applied Energy 2014; 124: 1–16.

[8] Claire J. Ferchaud, Robbert A.A. Scherpenborg, Herbert A. Zondag and Robert de Boer. Thermochemical seasonal solar heat storage in salt hydrates for residential applications - Influence of the water vapor pressure on the desorption kinetics of MgSO4.7H2O. Energy Procedia 2014; 57: 2436 – 2440.

[9] C.J. Ferchaud, H.A. Zondag, A. Rubino, R. de Boer. Seasonal Sorption Heat Storage – Research on Thermochemical Materials and Storage Performance. ECN-M--12-070 Conference 2012.

[10]Devrim Aydin, Sean P. Casey, Saffa Riffat. The latest advancements on thermochemical heat storage systems. Renewable and Sustainable Energy Reviews 2015; 41: 356–367.

[11] Gutierrez Andrea, Miró Laia, Gil Antoni, Rodríguez-Aseguinolaza Javier, Barreneche Camila. Advances in the valorization of waste and by-product materials as thermal energy storage (TES) materials. Renewable and Sustainable Energy Reviews 2016; 59: 763–783.

[12] Miró L, Navarro ME, Suresh P, Gil A, Fernández AI, Cabeza LF. Experimental characterization of a solid industrial by-product as material for high temperature sensible thermal energy storage (TES). Appl Energy 2014; 113:1261–8.

[13] Svetlana Ushak, Andrea Gutierrez, Hector Galleguillos, Angel G. Fernandez, Luisa F. Cabeza, Mario Grágeda. Thermophysical characterization of a by-product from the non-metallic industry as inorganic PCM Solar Energy Materials & Solar Cells 2015; 132: 385 –391.

[14] V. Mamani, A. Gutiérrez, S. Ushak. Development of low-cost inorganic salt hydrate as a thermochemical energy storage material. Solar Energy Materials and Solar Cells 2018; 176: 346–356.

[15] Andrea Gutierrez, Svetlana Ushak, Veronica Mamani, Pedro Vargas, Camila Barreneche, Luisa F. Cabeza, Mario Grágeda, Characterization of wastes based on inorganic double salt

hydrates as potential thermal energy storage materials, Sol. Energy Mater. Sol. Cells 2017;170:149-159.
[16] Andrea Gutierrez, Svetlana Ushak, Marc Linder. High Carnallite-Bearing Material for Thermochemical Energy Storage: Thermophysical Characterization. *ACS Sustainable Chem. Eng.*, 2018; 6 (5): 6135–6145.
[17] S. Ushak, A. Gutierrez, E. Flores, H. Galleguillos, M.Grageda., Development of Thermal Energy Storage Materials from Waste-Process Salts. Energy Procedia 2014; 57: 627-632.
[18] H.-H. Emons. Mechanism and kinetics of formation and decomposition of carnallitic double salts. Journal of Thermal Analysis 1988; 33: 113-120
[19] Emons, H.-H.; Naumann, R.; Pohl, T.; Voigt, H. Thermoanalytical investigations on the decomposition of double salts: I. the decomposition of carnallite. J. Therm. Anal. 574 Calorim. 1984; 29: 571-579.
[20] H.-H. Emons and Th. Fanghiinel. Thermal decomposition of carnallite ($KCl.MgCl_2 .6H_2O$)-comparison of experimental results and phase equilibria. Journal of Thermal Analysis. 1989; 35: 2161-2167.
[21] Boletín informativo del ministerio de energía, http://www.energia.gob.cl/energias-renovables (2016).
[22] Los hitos del 2014, ELECTRICIDAD, La revista energética de Chile, (2015).
[23] Korotkov, J. A.; Mikhkailov, E. F.; Andreevm, G. A.; Eltsov, B. I.; Plyakov, J. A.; Shestakov, B. G.; Kechina, G. D. Method of dehydrating carnallite. United States Patent Nr. 4,224,291, 1980.
[24] Meir Elam, Sara Ben-Ari, Nestor Leiderman. Carnallite having reduced moisture absorption and method of producing it. Patent WO2001083401A1 (2001).
[25] Bushra Khalid. Effect of Temperature and Humidity on Salt Mine Environment. Pakistan Journal of Meteorology 2010; 7:1-13.
[26] A. Minevich, Y. Marcus, L. Ben-Dor,] Densities of solid and molten salts hydrates and their mixtures and viscosities of the molten salts, Journal of Chemical & Engineering Data 2004; 48: 1451-1455.
[27] Nathaly Romero. Engineer undergraduate thesis, avalaible in spanish: Consumo de energía a nivel residencial en Chile y análisis de eficiencia energética en calefacción. Memoria de ingeniero civil. Universidad de Chile, 2011.
[28] Pedro Pavlovic. The industry of lithium in Chile. Available in spanish in journal: Ingenieros, Revista de Colegio de Ingenieros en Chile, 2014, 02: 30-35
[29] Shkatulov, Alexandr Aristov, Yuri. Modification of magnesium and calcium hydroxides with salts: An efficient way to advanced materials for storage of middle temperature heat. Energy 2015; 85: 667-676.
[30] Korhammer Kathrin, Druske Mona Maria, Fopah-Lele Armand, Rammelberg Holger Urs, Wegscheider Nina, Opel Oliver Thomas Osterland, Wolfgang Ruck. Sorption and thermal characterization of composite materials based on chlorides for thermal energy storage. Applied Energy 2016; 162: 1462–1472.
[31] Hongyu Huang, Jun Li, Huhetaoli, Yugo Osaka, Chenguang Wang, Noriyuki Kobayashi, Zhaohong He, and Lisheng Deng. Porous-Resin-Supported Calcium Sulfate Materials for Thermal Energy Storage. Energy Technol. 2016; 4: 1401 – 1408.

[32] Araten, David Ashboren. Carnallite Decomposition into Magnesia, Hydrochloric Acid and Potassium Chloride: A 'Thermal Analysis Study; Formation of Pure Periclase. J. appl. Chem. Biotechnol 1973; 23: 77-86.
[33] Danny Müller, Christian Knoll, Georg Gravogl, Werner Artner, Jan M. Welch, Elisabeth Eitenberger, Gernot Friedbacher, Manfred Schreiner, Michael Harasek, Klaudia Hradil, Andreas Werner, Ronald Miletich, Peter Weinberger. Tuning the performance of MgO for thermochemical energy storage by T dehydration – From fundamentals to phase impurities. Applied Energy 2019; 253: 113562.
[34] Elisa Guelpa, Vittorio Verda. Thermal energy storage in district heating and cooling systems: A review. Applied Energy 2019; 252: 113474.
[35] Xavier Fontanet. Estudio de Na_2S como material de almacenamiento termoquímico. Memoria ingeniería de materiales. Escuela técnica superior de ingeniería industrial de Barcelona, 2013.
[36] P.A.J. Donkers, L.C. Sögütoglu, H.P. Huinink, H.R. Fischer, O.C.G. Adan. A review of salt hydrates for seasonal heat storage in domestic applications. Applied Energy 2017; 199: 45–68.

***Credit Author Statement**

CRediT author statement

Mamani: Conceptualization, Investigation, partial original draft preparation. Gutierrez: Methodology, Investigation, Supervision of experimental work, partial original draft preparation. Ushak: Supervision, Funding acquisition, Writing. Fernandez: Supervision, Reviewing and Editing.

***Declaration of Interest Statement**

Declaration of interests

☒ The authors declare that they have no known competing financial interests or personal relationships that could have appeared to influence the work reported in this paper.

☐The authors declare the following financial interests/personal relationships which may be considered as potential competing interests:

Declarations of interest: none